Phase Transitions in Hard-Core Lattice Gases

A thesis presented by

Roger M. Nisbet

to the

University of St. Andrews

in application for the Degree of

Doctor of Philosophy

February 1972

Th

7014

Declaration

The accompanying thesis is my own composition. It is based on work carried out by me and no part of it has previously been presented in application for a Higher Degree.

Certificate

I certify that the conditions of the Ordinance and Regulations have been fulfilled.

Research Supervisor

I was admitted as a research student under Ordinance General No. 12 in October 1968, and as a candidate for the degree under this ordinance in October 1969.

Acknowledgements

I should like to express my thanks to the following:

Dr. I.E. Farquhar, my research supervisor, for his constant interest and encouragement, and for his many ideas and suggestions which appear unacknowledged in the thesis.

Professor R.B. Dingle, for the facilities made available to me in the Department of Theoretical Physics.

Dr. R. Erskine and the staff of the Computing Laboratory for the excellent computing facilities made available to me, including an enormous amount of computer time. Dr. Erskine also wrote me three subroutines which were essential to most of the work.

Dr. P. Keast (Department of Mathematics) whose lectures on Numerical Linear Algebra (Session 1969-70) provided the foundation for all the numerical work on matrices. Dr. Keast also solved a mathematical problem which had held up my numerical work for some time (see Chapter 2.3).

Dr. D.S. Gaunt (King's College, London) for two valuable discussions which led to the work on the superexchange model and the SQ12 model (defined in the text).

The Carnegie Trust for the Universities of Scotland for financial support throughout the course of the work.

plus many others who helped with a large number of smaller problems, especially Mr.D.J. Buchanan, Dr. N.C. McGill, and Miss V.A. Wynne.

CONTENTS.

ABSTRACT

The thesis contains the results of some numerical studies of two-dimensional "hard-core lattice gases" (HCLGs) i.e. collections of particles confined to the sites of a lattice and interacting only through a hard-core which excludes the occupancy of a set of lattice sites around an occupied site. The hope is that such models might display properties similar to hard discs for which the steric interactions are believed to cause a first-order Ehrenfest phase transition (EPT); as a step towards understanding the transition in the continuum system we try to identify which properties of an HCLG will lead to a first-order EPT.

We first discuss the different methods of characterising phase transitions in lattice gases — as discontinuities or singularities of the grand canonical pressure, as regions where the Gibbsian distribution on the lattice ceases to be unique, and as points where some "order parameter" vanishes. We examine the previous work on HCLGs and summarise the evidence for each of the three types of transition before introducing a conjecture of Orban and Bellemans that (provided the hard-core is not too small) an HCLG will have a first-order EPT provided the close-packed configuration is well-defined[1]. We then introduce the twin aims of the present work: to test this idea on a specific model and in the light of the results of this work (which provides a counter-example to the conjecture) to re-examine the evidence on which the conjecture was based.

In the second chapter we give a detailed account of the use of the transfer matrix to study lattices of infinite length, but of finite width, M sites. We consider the problems involved in using the properties of such semi-infinite lattices to predict the location and nature of any phase transition in a lattice of infinite width. All the methods under consideration are tested on three examples: the superexchange model (for which at one temperature an exact isotherm has been calculated by Fisher), a square-lattice gas with an attractive potential extending to nearest-neighbour sites (mathematically equivalent to the spin-$\frac{1}{2}$ Ising model whose behaviour in the transition region is known), and the square-lattice gas with nearest-neighbour exclusion (which has been studied numerically by several different groups who agree on the nature of the transition). The chapter concludes with a critical assessment of

the numerical methods in view of the results of these tests.

The third chapter contains the results for the square-lattice gas with first-, second-, and fourth-nearest neighbour exclusion. We conclude that there is no EPT in this model and thus have a counter-example to the conjecture that there will be a first-order EPT in an HCLG with a unique close-packed configuration.

The final chapter is a preliminary report of our re-examination of three HCLGs studied by other workers. The principal theme is the influence of boundary conditions on the results for semi-infinite lattices, the main result a demonstration that the phase transition believed to occur in the square-lattice gas with first- and second-nearest neighbour exclusion might be an artifact of the periodic boundary conditions. Completion of the work on some of these HCLGs is postponed till the arrival of an extra 100K of core for the St. Andrews computer.

The appendices deal with a few technical points. The only new material is a device for accelerating the convergence of Nesbet's algorithm for eigenvalues and eigenvectors of large matrices.

NOTATION

We list here some of the symbols which recur throughout the thesis:

(1) Standard Thermodynamic and Statistical Mechanical Quantities.

Ξ	grand partition function
P	grand canonical pressure
V	volume
ρ	density
T	temperature
k	Boltzmann's constant
μ	chemical potential
z	activity
u	$z/(1+z)$
R	order parameter

(2) Two-Dimensional Hard-Core Lattice Gases.

We define the models by a notation in which:

SQ12 is the case of first- and second-nearest neighbour exclusion on the square lattice.

TR1 is the case of nearest-neighbour exclusion on the triangular lattice.

H1 is the case of nearest-neighbour exclusion on the honeycomb lattice.

etc.

(3) Matrix Method.

M	width of the lattice
B	transfer matrix before symmetry reduction
d(M)	dimension of B for a lattice of width M
$\{\lambda_i\}$	eigenvalues of B
P	reduced transfer matrix
σ(M)	dimension of P for a lattice of width M
MNMINI, MNMAXI, MNEIGM	programs for deriving thermodynamic properties of $M\times\infty$ lattices.

(4) Quantities used to make deductions about $\infty \times \infty$ lattices.

For a given $M \times \infty$ lattice we define:

$u_o(M)$ value of u at which $d\rho/du$ attains its maximum value

$u_I(M)$ intersection point (where $\rho(M,u) = \rho(M+\Delta M,u)$; we are considering a sequence of values of M, the interval in M being ΔM.)

$u_1(M)$, $u_2(M)$ values of u where $d^2\rho/du^2$ attains respectively its maximum and minimum values.

$\rho_1(M)$, $\rho_2(M)$ density at respectively $u_1(M)$ and $u_2(M)$.

$u_{I1}(M)$, $u_{I2}(M)$, $\rho_{I1}^{M}(M)$, $\rho_{I2}^{M}(M)$, $\rho_{I1}^{M+\Delta M}(M)$, $\rho_{I2}^{M+\Delta M}(M)$: quantities used in the intersection method of determining the nature of a phase transition.

$u_{EV}(M)$ value of u at which λ_2/λ_1 attains its maximum value.

u_t transition point

CHAPTER I.

INTRODUCTION.

We shall be attempting to establish the existence and nature of phase transitions in some two-dimensional lattice gases of "hard-core" particles, by which we mean a collection of particles confined to the sites of a two-dimensional lattice, L, and interacting through a potential of the form

$$V(r) = \begin{cases} \infty & \text{for } r \in Y \\ 0 & \text{otherwise} \end{cases}$$

where Y is a simply connected, finite, subset of L containing the point r=0. The motivation for studying such models has been discussed elsewhere[1] in some detail; it is of course their similarity to the continuum cases of hard discs and spheres for which many workers have proposed a first-order Ehrenfest phase transition. However the relation between the lattice and continuum gases is not clear, and the reason for studying such oversimplified models has been cynically illustrated[3] by the story of the man who, returning late home from an alcoholic evening , was scanning the ground for his key under a lamp post; he knew he had dropped it somewhere else but only under the lamp post was there enough light to conduct a proper search!

1.1 Characterisation of a Phase Transition in Lattice Gases.

The grand canonical ensemble will be used throughout. The appropriate free variables are thus the volume, V, the chemical potential, μ, and the temperature, T; however for the special case of hard-core systems the effect of temperature is rather trivial and the grand partition function is a function of V and the activity, z, defined by

$$z = \Lambda^{-d} e^{\mu/kT} \quad \text{where} \quad \Lambda = (h/2\pi mkT)^{\frac{1}{2}} \qquad (1.1.1)$$

d = dimensionality of the system

m = mass of one particle

h = Planck's constant

k = Boltzmann's constant

Given $\Xi(V,\mu,T)$, the grand partition function of a (general) system, we obtain the equation of state from the relation

$$P(V,\mu,T) = (kT/V)\log \Xi(V,\mu,T) \qquad (1.1.2)$$

where P is the pressure. For finite V and stable* interactions it is not difficult to prove that the function P is analytic in μ and T for $-\infty < \mu < \infty$, $0 < T < \infty$**. This analyticity is obviously difficult to reconcile with the observed discontinuities in the experimental equation of state of many systems, the traditional solution to this problem being to consider the limit of infinite volume. Should the convergence to this limit be non-uniform, the grand canonical pressure need not remain an analytic function of μ and T. This mathematical necessity of considering the limiting infinite system is not physically as absurd as it might appear; to characterise a phase change by non-uniform convergence of some sequence as $V \to \infty$ is just to say that near a change of phase the corresponding property, X, of a large system varies in a peculiar manner with the volume. We shall be principally concerned with three choices for this property, X.

(1) The Grand Canonical Pressure.

This is the obvious approach to the problem of phase transitions. It is anticipated that after taking the limit $V \to \infty$, the grand canonical pressure will be a piecewise analytic function of μ and T, phase transitions occurring at the singularities and discontinuities of this function. The phase transitions are classified according to the nature of these non-analyticities, the most important being Ehrenfest phase transitions and λ-transitions.***

* An interaction is said to be stable if there exists $B \leq 0$ such that if n particles are situated at points $r_1, r_2, \ldots, r_n$, then the n-particle potential energy $U(r_1, r_2, \ldots, r_n)$ satisfies $U(r_1, r_2, \ldots, r_n) \geq nB$ for all $n \geq 0$ and all $r_1, r_2, \ldots r_n$.

** The key to proving this result is an un-numbered inequality on page 57 of ref. 4.

*** An n'th order Ehrenfest phase transition is one in which there is a finite discontinuity in an n'th derivative of a thermodynamic potential (e.g. the grand canonical pressure). At a λ-transition there is an infinity in a second derivative of a thermodynamic potential (e.g. an infinity in specific heat). See Pippard (ref. 5, chapter 9) for examples.

(2) The Grand Canonical Distribution Function.

Recent developments in algebraic techniques have made possible the discussion of probability distributions defined directly on the infinite system. There are a number of different approaches to the problem (e.g. those of Griffiths[6], Ruelle[4], Dobrušin[7]) each differing in the definition of an equilibrium state, and while they are very similar in spirit the relationships between them are not at all obvious. However for the particular case of the classical lattice gas, Brascamp[8] has demonstrated the equivalence of a number of the definitions. As the algebraic formalism is less familiar than the traditional grand canonical formalism, we now give a brief, non-technical sketch of the ideas involved.

Let **L** be the infinite lattice (e.g. for the two-dimensional square lattice L is isomorphic to $\mathbb{Z}^2$). A configuration of the lattice gas is defined by giving a set, X, of occupied lattice sites, so the configuration space of the system is just P(L), the set of subsets of L. A distribution, σ, is a probability measure on P(L); Dobrušin[7] quotes a theorem of Kolmogorov that specification of an infinite-dimensional distribution, σ, is equivalent to specifying a compatible* system of finite-dimensional distributions, σ_V, where $V \subset L$. The conditional distribution, $\sigma_V(X_V, Y_{L\setminus V}) : X_V \in \mathcal{P}(V),\ Y_{L\setminus V} \in \mathcal{P}(L\setminus V)$, is now easily defined; it is natural to interpret it as the probability of finding configuration X_V in the finite subset $V \subset L$, given $Y_{L\setminus V}$*, the known and fixed configuration in the remaining lattice sites. In statistical mechanics we are concerned with Gibbsian distributions; the conditional distribution σ_V is said to be Gibbsian if

$$\sigma_V(X_V, Y_{L\setminus V}) \qquad \frac{e^{-\beta U_V(X_V, Y_{L\setminus V})}}{Z_V(Y_{L\setminus V})} \tag{1.1.3}$$

where $U_V(X_V, Y_{L\setminus V}) = -\mu |X_V| + \Phi_1(X_V) + \Phi_2(Y_{L\setminus V}, X_V)$

$|X_V|$ is the number of elements of X_V,

$\Phi_1(X_V)$ is the potential energy due to interactions between particles in V,

$\Phi_2(Y_{L\setminus V}, X_V)$ is the potential energy due to particles in V interacting with particles outside V,

$$Z_V(Y_{L\setminus V}) = \sum_{X_V \in \mathcal{P}(V)} e^{-\beta U_V(X_V, Y_{L\setminus V})}$$

* defined in ref.7

According to Kolmogorov's theorem, specification of all the Gibbsian distributions $\sigma_\gamma(x_\Lambda|y_{\Lambda^c})$ now defines the limiting distribution σ on $P(L)$; however, this distribution may depend on the choice of y_{Λ^c} for the finite systems.

The connection with the problem of phases and phase transitions is through a theorem of Dobrušin[7], as a consequence of which it can be proved that uniqueness of the Gibbsian distribution implies continuity of the limit correlation functions, and it is well known[9] that at an n'th order EPT, the n-point correlation functions have a discontinuity. Thus the case where the Gibbsian distribution is unique corresponds to the case of no separation of phases. Alternatively, where the limiting distribution is not unique it is possible that two phases may co-exist. For example, consider the 2-D square-lattice gas with an attractive potential $-\epsilon$ between nearest neighbour sites. Then if $\mu = -2\epsilon$ and β is sufficiently large, it can be proved that there exist distributions σ_1 and σ_2 such that the respective probabilities P_1 and P_2 of occupancy of an arbitrary lattice site obey

$$P_1 \leq \gamma < \tfrac{1}{2}$$
$$P_2 \geq 1-\gamma > \tfrac{1}{2} \qquad (1.1.4)$$

from which it is immediate that there is a first-order EPT with a discontinuity in the density.

It is unfortunate that while the existence of an EPT implies non-uniqueness of the Gibbsian distribution for some values of μ and β, the converse proposition is not true. This observation is particularly relevant to the hard-core lattice gases as we shall now demonstrate. We consider again the 2-D square lattice gas, but this time with the potential consisting only of a hard-core extending to nearest neighbour sites. We divide the lattice into A and B sublattices as shown below:

A B A B A B A B A B A

B A B A B A B A B A B

A B A B A B A B A B A

B A B A B A B A B A B

For sufficiently large values of μ, Dobrušin has proved that there are two Gibbsian distributions σ_1 and σ_2. However, this time the respective probabilities P_1 and P_2 of occupancy of an arbitrary lattice site, i, obey:

$$P_1 \begin{cases} \leq \gamma < \frac{1}{2} & \text{if } i \in A \\ \geq \gamma > \frac{1}{2} & \text{if } i \in B \end{cases} \qquad (1.1.5)$$

$$P_2 \begin{cases} \geq \gamma > \frac{1}{2} & \text{if } i \in A \\ \leq \gamma < \frac{1}{2} & \text{if } i \in B \end{cases}$$

Since the observed properties, e.g. density, of the lattice gas involve averaging over both sublattices, it is not possible in this case to predict any discontinuities in these properties, the two co-existing "phases" in this case corresponding to preferential occupation of the A or B sublattices.

(3) An "Order Parameter".

This is in general a difficult quantity to define and interpret, but for the hard-core lattice gases* the situation is fairly simple and is best explained with the help of an example. We again consider the 2-D square-lattice gas with nearest-neighbour exclusion, and (formally) ascribe different chemical potentials μ_A, μ_B to the A and B sublattices. The grand canonical pressure is then a function of μ_A, μ_B, and V; differentiation with respect to μ_A (or μ_B) yields the density ρ_A (or ρ_B) on the A (or B) sublattice. The order parameter, R, is defined by

$$R(\mu) = \left[\lim_{\mu_A \to \mu_B} \lim_{V \to \infty} (\rho_A - \rho_B) \right]_{\mu_B = \mu} \qquad (1.1.6)$$

The limits must be taken in the order specified (cf. the definition of the spontaneous magnetisation of a ferromagnet). We talk of an order-disorder transition if for some μ_c

$$R(\mu) \begin{cases} = 0 & \text{for } \mu < \mu_c \\ > 0 & \text{for } \mu > \mu_c \end{cases} \qquad (1.1.7)$$

* The following discussion follows the ideas given in ref. 1

That R should be non-vanishing if and only if there are a number of Gibbsian distributions of the type (1.1.5) would be an appealing result, but one which, to the author's knowledge has not been proved. However, the interpretation of a non-zero R is identical to that of the relations (1.1.5); in particular it should be emphasised that to the best of our understanding the existence of an EPT cannot be rigorously deduced from information about R (though one may speculate that where a first-order EPT occurs, R will go to zero discontinuously at the transition point).

1.2 Previous Work on Two-dimensional Hard-Core Lattice Gases.

We are now in a position to review previous work on these models, and shall examine the evidence for EPTs and λ-transitions, for regions of the μ-T plane where the Gibbsian distribution is not unique, and for order-disorder transitions.

To provide evidence for the occurrence of EPTs we must resort to the "brute-force" method of attempting to evaluate the grand partition function. For no two-dimensional hard-core model has the grand partition function been found analytically, although there are some rather artificial models which resemble the hard-core lattice gases*. The available approximation methods fall into two classes, "shot-in-the-dark" approximations and systematic approximations. While the former are often useful when considering a single phase, they are unlikely to yield reliable information in the transition region**; however, two systematic approximation methods have proved useful and are now outlined.

(1) Series Expansions.

High- and low-density (or activity) expansions of the grand canonical pressure can be found[1], extrapolation to

* e.g. Fisher's superexchange model[10] and a three-colouring model due to Baxter[11]. It is quite possible however that the transitions found in these models are due to the features by which they differ from the hard-core lattice gases.

** Confirmation of this statement may be found in the diversity of the results obtained by applying different approximations to the case of nearest-neighbour exclusion on the square lattice (see ref. 1 for details and references).

regions near and beyond the radius of convergence of these series being effected by the construction of Padé approximants[12,13] (PAs). Provided enough terms in the relevant series are used it is possible to obtain reliable results even near a transition point. The graph reproduced in fig. 1.2.1 was published by Gaunt and Fisher[1] who applied this technique to the case of nearest-neighbour exclusion on the square lattice.

The drawback to the method is that it is imperative that sufficient terms be used; the Padé approximant technique uses detailed information about the early terms in a series to estimate the effect of later terms, and it is not unknown for the early terms in a series to behave in an apparently regular manner, but one which does not correspond to the correct higher order terms. Two examples may be mentioned to support this point:
(i) Gaunt[2] has studied the case of nearest neighbour exclusion on the triangular lattice and his plot of the PAs for the low- and high-density series is shown in fig. 1.2.2. The lower order PAs suggest a first-order EPT for the model which[2,18] is generally believed to exhibit a continuous transition.
(ii) Bellemans and Fuks[14] used low-density series to estimate the edge tension, γ, in monomer-dimer mixtures on the square lattice. It has been proved[15] that there is no phase transition at finite activity in this model, and consequently analytic continuation of the low-density series to all densities should be permissible. From terms up to ρ^6 PAs were constructed and consistent behaviour obtained. However, at close-packing (the pure dimer case where an analytic result is available), the value of γ/kT is in error by 50%.

(2) Use of the Transfer Matrix.

In this approach, which will be discussed in some detail in the next chapter, lattices of infinite length but of a finite width, M sites, are studied. A matrix $B(z)$ is constructed, thermodynamic quantities deriving from the eigenvalue of maximum modulus and its derivatives. The dimension of the matrix is approximately $e^{\alpha M}$ $(0<\alpha\leq \log 2)$, so for large values of M the eigenvalue problem is impossible, even on a large computer. Nevertheless it is possible to use the matrix method to evaluate to high accuracy the thermodynamic properties of a sequence of $M\times\infty$ lattices, and then to extrapolate to the corresponding properties of the $\infty\times\infty$ lattice. Associated with this extrapolation are two distinct

Table 1.2.1: Previous Work on Two-Dimensional Hard-Core Lattice Gases.

MODEL	WORKER(S)	METHOD USED (SERIES or MATRIX)	TRANSITION PARAMETERS	NATURE OF TRANSITION
SQ1	Gaunt and Fisher[1]	Series (L=13, H=9)	$z=3.80\pm2$, $\rho=0.740\pm8$	Continuous (no λ^*)
	Karayianis, Morrison, and Wortman[16]	Matrix (M=2(2)14)	$z=3.799$, $\rho=0.7356$ (EV)	Continuous (λ)
	Runnels and Combs[17,18]	Matrix (M=6(2)22)	$z=3.86$, $\rho=0.738$ (ref. 17)	Continuous (λ)
			$z=3.80\pm4$, $\rho=0.742$ (C) (ref.18)	Continuous (λ) (RC)
	Ree and Chesnut[23]	Matrix (M=4(2)18)	$z=3.7966\pm3$, $\rho=0.73552$ (EV)	Continuous (λ) (I)
SQ12	Bellemans and Nigam[25]	Series (L=10, H**=2), Matix (M=2(2)12)	$\mu/kT \simeq 4$ $\rho \sim 0.92$	Doubtful
	Ree and Chesnut[24]	Matrix (M=6(2)18)	$\mu/kT=5.3\pm5$, $\rho=0.953\pm2$	3rd. Order EPT
SQ123	Bellemans, Nigam, Orban[25-28]	Matrix (M=5(5)15)	$\mu/kT = 3.7$	1st. Order EPT (I)
SQ1234	Orban[28]	Matrix (M=4(4)20, also M=7 and M=14)	$\mu/kT \simeq 5$	Continuous (doubtful)
SQ12345	Orban[28]	Matrix (M=3(3)21)		No prediction
TR1	Gaunt[2]	Series (L=8,H=5)	$\mu/kT=2.40\pm1$, $\rho=0.832\pm20$	Continuous (λ)
	Runnels and Combs[18]	Matrix (M=6(3)21)	$\mu/kT=2.41\pm1$, $\rho=0.837\pm20$	Continuous (λ) (RC)
TR12	Orban and Bellemans[26,28]	Matrix (M=2(2)14), Series (L=10,H=7)	$\mu/kT=1.750\pm5$	1st. Order EPT (I and RC)
	Runnels, Craig, Streiffer[22]	Matrix (M=4(1)9, and M=10(2)14)	$\mu/kT=1.778$	Probable 1st. Order EPT
TR123	Orban and Bellemans[26,28]	Matrix (M=7,14), Series (L=7,H=3)	$\mu/kT=4.7\pm2$	1st. Order EPT (I)
TR1234	Orban and Bellemans[26,28]	Matrix (M=3(3)15), Series (L=6,H=5)	$\mu/kT=2.90\pm5$	1st. Order EPT (RC)
H1	Runnels, Combs, Salvant[19]	Matrix (M=6(2)18)	$\mu/kT=2.07\pm1$	Continuous (λ) (RC)
DIMERS (square)	Runnels[20]	Matrix (M=4(2)10)		No Phase Transition
	Gaunt[41]	Series (L=~~15~~ 15)		No Phase Transition
DIMERS (triangular)	Gaunt[41]	Series (L=~~15~~ 10)		No Phase Transition
TRIMERS (rectilinear, square lattice)	Van Craen[42]	Matrix (M=2(2)14)		No Phase Transition
	Bellemans and Van Craen[43]	Series (L=7)		No Phase Transition

LEGEND: Model — SQ12 means square-lattice gas with exclusion of first- and second- nearest neighbours.
TR1 means triangular-lattice gas with nearest-neighbour exclusion.
H1 means honeycomb-lattice gas with nearest-neighbour exclusion.
etc.

Method — Matrix (M=2(2)14) ; semi-infinite lattices of width M = 2,4,6,.....14 were studied.
Series (L=13,H=9); L=no. of terms available in the low-activity series, H=no. of terms available in the high-activity series (i.e. terms up to and including z^{-H})

Transition Parameters — we quote μ/kT or z according to whichever was used by the previous worker(s). Where ρ is quoted it is as a fraction of the close-packed density.
(C) and (EV) indicate that the results were obtained from the sequences of maxima in the compressibility and in the ratio of the leading eigenvalues of the matrix respectively.

Nature of Transition — (I) and (RC) indicate that the result was obtained respectively by inspection or by the method of Runnels and Combs.

NOTES: * Gaunt (private communication)has since suggested that this may be a λ-transition.
** The high-activity series is in powers of $z^{-\frac{1}{2}}$; terms up to order z^{-1} have been found.

problems: first locating the value of z at which a phase transition occurs and then determining the nature of the transition. At this point we merely mention that the former problem has been tackled in the past by extrapolating the sequence of maxima in the compressibility or the sequence of maxima in the ratios of leading eigenvalues while the latter problem has been tackled by the method of Runnels and Combs. Details and an assessment of these (and other) methods are given in chapter II; however we quote here one finding, namely that without considerable care the method of Runnels and Combs can erroneously predict a first-order EPT.

The previous work based on the use of series expansions and the transfer matrix is listed in table 1.2.1 and summarised in table 1.2.2

Table 1.2.2: Summary of predictions in table 1.2.1 for square and trianguar lattices.

Exclusion Region	Probable Type of Transition	
	Square Lattice	Triangular Lattice
1	λ	λ
12	3rd order EPT	1st order EPT
123	1st order EPT	1st order EPT
1234	λ	1st order EPT
12345	3rd order EPT (doubtful)	not studied

From this point we shall use the notation of table 1.2.1 to define the various models.

The results for the TR1 and TR12 models are supported by some Monte Carlo calculations of Chesnut[29] who predicted respectively a λ-transition and a first-order EPT for these models. Without practical experience of Monte Carlo methods it is inappropriate for us to comment on these results; there are certainly some unsolved theoretical problems associated with the use of pseudo-random numbers but whether these are serious in practice is uncertain.[30] If the results are valid, the evidence for the first-order transition in the TR12 model is very convincing; for a finite

system with $\mu/kT = 1.66$ the plot of $P(\rho)$, the probability of density ρ, against ρ shows two peaks.

So far we have reviewed the evidence for EPTs and λ-transitions. The state of knowledge with regard to non-uniqueness of Gibbsian distributions and to order-disorder transitions is less untidy. As far as we are aware, only for the SQ1 model has it been proved that for sufficiently large μ there exists more than one Gibbsian distribution. However, for the following models (all the models studied with a unique close-packing configuation) an order-disorder transition has been established*: SQ1, SQ123, TR1, TR12, TR123, TR1234.

1.3 Outline of Present Work.

To sum up the previous section, in all the models with a well-defined unique, close-packed configuration there is little room for doubt that an order-disorder transition is present. The situation as regards EPTs and λ-transitions is less clear; however, the work listed in table 1.2.1 provides evidence for the behaviour listed in table 1.2.2. The irregularity of the predictions in this table is disappointing since the work is largely motivated by the search for models similar to hard spheres and discs; the principal point of interest in this context is the presence or absence of a first-order EPT.

Orban and Bellemans[26] have suggested that the irregularity of the predictions for the square lattice is probably due to the residual degrees of freedom persisting at close-packing in the SQ12, SQ1234, and SQ12345 models, which allow adjacent rows of molecules to slide freely with respect to each other, unlike the triangular lattice where the close-packed configurations are well defined in all cases studied. On both lattices (excluding the case of nearest neighbour exclusion where the hard core may be too small) it is evident that in each case a first-order EPT is predicted when the close-packed configuration is well defined. The first objective of the present work was to test this idea by using the matrix method to establish the nature of the phase transition in the SQ124 model where the close-packing configuration is well defined and thus a first-order EPT should be expected. The work is described in chapter

*We regard the order-disorder transition as "established" if all the coefficients in the low activity (density) expansion of R vanish while the high-activity (density) expansion exists and has an apparently non-zero radius of convergence.

III where it is shown that while preliminary calculations using the method of Runnels and Combs indeed suggested a first-order EPT for the model, the more detailed work predicted no EPT. Having established this result which of course contradicts the idea of Orban and Bellemans, the obvious next step was to re-examine by the same methods a few of the models studied by other workers to see if the transitions given in the two tables were in fact correct. This second part of the work is described in chapter IV.

CHAPTER II.

THERMODYNAMIC PROPERTIES OF Mx∞ AND ∞x∞ LATTICE GASES.

All the numerical methods used in the work are described in this chapter. The first four sections are devoted to a description of the use of the transfer matrix to analyse Mx∞ systems. The method is conceptually very simple and, possibly for this reason, the derivations in the literature tend to lack detail and/or rigour. We thus make no apology for including the rather lengthy derivations in the text. In the next section we consider the extrapolation from results for Mx∞ lattices to those for ∞ x∞ lattices. The methods are then tested on three models, and the chapter concludes with an assessment of the methods on the basis of these tests.

2.1 General Description of the Matrix Method.*

Following Bellemans and Nigam[25] we assume the lattice to be bent in the form of a torus of length N, and circumference, M. We assume that the "hard-core" repulsion causes interaction between the states of q consecutive rings of sites on the torus (e.g. for 1-2-4 exclusion on the square lattice, q=3). Denoting by i,j,....k, permitted configurations on a single ring of M sites, and by ψ_α {i,j,....k}, ψ_β {l,....,r,s}, etc., permitted configurations on (q-1) consecutive rings of sites, we define

$$\epsilon_{\alpha\beta} \equiv \begin{cases} 1 \text{ if } \begin{cases} \text{(i) } \{j,\ldots k\} = \{\ell,\ldots r\} \\ \text{(ii) } i, s, \text{ are compatible when separated by a distance } q \end{cases} \\ 0 \quad \text{otherwise} \end{cases} \qquad (2.1.1)$$

Finally, we define $B_{\alpha\beta} = \epsilon_{\alpha\beta} z^{\nu_\beta}$ where ν_β is the number of molecules on a single ring in state s. Then the grand partition function $\underline{\tilde{\Xi}}(MxN)$ is given by

$$\underline{\tilde{\Xi}}(MxN) = \text{Trace } (B^N) = \sum_i \lambda_i^N \qquad (2.1.2)$$

where $\{\lambda_i\}$ are the eigenvalues of B. The grand canonical pressure, P, is given by

$$P/kT = (MN)^{-1} \log \underline{\tilde{\Xi}}(MxN) \qquad (2.1.3)$$

* This section is based on references 25 and 31.

For a semi-infinite system ($N \to \infty$)

$$P/kT = M^{-1} \log \lambda_1 \tag{2.1.4}$$

where λ_1 is the eigenvalue of maximum modulus of B. To prove (2.1.4), note that

$$(MN)^{-1} \log \underline{\mathcal{H}}(MxN) = M^{-1} \log \lambda_1 + (MN)^{-1} \log R(M,N) \tag{2.1.5}$$

with $R(M,N) = \sum_i \{\lambda_i(M)/\lambda_1(M)\}^N$. Since the dimension of B is less than 2^M, it is immediate that

$$M^{-1} \log R(M,N) < \log 2 \tag{2.1.6}$$

For <u>even</u> N, $R(M,N) > 1$, and result (2.1.4) is trivial.

For <u>odd</u> N, a lower bound may be found for $M^{-1} \log R(M,N)$ by comparing the system with a periodic system of length (N-1) and circumference M. For any permissible configuration, k, of particles on the $(Mx\overline{N-1})$ lattice, a permissible configuration on the (MxN) lattice may be found by inserting an empty column between any two columns of k. Thus $Q(n,M,\overline{N-1}) \leqslant Q(n,M,N)$ where Q(n,M,N), the configurational part of the canonical partition function, is 1/n! times the number of permitted ways of placing n distinguishable particles on the (MxN) lattice. Since $\underline{\mathcal{H}}(MxN) = \sum_n Q(n,M,N) z^n$ with $z>0$, it follows that $\underline{\mathcal{H}}(Mx\overline{N-1}) \leqslant \underline{\mathcal{H}}(MxN)$, and hence that

$$\exp\{\Pi(M).M.(N-1)\}\ R(M,\overline{N-1}) \leqslant \exp\{\Pi(M).M.N\}\ R(M,N) \tag{2.1.7}$$

where $\Pi(M) = M^{-1} \log \lambda_1(M)$. For odd M, we have $R(M,\overline{N-1}) \geqslant 1$ and hence

$$-N^{-1}\Pi(M) \leqslant (NM)^{-1} \log R(M,N) < N^{-1} \log 2 \tag{2.1.8}$$

But $kT\Pi(M)$ is the grand canonical pressure of an $(Mx\infty)$ lattice, regarded as the limit of an (Mx2N) lattice, and so the existence of an upper bound for $\Pi(M)$ is guaranteed (since $1 < \underline{\mathcal{H}}(Nx2M) < \underline{\mathcal{H}}_0(Nx2M)$, where $\underline{\mathcal{H}}_0$ is the grand partition function of a non-interacting lattice gas whose grand canonical pressure can be evaluated directly). It follows that $(NM)^{-1} \log R(M,N) \to 0$ as $M,N \to \infty$. This completes the proof of equation (2.1.4).

Expressions for different thermodynamic quantities may now be found in terms of λ_1 and its derivatives, e.g. the density, ρ.

$$\rho = z \frac{dP}{dz} = \frac{z}{M\lambda_1} \cdot \frac{d\lambda_1}{dz} \tag{2.1.9}$$

The derivatives of λ_1 may be found from the other eigenvalues and eigenvectors of B. Let $\{x_i\}$, $\{y_i\}$, be the sets of right and left eigenvectors of B. Then denoting by B' and by B'' respectively the matrices with $(i,j)^{th}$ elements dB_{ij}/dz and d^2B_{ij}/dz^2, we find from arguments similar to those of Wilkinson*

$$\frac{d\lambda_1}{dz} = \frac{(y_1, B' x_1)}{(y_1, x_1)} \tag{2.1.10}$$

and

$$\frac{d^2\lambda_1}{dz^2} = \frac{1}{(y_1, x_1)} \left\{ (y_1, B'' x_1) + 2 \sum_{j \neq 1} \frac{(y_j, B' x_1)(y_1, B' x_j)}{(\lambda_1 - \lambda_j)(y_j, x_j)} \right\} \tag{2.1.11}$$

<u>provided B is not defective</u> (i.e. provided B possesses a complete set of left and right eigenvectors).

2.2 Symmetry Considerations.**

The rows and columns of the matrix, B, defined in the previous section are labelled by $\{\psi_\alpha\}$, the set of allowed configurations on (q-1) consecutive rings of M sites. Suppose that the sites of these rings are permuted by an operation of S_M, the symmetric group on M objects. Then it is possible that for some operations of S_M, each allowed state is changed into another allowed state. Let H be a collection of such operations and consider the special case where H is a subgroup of S_M. Given $h \in H$, we denote by P(h) the corresponding operation on the set of allowed configurations, $\{\psi_\alpha\}$, and write $\psi_\beta = P(h)\psi_\alpha$ if the effect of a permutation, h, of the M lattice sites is to change configuration ψ_α to ψ_β. We define a binary relation E on $\{\psi_\alpha\}$ by $\psi_\alpha E \psi_\beta$ if and only if there exists $h \in H$ such that $\psi_\alpha = P(h)\psi_\beta$. It is trivial to prove that E is an equivalence relation on $\{\psi_\alpha\}$ and hence[33] that E splits $\{\psi_\alpha\}$ into a set of disjoint equivalence classes, K_1, K_2, K_3, ... We now call H an admissible subgroup if, for all pairs of equivalence classes, K_i, K_j:

$$L_{\alpha j} \equiv \sum_{\psi_\beta \in K_j} B_{\alpha\beta} \quad \text{is independent of the state } \psi_\alpha \text{ of } K_i \tag{2.2.1}$$

The interpretation of (2.2.1) becomes clearer if we note that

$$L_{\alpha j} \equiv \sum_{\psi_\beta \in K_j} B_{\alpha\beta} = \sum_{\psi_\beta \in K_j} \varepsilon_{\alpha\beta} z^{\nu_\beta} = z^{\nu_\beta} \sum_{\psi_\beta \in K_j} \varepsilon_{\alpha\beta} \tag{2.2.2}$$

* Chapter 2 of reference 32.

**Based on references 18 and 19.

Thus $L_{\alpha j}$ is just z^{v_β} times the number of states in K_j which are compatible (in the sense of equation (2.1.1)) with a representative state $\psi_\alpha \in K_i$: the requirement is that $L_{\alpha j}$ be independent of this representative state. Finally we define <u>the</u> symmetry group, G, of a particular model to be the maximal admissible subgroup, H.

The states $\{\psi_\alpha\}$ form a basis for a representation, Γ, of G, since every operation, P(g): $g \in G$, changes ψ_α into another allowed configuration. However, Γ is in general reducible, and it is easily proved that $\sigma(M)$, the number of equivalence classes K , is equal to the number of times the symmetric representation, A , occurs in the decomposition of Γ into the direct sum of irreducible representations (IRs) of G. (A is the IR with $A_1(g) = 1$ for all $g \in G$). Moreover, if V is the vector space on which the transfer matrix operates, and x is an arbitrary vector in V, then x belongs to A if and only if $\psi_\alpha \equiv \psi_\beta \Rightarrow x_\alpha = x_\beta$.

In section 2.1 it was proved that the thermodynamic properties of the system derive from λ_1, the maximum eigenvalue of B. Suppose we could prove that x, the corresponding right eigenvector of B belongs to A_1 ; then denoting by d(M) the dimension of B, the eigenvalue equation $Bx = \lambda_1 x$, written out in full becomes

$$\sum_{\beta=1}^{d(M)} B_{\alpha\beta} x_\beta = \lambda_1 x_\alpha \qquad \alpha = 1, 2, \ldots\ldots, d(M) \tag{2.2.3}$$

When $x_\alpha = x_\beta$ $(= x_i)$ for α, β, in the same class K_i, equation 2.2.3 becomes

$$\sum_{\{K_i\}} \sum_{\psi_\beta \in K_i} B_{\alpha\beta} = \lambda_1 x_\alpha \tag{2.2.4}$$

But from (2.2.1), $\sum_{\psi_\beta \in K_i} B_{\alpha\beta}$ is independent of the choice of α from its class, j say. So if we set

$$P_{ji} = \sum_{\psi_\beta \in K_i} B_{\alpha\beta} \tag{2.2.5}$$

then

$$\sum_{\{K_i\}} P_{ji} x_i = \lambda_1 x_j \tag{2.2.6}$$

i.e. λ_1 is an eigenvalue of the <u>reduced matrix</u> P defined by (2.2.5), a matrix of dimension $\sigma(M)$.

To justify the use of the reduced matrix, it remains to show that if $\psi_i \equiv \psi_j$, then $x_i = x_j$, i.e. that x belongs to A . The remainder

of this section is devoted to a proof of this result. The proof is in five parts.

(1) It is possible to identify each eigenvalue of B with one of the IRs of G (in the same way that quantum mechanical states may be identified with IRs of the group of the Schrödinger equation). This is immediate if B commutes* with T where T is a matrix representing the rearrangement of states arising when the sites are permuted by an operation of G (e.g. for a permutation which switches states 1 and 2 but leaves the rest unchanged

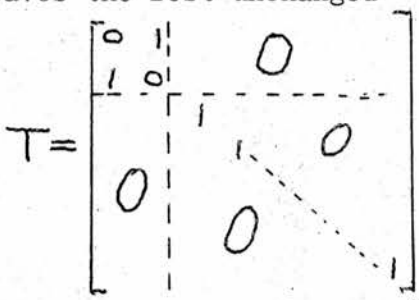

(2) The matrix B is irreducible.** This result is an immediate consequence of the definition of an irreducible matrix. The concept of an irreducible matrix is clarified by the following theorem[34]:

If the directed graph of a matrix, A, of order $n \times n$, is a set of n points $p_1, p_2, \ldots\ldots p_n$ with a directed line joining p_i to p_j when the matrix element $A_{ij} \neq 0$, then A is irreducible if and only if there is a path from any p_i to any p_j in the directed graph.

Now let $\psi_k = \{i,j,\ldots\ldots k\}, \psi_\beta = \{1,\ldots\ldots,r,s\}$ as in section 2.1, and consider the sequence of states:

*Usually B will commute with T. However, it occasionally happens (e.g. in the H1 model[19]) that due to the choice of boundary conditions, T does not commute with B but does commute with the matrix B obtained from B by some rearrangement of the columns corresponding to different configurations within given classes. The present argument is now valid for the matrix B and in all cases encountered it has been possible to show that B and B have the same maximum eigenvalue.

**It is unfortunate that the word "irreducible" appears in the theory with applied to both matrices and the representations of the group, G. A matrix, A, is irreducible if there is a permutation matrix, S, such that

$$S^T A S = \begin{bmatrix} C & E \\ 0 & D \end{bmatrix}$$

where C,D, are square matrices. Otherwise it is irreducible. The matrix B can of course be decomposed to this form by similarity transformations with matrices other than permutation matrices (e.g. the decomposition being derived in this section!).

$\psi_\alpha \equiv \psi_1 = \{i, j, \ldots\ldots, k\}$
$\psi_2 = \{j, \ldots\ldots, k, 0\}$ where 0 denotes the empty state on a single ring.
$\psi_3 = \{\ldots\ldots k, 0, 0\}$

$\psi_\ell = \{a, 0, \ldots\ldots 0\}$
$\psi_{\ell+1} = \{0, 0, \ldots\ldots \ell\}$

$\psi_{2^{n-1}} = \{\ell, \ldots\ldots i, j, s\} \equiv \psi_\beta$

Clearly there is a directed line from the point representing ψ_ℓ to that representing $\psi_{\ell+1}$ to that representing $\psi_{\ell+1}$ in the above sequence. Thus there is a path from the point representing <u>any</u> state ψ_α to <u>any</u> state ψ_β. Hence B is irreducible.

<u>(3) λ_1 is a simple eigenvalue of B.</u> This is a direct consequence of the Perron-Frobenius theorem which applies to irreducible, non-negative matrices.

<u>(4) λ_1 is an analytic function of z.</u> From (3) λ_1 is a simple eigenvalue of B and thus a simple root of a polynomial of the form:

$$f(\lambda, z) = \lambda^n + P_{n-1}(z)\lambda^{n-1} + \ldots\ldots\ldots + P_0(z) \qquad (z \geq 0)$$

It follows* that λ_1 is an analytic function of z in a region of the complex ~~plain~~ plane enclosing the positive real axis.

(5) For z 0, λ_1 belongs to A_ℓ. But we have just shown that λ_1 is an analytic function on and around the positive, real z-axis. <u>Thus λ_1 belongs to A_ℓ for all z.</u>

2.3 Zero eigenvalues.**

The problem here is best illustrated with an example. Consider the SQ124 model with M=4. The reduced matrix, P, is

$$P = \begin{bmatrix} 1 & 4z & 2z^2 & 0 & 0 \\ 0 & 0 & 0 & 1 & 0 \\ 0 & 0 & 0 & 0 & 1 \\ 1 & 2z & z^2 & 0 & 0 \\ 1 & 2z & z^2 & 0 & 0 \end{bmatrix} \qquad (2.3.1)$$

The characteristic equation of P is

$$c(\lambda) \equiv \lambda^2(-\lambda^3 + \lambda^2 + (2z + z^2)\lambda + (2z + z^2)) = 0 \qquad (2.3.2)$$

* See e.g. reference 32, page 65, theorem 1.

**The method derived in this section is based on a suggestion of Dr. P. Keast.

It is not difficult to show that the elementary divisors of P are $\lambda^2, (\lambda_1 - \lambda), (\lambda_2 - \lambda), (\lambda_3 - \lambda)$ where λ_1, λ_2, λ_3 are the roots of $-\lambda^3 + \lambda^2 + (2z + z^2)\lambda + (2z + z^2) = 0$. Note the non-linear elementary divisor λ^2, due to the matrix P being defective. Thus equation (2.1.11) is not valid for the matrix P. Clearly it would be desirable to find a 3x3 matrix with elementary divisors $(\lambda_1 - \lambda), (\lambda_2 - \lambda), (\lambda_3 - \lambda)$. More generally the problem may be stated as follows:

Given an nxn matrix P of rank r with a zero eigenvalue of multiplicity p (p not necessarily equal to n-r), can we convert P to the form $P \oplus \underset{\sim}{0}$ by a sequence of similarity transformations, where P is an $\overline{n-p} \times \overline{n-p}$ matrix and $\underset{\sim}{0}$ is the p×p matrix of zeros?

Method: Let $\{r_i\}$, i=1,2,.....n be the rows of P. There is a relation between the rows, $\sum \alpha_i r_i = 0$ with (say) $\alpha_k = 1$. Consider a similarity transformation with a matrix H defined by

$$H = \begin{bmatrix} 1 & & & & & & \\ & 1 & & & & & \\ & & \ddots & & & & \\ & & & 0 & & & \\ & & & & \ddots & & \\ & & & & & 1 & \\ -\alpha_1 & -\alpha_2 & \cdots & -\alpha_{k-1} & -\alpha_{k+1} & \cdots & 0 \end{bmatrix} \leftarrow k^{th} \text{ row} \qquad (2.3.3)$$

Then

$$H^{-1} = \begin{bmatrix} 1 & & & & & & \\ & 1 & & & & & \\ & & \ddots & & & & \\ & & & 0 & & & \\ & & & & \ddots & & \\ & & & & & 1 & \\ +\alpha_1 & +\alpha_2 & \cdots & +\alpha_{k-1} & +\alpha_{k+1} & \cdots & 0 \end{bmatrix} \leftarrow k^{th} \text{ row} \qquad (2.3.4)$$

It is easy to prove by direct evaluation that $H^{-1}PH$ has its k'th row and column consisting entirely of zeros and that

$$\det (P - \lambda I) = \lambda \det (P' - \lambda I) \qquad (2.3.5)$$

where P' is the $\overline{n-1}$ $\overline{n-1}$ matrix obtained by deleting the null rows of $H^{-1}PH$, i.e.

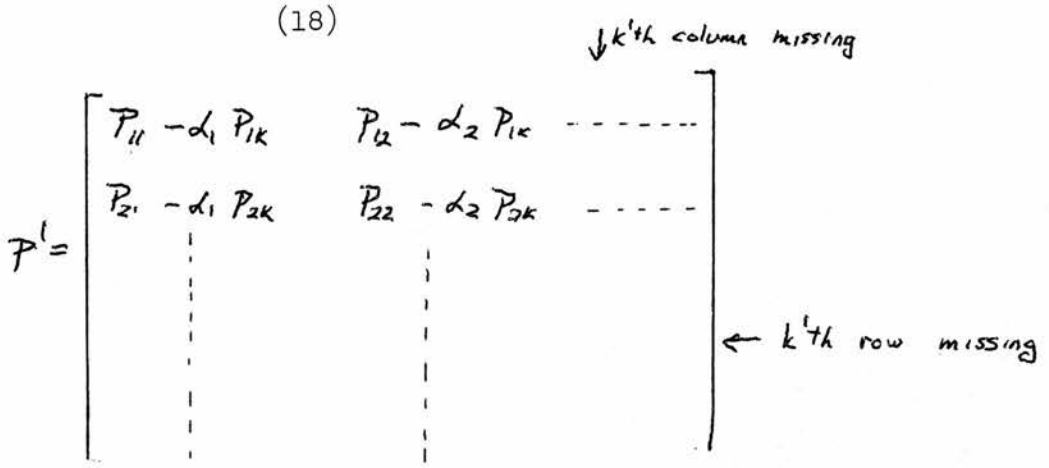

If P' is singular, the process is repeated till a non-singular matrix, P_1, is obtained The process is then complete and P has been transformed to the form $P_1 \oplus \underset{\sim}{0}$. As an example, consider P given by equation (2.3.1). Here n=5, p=2, r=4. Successive transformations yield the matrices

$$\begin{bmatrix} 1 & 4z & 2z^2 & 0 \\ 0 & 0 & 0 & 1 \\ 0 & 0 & 0 & 1 \\ 1 & 2z & z^2 & 0 \end{bmatrix} \quad \text{and then} \quad \begin{bmatrix} 1 & 4z+2z^2 & 0 \\ 0 & 0 & 1 \\ 1 & 2z+z^2 & 0 \end{bmatrix}$$

This method is particularly useful for two reasons:
(a) We are concerned with matrices P of the form SD(z) where S is a constant matrix and and D(z) is a diagonal matrix with elements dependent on the activity, z. The method of reduction uses purely <u>row</u> relations of P which are independent of z, and thus the matrices H need be found only once (for a given value of M).
(b) A second consequence of H being independent of z is that if $H^{-1}PH = P_1 \oplus \underset{\sim}{0}$, then $H^{-1}P'H = P_1' \oplus \underset{\sim}{0}$ and $H^{-1}P''H = P_1'' \oplus \underset{\sim}{0}$, where the dashes denote differentiation with respect to z. Thus it is a simple matter to apply formula (2.1.10) and (2.1.11) to the matrices reduced by this method.

2.4 Numerical Analysis of M×∞ Lattices.

The first step is to construct the matrix P using the prescription of (2.2.5). The program used was extremely unsubtle; it was written in FORTRAN IV and followed roughly the procedure of Ree and Chesnut.[23] The

configurations were manipulated in arrays of half-length (2 byte) integers but were stored as bit strings. Access to the configurations was by two ASSEMBLER language subroutines written by Dr. R. Erskine. The matrix S (see previous section) was kept on cards or on disk* together with the set $\{\lambda_s : s=1,2,\ldots\sigma(M)\}$.

Satisfactory checking of the matrix elements obtained is difficult though the values of d(M) and $\sigma(M)$ may be checked, d(M) is given by a simple recurrence relation** while $\sigma(M)$ obeys $\sum_{i=1}^{\sigma(M)} \omega_i = d(M)$, ω_i being the number of equivalent configurations in the equivalence class K_i. In addition, for some models $\sigma(M)$ may be derived from the Polya theorem.** However, to check the matrix elements themselves, it is usually necessary to construct the lower-order matrices by hand, taking care in cases where there is dihedral symmetry to cover cases where M is sufficiently large for reflections to introduce new inequivalent configurations to some equivalence classes.

To deal with the eigen-problem, three procedures were used involving the programs MNMINI, MNMAXI, and MNEIGM.

(a) MNMINI

The maximum eigenvalue of P was found by the power method[32] for each value of z; ρ and $d\rho/d\mu$ then followed by numerical differentiation. The convergence of the power method is controlled by the ratios of the other eigenvalues to λ_1, being slow if $|\lambda_i/\lambda_1|$ approaches unity for any i. Where long-range order is present in hard-core models, we frequently have an eigenvalue $\lambda_2 \sim -\lambda_1$ and where a phase transition occurs there must[35] be eigenvalues asymptotically equal to λ_1. Thus convergence is slow in regions of interest and we can show that no shift of origin[32] will help substantially. The convergence can be accelerated by using a device of Orban[28] based on the standard method for locating complex conjugate pairs of eigenvalues,[32] but this procedure was not used in the present work. Rather, MNMINI used the simplest version of the power method; it was easy to write and its principal purpose was to aid the debugging of MNMAXI.

*Resorting to the use of cards was a reaction to some trouble with the direct access input/output routines. In the end two decks were kept for all the larger matrices after a hungry card reader devoured part of the SQ124, M=14 matrix!

**See appendix III.

(b) MNMAXI.

The method of section 2.3 is used to deflate* the matrix, P, if it possesses any zero eigenvalues. The eigenvalues and right eigenvectors of P (or P_1) are then found by a subroutine[36] which uses the QR double-step process and inverse iteration. The subroutine is then used on the transpose, P^T, of P (or P_1) to yield the left eigenvectors. This also gives a (poor) test of the stability of the eigenvalues since a matrix and its transpose have the same eigenvalues.** The pressure, density, and compressibility now follow from λ_1 and its first and second derivatives computed according to equations (2.1.10) and (2.1.11).

MNMAXI proved very reliable when used on smaller matrices, but has the following disadvantages when used on large matrices:

(i) The property of sparseness (possession of a high proportion of zero matrix elements) is not exploited either to save execution time or reduce the storage space required.

(ii) All the right and left eigenvectors are required to compute the compressibility exactly, while to compute the density only the eigenvectors corresponding to λ_1 are required. However, the large number of arithmetic operations required to evaluate $d\rho/d\mu$ from (2.1.11) leads to a substantial rounding error in the compressibility, and it turns out that for the larger matrices the extra computer time is spent obtaining a result no better than would be obtained from numerical differentiation of the density.

(iii) The subroutine of Grad and Brebner[36] is complex (750 FORTRAN cards) and, as written, requires having three arrays of the size of the original matrix in core at one time. This limits the matrices to a final dimension of about 50 on the St. Andrews machine, the complexity of the subroutine precluding the use of external disk storage.

(c) MNEIGM.

Here we use an algorithm due to Bender and Shavitt[37] appropriate to large, sparse, non-symmetric matrices. We have introduced a device which accelerates the convergence substantially (see appendix II). The non-zero elements of the matrix are stored on disk; this is not excessively inefficient as the algorithm only requires access to each row once per iteration. The maximum eigenvalue is found together with the corresponding right and left eigenvectors, thus yielding the density exactly.

*i.e. reduce to a matrix P of dimension $\overline{n-p}$, where p is the number of zero eigenvalues.

**Equality of the eigenvalues obtained from P and P^T is not a good test of their accuracy (see ref.38)

Derivatives of the density are found numerically. To a purist this algorithm is unsatisfactory as there is no rigorous proof that the eigenvalue found is in fact the largest. However, in practice for a given model it is possible to use MNMAXI to check all results on the smaller matrices; a check on the larger matrices is provided by the requirement that for fixed z the sequence of density values behaves regularly with M.

2.5 Deductions about $\infty \times \infty$ Lattices.

Suppose that one of the above programs has yielded, for each value of M, a table of values of P/kT, ρ, and $d\rho/d\mu$ for given values of u $(=z/(1+z))$; we use u rather than z as independent variable since the range $(0,\infty)$ in z corresponds to (0,1) in u. There remains the problem of locating and determining the nature of any phase transition.

Location of any Phase Transition.

We now describe three methods which are useful for models with a first-order EPT or a λ-transition.

(a) Maximum in $d\rho/d\mu$.

For each value of M we estimate the point $u_0(M)$ at which $d\rho/d\mu$ has its maximum value by constructing a parabola through the three points nearest the maximum. It is often difficult to achieve high accuracy in $u_0(M)$; nevertheless the sequence of values obtained can give an approximate value for the transition point, u_c.

(b) Maximum in $|\lambda_2/\lambda_1|$.

At a phase transition λ_1 must be asymptotically degenerate (as $M \to \infty$); thus it is reasonable to find a sequence of values, $u_{EV}(M)$ at which $|\lambda_2/\lambda_1|$ has a maximum. The method has been applied to the SQ1 model[16,23] where the maximum proved very sharp and led to a very accurate estimate of u_c. The drawback is of course that it is necessary to compute λ_2; this was not possible with MNEIGM and thus we could not use the method on matrices of dimension greater than about fifty.

(c) Intersection Method.

Suppose we have isotherms for a sequence of M values, the interval in M being ΔM. To locate the transition point we exploit a readily observed feature of the isotherms, present in many of the models studied. Comparison of the plots of ρ against u for lattices of width M and M+ ΔM reveals an intersection point, $u_I(M)$ with the property that for $u \gtrsim u_I(M)$, $\rho(M,u) \lesssim \rho(M+\Delta M,u)$. The point $u_I(M)$ may be determined to high accuracy by using Aitken's Process[39] to locate a zero of the function $\rho(M,u) - \rho(M+\Delta M,u)$. Extrapolation of the sequence $\{u_I(M)\}$ to infinity then gives the transition point, u_t.

Nature of any Phase Transition.

In the context of the present work, the primary problem is to decide whether any observed transition is first-order; we discuss three approaches to the problem.

(a) Method of Runnels and Combs.[18]

By numerical differentiation of $d\rho/d\mu$ we estimate $d^2\rho/d\mu^2$ at the table points for each value of M. The positions $u_1(M)$ and $u_2(M)$ of the maximum and minimum values of $d^2\rho/d\mu^2$ are found, again by fitting parabolas to the three nearest table points, and the corresponding densities $\rho_1(M)$ and $\rho_2(M)$ determined. In addition we examine the sequence of maximum values of $d\rho/d\mu$ to see if this quantity diverges at u_t. It is evident that if the sequences $\{\rho_1(M)\}$ and $\{\rho_2(M)\}$ have different limits and if $d\rho/d\mu$ diverges at u_t, then the system has a first-order EPT. A consistency test is provided by the requirement that both the sequences $\{u_1(M)\}$ and $\{u_2(M)\}$ should have a limit equal to u_t. The method of Runnels and Combs has, a priori, two principal defects:

(i) The justification of the method relies on showing that $(d\rho/d\mu)_{max}$ diverges as $M \to \infty$. When this divergence is slow (e.g. logarithmic with M), this may be difficult to demonstrate convincingly if the number of points available is small.

(ii) The sequences to be extrapolated are not obtained to high accuracy, being estimates of maxima or minima in a table which itself is found by twice carrying out a numerical differentiation.

Thus the chances of estimating a limit for the sequences must be regarded as poor; moreover an error in estimating the limit of one of the sequences will lead to an erroneous prediction of a first-order EPT. A good example is the TR1 model where Runnels and Combs[18] quoted a sequence of values of $\rho_2(M)$; from a plot of $\rho_2(M)$ against $M^{-\frac{3}{4}}$ they obtain a limit of 0.837 ± 0.02 whereas a good fit is also obtained by assuming $\rho_2(M) = A + B\lambda^M$ ($\lambda < 1$) with $A = 0.852$.

(b) Intersection Method.

Whatever the numerical difficulties, there is considerable appeal in the basic idea behind the previous method, namely, to find sequences $\{u_1(M)\}$ and $\{u_2(M)\}$ with limits u_t^- and u_t^+ respectively, and then to examine the corresponding sequences of densities. It is thus natural to try and find two such sequences with limits u_t^- and u_t^+, but more tractable numerically than those of maxima and minima in $d^2\rho/d\mu^2$. This is possible in some cases by exploiting another "intersection property". If the plot of $d\rho/d\mu$ against u for successive values of M takes the form of fig. 2.5.1 then the sequences $\{u_{I1}(M)\}$ and $\{u_{I2}(M)\}$ (defined in fig. 2.5.1) may be expected to approach u_t from below and above. If $\rho_{I1}^{M}(M)$ and $\rho_{I1}^{M+\Delta M}(M)$ are the densities of the lattice gases of width M and M+ ΔM evaluated at $u_{I1}(M)$, and $\rho_{I2}^{M}(M)$ and $\rho_{I2}^{M+\Delta M}(M)$ are similarly defined, then for a first-order EPT we must have as $M \to \infty$:

$$\left(d\rho/d\mu\right)_{max} \longrightarrow \infty \qquad (2.5.1)$$

$$u_{I1}(M) \longrightarrow u_t^- \qquad (2.5.2)$$

$$u_{I2}(M) \longrightarrow u_t^+ \qquad (2.5.3)$$

$$\rho_{I1}^{M}(M) \text{ and } \rho_{I1}^{M+\Delta M}(M) \longrightarrow \text{equal limits } \rho_{I1} \qquad (2.5.4)$$

$$\rho_{I2}^{M}(M) \text{ and } \rho_{I2}^{M+\Delta M}(M) \longrightarrow \text{equal limits } \rho_{I2} \qquad (2.5.5)$$

$$\rho_{I1} \neq \rho_{I2} \qquad (2.5.6)$$

(c) Exact Isotherm for the $\infty \times \infty$ Lattice.

For each value of u we have a sequence of values of P/kT and of ρ, and we extrapolate to the limits of each sequence by two totally independent methods: by accelerating convergence using the e_1 transform[40] and by considering P/kT and ρ as functions of M^{-1} and extrapolating to $M^{-1}=0$. In the absence of prior information on the limiting process we accept a numerical estimate of the limit if it is independent of the method used. As a further check we

differentiate numerically the results for P/kT at each value of u and test for consistency with the values of ρ obtained by direct extrapolation of the sequences $\{\rho(M)\}$. The nature of any phase transition follows by inspecting the isotherm of the infinite lattice.

2.6 Tests of the Methods.

The methods described in the previous sections have been tested on three models: the superexchange model, a square-lattice gas with an attractive potential between nearest neighbour sites, and the square-lattice gas with nearest neighbour exclusion.

(a) Superexchange Model.

This is a non-trivial model for which, at one temperature, an exact isotherm has been calculated by Fisher.[10] The particles are on a square lattice, the potential consisting of nearest-neighbour exclusion plus an attractive potential, V_0, which extends only across alternate squares, those joined by dotted lines in fig.2.6.1.

At one temperature, $T=V_0/k.\log 2$, Fisher[10] has derived the equation of state analytically. The model has a λ-transition at $z_+ = \frac{1}{2}(1+\sqrt{2})$, i.e. at $u = 0.54692$. The model is thus very suitable for testing the methods of section 2.5; not only can we test the estimates of the location and nature of the transition but in addition the result of direct extrapolation to the isotherm of the $\infty\times\infty$ lattice may be compared with the exact isotherm.

To apply the matrix method we first impose periodic boundary conditions in the vertical direction and then distort the lattice by twisting each vertical ring by one lattice site relative to the ring on its left. Fig. 2.6.1 then takes the form shown in fig.2.6.2. This twisting of the lattice permits the transfer matrix to be defined in terms of the interaction between single, rather than double, rings of M sites, and the dimension of the transfer matrix is consequently reduced. Some care is required in determining the symmetry group, G, for the model; it turns out to be the group of rotations by multiples of $4\pi/M$ together with the combinations of such rotations with a reflection in the axis $00'$ of fig. 2.6.2.* (That G is not the cyclic group C_M is demonstrated by

*This group should be carefully distinguished from the dihedral group, $D_{M/2}$ which occurs in the H1 model.[19]

considering the matrix elements for M=10 between configurations of the type (1010010000) and (1010000000)).

The sequence $\{u_0(M)\}$ of locations of maxima in dp/du is shown in table 2.6.1 and suggests $u_t = 0.545 \pm 0.005$. The intersection method gave a sequence $\{u_I(M)\}$ in which $u_I(M)$ was constant for all M studied. The value of u_t obtained from the intersection method was $u_t = 0.5469$, in agreement with the exact value.

Table 2.6.1: Locations of maxima in dp/du for the superexchange model. (The accuracy of the points $u_0(M)$ is uncertain)

M	$u_0(M)$
4	0.46774
6	0.50784
8	0.52348
10	0.53106
12	0.53549
∞	0.545 ± 0.005

All three methods of determining the nature of the phase transition were tried:

Method of Runnels and Combs

In table 2.6.2 are displayed the various sequences:

M	$u_1(M)$	$\rho_1(M)$	$u_2(M)$	$\rho_2(M)$
4	...*	...*	0.65720	0.40987
6	...*	...*	0.63407	0.40502
8	0.44750	0.28462	0.61901	0.40032
10	0.47065	...**	0.60538	0.39443
12	0.48284	0.30421	0.59839	0.39147
∞	EXTRAPOLATION NOT POSSIBLE			

Table 2.6.2: Application of the method of Runnels and Combs to the Superexchange model.

* Not in range 0.41 - 0.70.
**Not computed because of a numerical quirk of the data not considered worth repeating.

It is evidently impossible to obtain accurate limits by numerical methods in view of the small number of points (for u_1 and ρ_1), the low accuracy of the points obtained, and the obviously slow convergence. In figs. 2.6.3 and 2.6.4 the sequences are plotted as functions of M^{-1}; in so far as such graphs may be trusted, the conclusion from them (taken with the apparent logarithmic divergence of $(d\rho/d\mu)_{max}$ — see fig. 2.6.5) is that there is either a continuous transition or a very weak first-order EPT.

Intersection Method.

This method fails completely in the absence of results for M greater than 12. For $M=4$ the compressibility peak has not yet become well defined and consequently any conclusions must come from extrapolating sequences of three points, which is a meaningless exercise*.

Exact Isotherm for the $\infty\times\infty$ Lattice.

The sequences of density values for a given u tended to converge fast over most of the density range. Extrapolation by the use of the e_1 transform yielded internal consistency at all points studied, but it was not possible to perform a satisfactory extrapolation when the sequences were treated as functions of M^{-1} and Aitken's process used to find the value at $M^{-1}=0$. We have tabulated the extrapolated values of ρ from the use of the e_1 transform and for comparison the known exact values of ρ from Fisher's exact formula[10].

$$\rho = \tfrac{1}{4}(1 - e^{-4K'})(1 + \omega_1(K')) \qquad (2.6.1)$$

$$\text{where } \omega_1(x) = \tfrac{1}{2}\coth(2x)\left\{1 + (2/\pi)k_1''K(k_1)\right\} \qquad (2.6.2)$$

$$k_1(x) = 2\tanh(2x)/\operatorname{ccsh}(2x) \qquad (2.6.3)$$

$$k_1''(x) = 2\tanh^2(2x) - 1 \qquad (2.6.4)$$

$$e^{4K'} = 1 + 4z \qquad (2.6.5)$$

and $K(k_1)$ is the complete elliptic integral**

$$K(k_1) = \int_0^{\pi/2} (1 - k_1^2\sin^2\phi\ )^{-\frac{1}{2}}d\phi \qquad (2.6.6)$$

* though not an unpractised one — see ref. 26, fig.9!

**Note that this definition of $K(k_1)$, apparently used by Fisher[10] who followed the notation of Onsager (ref.44) is different from that in the National Bureau of Standards "Handbook of Mathematical Functions" which defines (page 590):

$$K(m) = \int_0^{\pi/2} (1 - m\sin^2\phi\ )^{-\frac{1}{2}}d\phi$$

In spite of the fact that the extrapolations were, according to our criteria, doubtful, the agreement between them and the exact results is very encouraging.

Table 2.6.3: Superexchange Model — comparison with the known exact results of values of density obtained by extrapolation from values for $M \times \infty$ lattices.

u	ρ (from extrapolation)	ρ (exact)
0.41	0.2587	0.2587
0.42	0.2641	0.2641
0.43	0.2696	0.2695
0.44	0.275	0.2751
0.45	0.281	0.2808
0.46	0.287	0.2866
0.47	0.293	0.2926
0.48	0.299	0.2987
0.49	0.305	0.3052
0.50	0.312	0.3119
0.51	0.320	0.3190
0.52	0.328	0.3266
0.53	0.337	0.3350
0.54	0.346	0.3446
0.55	0.357	0.3580
0.56	0.366	0.3680
0.57	0.375	0.3768
0.58	0.383	0.3841
0.59	0.390	0.3906
0.60	0.396	0.3967
0.61	0.402	0.4022
0.62	0.407	0.4074
0.63	0.412	0.4122
0.64	0.417	0.4168
0.65	0.421	0.4211
0.66	0.4251	0.4252
0.67	0.4290	0.4291
0.68	0.4327	0.4327
0.69	0.4362	0.4363
0.70	0.4396	0.4396

(b) Square-Lattice Gas with Nearest-Neighbour Attraction.

As all the present work is directed towards determining whether or not certain models have a first-order EPT., we have tested the methods described in the previous sections on the square-lattice gas with an attractive potential, $-V_0$, extending only to nearest-neighbour sites. This model is mathematically equivalent to the spin-$\frac{1}{2}$ Ising Model in a magnetic field for which no analytic solution is available[45], but the transition point, u_t, in the lattice gas corresponds to the case of zero magnetic field in the Ising model, allowing us to obtain the transition parameters from the results of Onsager[44] and Yang[46] for the free energy and spontaneous magnetisation respectively. Setting $\xi = e^{V_0/kT}$, we have chosen to study the case $\xi = 6$ for which we should observe a strong first-order EPT. The transition occurs at $u_t = 0.027027$ with a density jump from $\rho = 0.136286$ to $\rho = 0.863714$.

MNMAXI was used to obtain results for lattices of width $M = 2,3,....8$ with u running from 0.0261 to 0.0280 in intervals of 0.0001. The $M\times\infty$ lattices studied were oriented at 45°; however the reason for this arose from other work being performed concurrently and need not concern us here.

The transition in this model was very easily located: studying the sequence of maxima in $d\rho/d\mu$ gave $u_t = 0.027025 \pm 0.000005$ while the intersection method gave $u = 0.027027 \pm 0.000001$. In both cases the extrapolation was trivial as both $u_o(M)$ and $u_I(M)$ are independent of M.

To determine the nature of the transition, we used the three methods of section (2.5):

Method of Runnels and Combs.

We first noted that $(d\rho/d\mu)_{max}$ diverges very fast with M. We have plotted $(d\rho/d\mu)_{max}$ and $\log(d\rho/d\mu)_{max}$ against log M (figs. 2.6.6 and 2.6.7); the former graph showed that the divergence was faster than logarithmic, indeed the latter suggested that $(d\rho/d\mu)_{max} \sim M^{\alpha}$ with $1.8 < \alpha < 1.9$. Plots of $\rho_1(M)$ and $\rho_2(M)$ are shown in fig. 2.6.8; while it is not possible to extrapolate to $M^{-1}=0$ it is obvious that the sequences are tending to unequal limits. The consistency check is that $\{u_1(M)\}$ and $\{u_2(M)\}$ should tend to $u_t = 0.027027$ and in fig. 2.6.9 these quantities are plotted against M^{-1}. From the graph all that we can say is that the plots are not inconsistent with limits around 0.027. To sum up, the method of Runnels and Combs gives strong indications of a

first-order EPT, but leaves the values of ρ_1 and ρ_2 undetermined.

Exact Isotherm for the $\infty \times \infty$ Lattice .

The isotherm obtained from the extrapolation is shown in fig. 2.6.10. For every point shown, the results of numerical differentiation of the pressure are consistent with the values obtained for the density. While one can never by this method exclude the possibility of a very sharp continuous transition, the graph suggests strongly a first-order EPT with a density discontinuity from $\rho = 0.12$ to $\rho = 0.88$.

Intersection Method.

The sequences are given below in table 2.6.4:

Table 2.6.4: Lattice Gas with Attraction — Intersection Method for Nature of Transition.

M	$u_{I1}(M)$	$\rho_{I1}^{M}(M)$	$\rho_{I1}^{M+1}(M)$	$u_{I2}(M)$	$\rho_{I2}^{M}(M)$	$\rho_{I2}^{M+1}(M)$
3	0.02643	0.2957	0.2091	0.02764	0.7051	0.7917
4	0.02666	0.2906	0.2231	0.02740	0.7098	0.7773
5	0.0267	0.242	0.189	0.0273	0.726	0.782
6	0.0268	0.246	0.201	0.0272	0.709	0.756
7	0.026(9)	0.291	0.250	0.0272	0.756	0.795
∞	0.027	...	...	0.027	...	...

The entries in the table are very inaccurate as may be seen from the fact that we would expect $\rho_{I1}^{M}(M) + \rho_{I2}^{M}(M) = 1$ and a similar result for ρ_{I2}^{M+1}. This inaccuracy is due to inaccuracy in the "raw" compressibility data caused by the sharpness of the transition, and suggests that where such a sharp transition is present the compressibility should be computed exactly from the eigenvectors.

No conclusion concerning the transition in this model can be drawn from the above table.

(c) Nearest-Neighbour Exclusion on the Square Lattice.

Although no analytic results have been found for this model, it has been studied numerically by several independent groups of workers (see table 1.3.1) with very close agreement in the results obtained. It has been established "beyond reasonable doubt" that this model exhibits an order-disorder transition but not a first-order EPT. Moreover there is close agreement in the transition parameters obtained, the most precise estimate of u_t being that of Ree and Chesnut[23], namely $u_t = 0.79152$, using the sequence of maxima in $|\lambda_2/\lambda_1|$.

We have used both MNMAXI and MNEIGM to study lattices of width M=2,3,...9 sites and have used MNEIGM to continue to lattices of width 13 sites. As with the previous model, the lattices are oriented at 45°. This ensures that the close-packed configuration corresponds to that of the infinite lattice for lattices of both odd and even width.

The transition was located by examining the sequences $\{u_0(M)\}$ and $\{u_I(M)\}$. The results are shown in table 2.6.5. From the sequence $\{u_I(M)\}$ we can estimate $u_t = 0.79151 \pm 0.00001$. We have found difficulty in satisfactory extrapolation of the sequence $\{u_0(M)\}$; the only conclusion is that $u_t \simeq 0.79$.

To determine the nature of the phase transition we again used the three methods of section (2.5):

Method of Runnels and Combs.

We first observe from fig. 2.6.11 that $(d\rho/d\mu)_{max}$ seems to diverge logarithmically with M, permitting us to attempt to apply the method. In table 2.6.6 are listed the sequences $\{u_1(M)$, $u_2(M)$, $\rho_1(M)$, and $\rho_2(M)$: M=3,4,....13$\}$ and a few minutes at a desk calculator is sufficient to prove that an honest numerical extrapolation of the sequences is impossible in the absence of prior information on how the limit is approached. We have plotted the different functions against $M^{-\alpha}$ for a few values of α but our graphs merely demonstrated that we could "prove" anything in this way and we have not reproduced them.

Intersection Method.

As with the method of Runnels and Combs, an honest numerical analysis of the sequences (table 2.6.7) leads to no unambiguous result

Table 2.6.5: SQ1 Model — Variation of $u_0(M)$ and $u_I(M)$ with M.

M	$u_0(M)$	$u_I(M)$
4	0.75580	....
5	0.76898	0.79240210
6	0.77591	0.79195093
7	0.77974	0.79175301
8	0.78233	0.79165468
9	0.78421	0.79160094
10	0.78552	0.79156937
11	0.78641	0.79154977
12	0.78709	0.79153703
13	0.78762	....

The accuracy of the points $u_0(M)$ is uncertain. The last figure in the points $u_I(M)$ is an estimate, the remaining figures are accurate.

Table 2.6.6: SQ1 Model — Method of Runnels and Combs.

M	$u_1(M)$	$\rho_1(M)$	$u_2(M)$	$\rho_2(M)$
3	.....	.....	0.87182	0.84185
4	.....	.....	0.85995	0.83347
5	.....	.....	0.85022	0.82454
6	0.71142	0.62530	0.84267	0.81672
7	0.72542	0.63904	0.83687	0.81029
8	0.73505	0.64909	0.83230	0.80496
9	0.74163	0.65620	0.82871	0.80063
10	0.74718	0.66257	0.82523	0.79605
11	0.75130	0.66743	0.82294	0.79314
12	0.75539	0.67260	0.82103	0.79068
13	0.75771	0.67542	0.81929	0.78832

Table 2.6.7: SQ1 Model — Intersection Method for determining the Nature of the Phase Transition.

M	$u_{I1}(M)$	$\rho_{I1}^{M}(M)$	$\rho_{I1}^{M+1}(M)$	$u_{I2}(M)$	$\rho_{I2}^{M}(M)$	$\rho_{I2}^{M+1}(M)$
3	0.65652	0.5893	0.5788	0.8881	0.8635	0.8721
4	0.68957	0.6115	0.6055	0.8682	0.8450	0.8502
5	0.71008	0.6277	0.6238	0.8553	0.8325	0.8358
6	0.7239	0.6398	0.6371	0.8462	0.8218	0.8243
7	0.7338	0.6491	0.6471	0.8396	0.8139	0.8158
8	0.7411	0.6571	0.6555	0.834	0.8077	0.8091
9	0.747	0.6638	0.6623	0.8301	0.8029	0.8041
10	0.751	0.6685	0.6674	0.826	0.7982	0.7991
11	0.755	0.6729	0.6720	0.823	0.7932	0.7941
12	0.758	0.6766	0.6759	0.821	0.7906	0.7913

but if we indulge in more graphical extrapolations, we find the following evidence for a continuous transition or a very weak first-order one.

(a) $(d\rho/d\mu)_{max} \longrightarrow \infty$ as log M (see fig. 2.6.11)

(b) From plots of $u_{I1}(M)$ and $u_{I2}(M)$ against M^{-1} and $(M+1)^{-1}$ it is likely that they tend to u_t (=0.792) from below and above respectively while the corresponding density sequences have close limits (see fig. 2.6.12 and fig. 2.6.13)

Exact Isotherm for the $\infty \times \infty$ Lattice.

The exact isotherm is plotted in fig. 2.6.14 for the range (0.63,0.96) in u. In order to show how points away from the transition region may be useful in determining the nature of the transition, we show this isotherm in detail for the range (0.75,0.84) in fig.2.6.15, and finally in fig.2.6.16 we have expanded the graph yet again to illustrate the range (0.788,0.794).

Although there is no analytic expression for the isotherm, we can obtain some test of the isotherm by comparison with the isotherm obtained by constructing Padé approximants to some of the low- and high-density series of Gaunt and Fisher[1]. In fig.2.6.14 we have inserted the (6,6), (7,6) and (6,7) PAs to the low-activity $\rho(z)$ series, but since these are not consistent with each other they do not give a good test of the isotherm. However, the PAs to the high-activity $\rho(u')$ series ($u' \equiv 1-u$) provide a good test of part of the isotherm as, to graphical accuracy, the (3,4), (4,4), and (5,4) PAs are identical to each other and to our isotherm for $u \geq 0.82$.

There is one new feature which appears in the computation of the exact isotherm for this model and which limits the amount of information available near u_t. We considered lattices of width up to 13; suppose that $u_t < u < u_I(13)$. Then the variation of $\rho(M)$ with M for this value of u will be of the form:

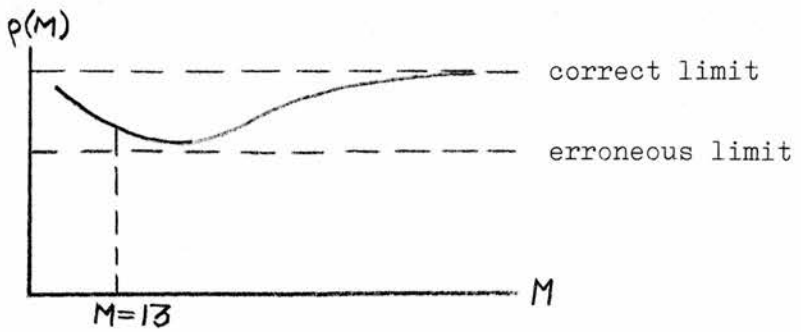

Extrapolation from the sequence $\{\rho(M)\colon M=2,3.....13\}$ will give the erroneous limit shown, and thus there is a small range of u for which extrapolation should not be attempted.

The conclusion from the isotherm is evidently that the model does not have a first-order EPT. This is indicated both by the behaviour of the points away from u_t and from the less accurate points around u_t. The question of whether or not the compressibility diverges at u_t is unanswered by this isotherm, there being nothing in fig. 2.6.5 to contradict the divergence suggested by fig. 2.6.11.

2.7 Assessment of the Methods for $\infty\times\infty$ Lattices.

(i) Location of the phase transition.

On the grounds of numerical convenience there can be no doubt that the intersection method is by far the best of the three. For the superexchange model the method yielded an exact value of u_t, for the lattice gas with attraction, where both it and the sequence of maxima in $(d\rho/d\mu)$ gave exact results, higher accuracy was obtained, and for the SQ1 model it yielded a value of u_t in five-figure agreement with that obtained from ratios of eigenvalues, numerically a much more difficult procedure to carry out.

The principal objection to the intersection method is theoretical; although intuitively it seems very likely, we have no rigorous proof even of the existence of the intersection property in any models, far less of the sequence $u_I(M)$ tending to u_t^*.

(ii) Nature of the Transition.

Here the problem is to choose between three unsatisfactory methods and it is not possible to recommend any one of them without qualifications. On theoretical grounds both the method of Runnels and Combs and the intersection method are appealing, but for each we obtained sequences which were too inaccurate for satisfactory numerical extrapolation. The pitfalls of graphical extrapolation from these sequences are well illustrated by fig. 2.6.13. If we only had

* Note Added: we have recently proved the existence of the intersection property for two-dimensional hard-core lattice gases with a unique close-packed configuration — February 1972.

results for lattices of width up to 8 sites then a qualitatively different conclusion (that there is a first-order EPT) might be drawn. However, this problem is slightly less serious for the intersection method since there we are studying the limits of pairs of sequences rather than of single sequences.

When the extrapolation is possible, it is obvious that the study of the exact isotherm is the best method as the raw data for extrapolation may be obtained to an accuracy of 10 or 12 significant figures. The basic weakness is of course that near the transition point the extrapolation frequently fails and in addition there is a (very small) region near u_t where misleading results may be obtained due to the intersection property. On the other hand, the strength of the method is that information about the transition region may be found (as in the SQ1 and superexchange models) from points on the isotherm distant from the transition. A final drawback with this method is that our experience with the SQ1 model and the superexchange model suggests that it is impossible to detect a divergence in $(d\rho/d\mu)$ from the isotherm obtained.

CHAPTER III.

1-2-4 EXCLUSION ON THE SQUARE LATTICE.

In section 1.3 we have already discussed the twin aims of this thesis: to test the idea that for an extended hard core the existence of a unique close-packed configuration is a sufficient condition for a first-order EPT in the model, and in the light of the results of this work to re-examine some models studied by other workers. This chapter is concerned with the first problem.

We have already pointed out that the SQ124 model possesses a well-defined close-packed configuration and according to this idea should thus show a first-order EPT. The results of this chapter, based on studies of semi-infinite lattices with both free and periodic boundary conditions, suggest on the contrary that there is no first order EPT in the SQ124 model.

3.1 Semi-infinite Lattices.

Periodic lattices of even width, M, up to 14 sites and of odd width up to 9 sites have been studied over the entire range of u in intervals of 0.025. For even lattices a pronounced maximum in $d\rho/d\mu$ is present for $M \geq 6$ whereas for odd lattices this maximum is very weak. The growing maximum for even lattices is illustrated in fig. 3.1.1. For the even lattices we have re-examined the vicinity of these peaks at intervals of 0.001 in u.

Semi-infinite lattices of width 3,4,5, and 6 sites but with free boundary conditions have also been studied over the entire range of u. For M=3 and M=5 there is again an obvious maximum in $d\rho/d\mu$ but this maximum is absent when M=4 or M=6. From these results and from those for the periodic lattices, it is tempting to speculate that the appearance of a peak in $d\rho/d\mu$ is a consequence of the availability of a well-defined, close-packed configuration, a situation present in the even-periodic and odd-free lattices but absent in the odd-periodic and even-free lattices. Also of interest is the similarity between this observed behaviour in semi-infinite lattices for which there can of course be no true phase transition, and the main problem under investigation i.e. the relation between the existence of a unique close-packed configuration and the occurrence of a first-order EPT in the infinite system.

3.2 Infinite Lattices: Location of any phase transition.

All three methods given in section 2.5 have been used to estimate the location of the phase transition and the results are shown in table 3.2.1.

Table 3.2.1: Estimates of the transition point for the SQ124 model.

M	$u_o(M)$	$u_I(M)$	$u_{EV}(M)$
4	0.697	0.7875(9)	.....
6	0.762	0.77247(3)	0.7584
8	0.77049	0.76934(9)	0.7630
10	0.77258	0.76857(2)	0.7667
12	0.77340	0.76847(5)	0.7683
14	0.77409	.....	.....
∞	0.775	0.768(3)	?

It was not the original intention to study the ratio of leading eigenvalues, as the study of lattices of width up to 12 sites with $\Delta u=0.025$ suggested that the compressibility diverged logarithmically with M at a point around $u=0.77$ consistent with the a more accurate value of around 0.768 obtained by the intersection method. However, when the results for M=14 were obtained it became evident that the limits of the sequences $\{u_o(M)\}$ and $\{u_I(M)\}$ are in all probability unequal, and the ratios of leading eigenvalues were studied in an attempt to resolve the apparent contradiction between the two values of u_t, namely

$$u_t = 0.775 \pm 0.001 \quad \text{from maxima in } d\rho/d\mu. \tag{3.2.1}$$

$$u_t = 0.7683 \pm 0.0001 \quad \text{from intersection method.} \tag{3.2.2}$$

As is evident from table 3.2.1, this study of the sequence $u_{EV}(M)$ has not resolved the contradiction although it seems that knowledge of $u_{EV}(14)$

might be sufficient to rule out one or other of the values of the limit. With the present programs it is not possible to compute $u_{\epsilon v}(14)$ since the matrix (of dimension 241) is too large to store in the computer as a two dimensional array, and we have no subroutines using iterative methods (as opposed to methods based on similarity transformations) which compute non-extremal eigenvalues of large matrices.

The author's prejudice is that the "true" transition point (i.e. the point at which long-range order appears) is that given by the intersection method. This belief is based on a more detailed examination of the variation of $(d\rho/d\mu)_{max}$ with log M (see fig.3.2.1) and on the exact isotherm for the $\infty \times \infty$ lattice. Both suggest that $d\rho/d\mu$ may remain finite and continuous at u_t in which event the precise location of the maximum in $d\rho/d\mu$ is not necessarily meaningful (since for example $\rho^{-1}.d\rho/d\mu$ may have a maximum at a different point from $d\rho/d\mu$ and why pick on $d\rho/d\mu$?).

3.3 Infinite Lattices: Nature of any Phase Transition.

We have already noted the rather surprising result (fig. 3.2.1) that $(d\rho/d\mu)_{max}$ increases with M slower than log M, although it is not impossible that $(d\rho/d\mu)_{max}$ may still diverge. Nevertheless, even if such a weak infinity in the compressibility is present it is strongly suggestive of the absence of a first-order EPT; in all cases where a first-order EPT has been proved or (convincingly) suggested by numerical evidence, $(d\rho/d\mu)_{max}$ has diverged as some power of M.

In the absence of an obvious divergence in $d\rho/d\mu$, there was little prospect of obtaining much information on the nature of the transition either from the method of Runnels and Combs or from the intersection method. The sequences $\{\rho_1(M)\}$, $\{\rho_2(M)\}$ apparently had different limits, but the corresponding sequences $\{u_1(M)\}$, $\{u_2(M)\}$ did not tend to u_t, a result consistent both with the possibility that the compressibility remains finite through the transition and with the probability that the numerical values were too inaccurate to be meaningful. Similar ambiguities appeared when attempting to apply the intersection method and the work was not pursued.

In contrast to these uncertaintities, the result of the extrapolation to the exact isotherm for the $\infty \times \infty$ lattice was very convincing indeed. All the consistency tests mentioned in section 2.5 were stringently applied; the variation of ΔP and $\Delta\rho$ with u is shown in figs. 3.3.1 and 3.3.2. In fig. 3.3.3 is shown the variation of $\Delta\rho$ with u near u_t; these extrapolations are slightly less reliable than those of the previous graphs. As a further check we have tested whether the extrapolation is independent of the boundary conditions imposed; this we have done by studying, for four values of u, lattices of odd width up to 11 sites and with free boundaries. The four points obtained, marked on fig. 3.3.2 are consistent with the proposed isotherm.

To sum up, both the behaviour of $\Delta\rho$ near u_t (fig.3.3.3) and its behaviour farther from u_t (fig.3.3.2) make it difficult to conclude other than that the SQ124 model does not exhibit a first-order EPT.

CHAPTER IV

SOME OTHER TWO-DIMENSIONAL HARD-CORE LATTICE GASES.

The result of the work on the SQ124 model (no first-order EPT) is inconsistent with the idea of Orban and Bellemans that the existence or otherwise of a unique close-packed configuration is the factor that determines whether or not a hard-core lattice gas exhibits a first-order EPT. Having this counterexample we found it natural to re-examine the evidence on which the conjecture was based, i.e. to test the reliability of the pattern of transitions summarised in table 1.2.2. Of greatest interest to us are the models for which a first-order EPT has been proposed; consequently we shall examine the simplest * such model, the TR12 model, and the only such model on a square lattice, the SQ123 model. Also of interest are the models (e.g. SQ12 and SQ12345) for which very weak transitions have been observed; we have studied the SQ12 model with both free and periodic boundary conditions in an attempt to understand the very strange properties reported for this model.

In this chapter we give a preliminary report of our work on these three models.

* i.e. the model with the smallest transfer matrices for a lattice of a given width.

4.1 1-2 Exclusion on the ~~Square~~ Triangular Lattice.

As mentioned in chapter I, the TR12 model has been studied by Orban and Bellemans[26,28] who used both series expansions and the matrix method. It has also been studied by Chesnut using Monte Carlo methods[29]. In every case a first-order EPT has been reported.

Orban and Bellemans used the matrix method on periodic lattices of even width up to 14 sites. From the study of the sequence $\{u_o(M)\}$ of maxima in $d\rho/d\mu$ they concluded that a transition occurred at $\mu/kT = 1.750 \pm 0.005$, i.e. at $u=0.852 \pm 0.001$. The nature of the transition was determined by the method of Runnels and Combs. In fig. 3 of ref. 26 they have plotted the sequences $\{\rho_1(M)\}$ and $\{\rho_2(M)\}$ against respectively M^{-1} and M^{-2}. The corresponding plots of $\{u_1(M)\}$ and $\{u_2(M)\}$ were not published; however Orban (private communication) has kindly provided the present author with a copy of the plots which are reproduced in fig. 4.1.1 We have repeatedly emphasised the dangers inherent in the method of Runnels and Combs; nevertheless this analysis has demonstrated that there is a sharp transition which may well be first-order.

We have repeated this work of Orban and Bellemans using periodic lattices of width up to 12 sites.

Location of the Transition.

The sequences $\{u_o(M)\}$ and $\{u_I(M)\}$ are listed in table 4.1.1, with estimates of their limits. The results agree with those of Orban and Bellemans[26,28] i.e. there is a phase transition around $u_t = 0.852$.

Table 4.1.1: TR12 Model — Variation of $u_o(M)$ and $u_I(M)$ with M.

M	$u_o(M)$	$u_I(M)$
4	....	0.8610
6	0.8346	0.8574
8	0.8465	0.8543
10	0.8498	0.8532
12	0.8517	....
∞	0.853±0.002	0.852±0.001

Nature of the Transition.

We have already mentioned the evidence of Orban and Bellemans for a first-order EPT, evidence based on the method of Runnels and Combs. We have attempted to test this result by performing the extrapolation to the exact isotherm of the infinite lattice for a number of values of u near u_t. At no point in the range (0.825,0.875) have we obtained a satisfactory* extrapolation to the density of the $\infty\times\infty$ lattice.

4.2 1-2-3 Exclusion on the Square Lattice.

The only previous work on this model is that of Bellemans and co-workers[25,27,28] who applied the matrix method to periodic lattices of width 5,10, and 15 sites, constructed four terms of the low-activity and two of the high-activity series, and also used a "shot-in-the-dark" approximation. Their most striking results came from the matrix method; a sharp peak appears in the plot of $(d\rho/d\mu)$ against μ/kT for M=10, and this peak becomes dramatically sharper with M=15. Yet the power of the matrix method lies in the possibility of a high accuracy computation of the thermodynamic properties of sequences of semi-infinite lattices, followed by a systematic extrapolation to the properties of the infinite lattices; to effect this extrapolation it is obviously desirable to have results for more values of M.

Why then did Bellemans et al. only look at lattices of width 5, 10 and 15 sites and ignore intermediate values of M? We can answer this by referring back to our experience with the SQ124 model where we saw that to obtain in a semi-infinite lattice of a reasonable width, behaviour resembling that of an infinite lattice, it is necessary to choose the width of the lattice and the boundary conditions in the finite direction so that the close-packed configuration is of the same form as that of the infinite lattice. This requirement on the SQ123 model with periodic boundary conditions immediately leads to the restriction that M be a multiple of five.

It is natural now to see if we can get round the above restriction by transforming or distorting the lattice to a form where the correct

* i.e fulfilling the criteria give in section 2.5

close-packed configuration occurs for a larger number of small values of M (as in the SQ1 model where we oriented the periodic lattice at 45° to get the correct close-packed configurations on lattices of both odd and even width — see section 2.6). We should bear in mind however that no computational advantage will be obtained if, as a consequence of the transformation, there is an increase in the range of the interaction in the infinite direction, i.e. in the notation of section 2.1 an increase in the value of q, since then, for a given value of M, the dimension of the transfer matrix will be greatly increased. In short, to increase the number of useful finite lattices which are computationally tractable, we must, without increasing q, transform the lattice to a form where the correct close-packed configuration occurs with a larger number of small values of M.

For the SQ123 model with the periodic boundary conditions of Bellemans et al. we can find no helpful transformation of the lattice.

For the SQ123 model with free boundary conditions the close-packed configuration of the infinite system is always permitted on a lattice of finite width; however, for a number of values of M, the free boundaries permit other, denser, configurations which will be preferred at close-packing. We illustrate this for M=4 in fig. 4.2.1.

So we rule out the use of free or periodic boundary conditions in our study of the SQ123 model. Instead, we have introduced "almost-periodic" boundary conditions. The lattice of width M is considered as a sublattice of a periodic lattice of width (M+1) with the constraint that the $(M+1)^{th}$ line of sites be empty. This is illustrated for M=4 in fig. 4.2.1. As far as we can see, the choice of almost-periodic boundary conditions leads to the correct close-packed configuration for $M \geq 4$ except when $M=5n+1$, $n=1,2,3,\ldots\ldots$

Numerical Work.

Transfer matrices have been constructed for the SQ123 model with almost-periodic boundaries for M=3,4,....10. For a number of values of u around u=0.98 (i.e. around $\mu/kT = 3.7$, the transition point of Bellemans et al.) we have used MNEIGM to compute, as usual, P/kT and ρ.

The quantity of greatest interest is $d\rho/d\mu$ and in fig. 4.2.2 we show the variation of $d\rho/d\mu$ with u in the region of interest. A peak is

beginning to appear for M=9,10, but it is much weaker than that observed by Bellemans for a periodic lattice of width 10. However, we believe that this peak corresponds to the appearance of Bellemans transition for the following reasons:

(1) For $M \geq 7$ there is an intersection property evident in the vicinity of the peak, i.e. there is a point $u_I(M)$ with $\rho(M+1,u) \leq \rho(M,u)$ for $u \leq u_I(M)$. The values of $u_I(M)$ are given in table 4.2.1. This is consistent with the "growth" of a phase transition in this region.

(2) We can compare the data in table 4.2.1 with the values of $u_o(M)$ quoted by Orban and Bellemans[27] (reproduced in table 4.2.2) It is certainly plausible that both our sequences and theirs have equal limits around u=0.98, $\rho = 0.875$.

Table 4.2.1: SQ123 Model — Intersection points and maxima in $d\rho/du$ for lattices with almost-periodic boundary conditions.

M	Intersection point		Maximum in $d\rho/du$	
	$u_I(M)$	corresponding value of ρ	$u_o(M)$	corresponding value of ρ
7	0.9969	not computed	no max.	.....
8	0.9943	0.9175	no max.	.....
9	0.9907	0.8960	0.995(7)	0.9300
10	.....	.....	0.994(4)	0.9245

Table 4.2.2: SQ123 Model — maxima in $d\rho/du$ for periodic lattices (results of Orban and Bellemans[27])

M	$u_o(M)$	corresponding value of ρ
5	no max.	....
10	0.973	0.873
15	0.975	0.878

Our results to date are rather meagre; we have confirmed the phase transition observed by Orban and Bellemans, but have not enough information even to venture a guess as to its nature. However, we are not too

discouraged as we believe that results for M=12 and M=13 (M=11 is of the form M=5n+1 and hence useless) would be sufficient to give a fair indication of the nature of the transition. In the summer of 1972, an extra 100K bytes of core will be available on the St. Andrews computer. At present when MNEIGM is used on large matrices, a fair proportion of the computer time is spent transferring blocks of matrix elements to and from core; given this extra core we believe that the matrix for M=13 will prove computationally tractable (the dimension of the matrix will be about 1900 — see fig. 4.2.3). This work should be completed during the summer of 1972.

4.3 1-2 Exclusion on the Square Lattice.

The conjecture of Orban and Bellemans relating the occurrence of a first-order EPT in a model to the existence of a unique close-packed configuration, relies heavily for support on the apparent lack of a first-order EPT in this SQ12 model. Although three models (SQ12, SQ1234, and SQ12345) lacking unique close-packed configurations have been studied[24,25,28] we only have detailed evidence on the nature of the transition for the SQ12 model, the most thorough analysis being that of Ree and Chesnut[24] who proposed a third-order EPT at $u_t = 0.995 \pm 0.002$*.

All the reliable previous work on the model has used the matrix method as there are serious problems associated with the low- and high-activity series expansions; the low-activity series has a very small radius of convergence, while the normal high-activity series of the form

$$P/kT \propto \log z + a_1 z^{-1} + a_2 z^{-2} + \ldots\ldots \qquad (4.3.1)$$

does not exist because of the absence of a well-defined sublattice structure at close-packing. Bellemans and Nigam[25] claim that the correct high-activity expansion is of the form

$$P/kT = \tfrac{1}{4}\log z + \tfrac{1}{4}z^{-\frac{1}{2}} + \tfrac{1}{4}z^{-1} + O(z^{-\frac{3}{2}}) \qquad (4.3.2)$$

but the present author does not see (even in principle) how to extend their argument to obtain a systematic recipe for the higher terms in the series. This means that there has been no check on the results obtained by the matrix method and it remains possible that the (very accurate) results of Ree and Chesnut are an artifact of the matrix method.

We can make this point more precise by noting that for the periodic $M\times\infty$ lattices used by Ree and Chesnut, P/kT has the following high-activity expansion[25]:

$$P(M)/kT = \tfrac{1}{4}\log z + \tfrac{1}{16}(M+4)z^{-1} + O(z^{-2}) \qquad (4.3.3)$$

We also note from equation (4.3.2) that the function** Q(z) defined by $Q(z) \equiv P/kT - \tfrac{1}{4}\log z$ has an essential singularity at $z=\infty$; the question arises as to whether the behaviour in $M\times\infty$ lattices observed by

* Note that there is a misprint in the statement of this result in ref. 24.
**At close-packing $kQ(z)$ is just the entropy per lattice site.

Ree and Chesnut for values of u very close to u=1 signalled the "growth" of a phase transition at some point $z_t \neq \infty$, or was merely a manifestation in the finite system of non-uniform convergence of $Q(M,z)$ ($\equiv P(M)/kT - \frac{1}{4}\log z$) to $Q(z)$ in the neighbourhood of the essential singularity at $z=\infty$?

We have tried to answer this question by studying $M \times \infty$ lattices with different boundary conditions. A change in boundary conditions will lead to a change in the high-activity expansion of the pressure of the semi-infinite lattice; we have no reason to believe that the essential singularity at z_t will "grow" in the same way out of different sequences of analytic functions.

There is a drawback. The reader will by now be familiar with the point that to observe the growth of a (true) phase transition in our semi-infinite lattices, we must choose boundary conditions which preserve the close-packed configuration of the infinite system. However, this observation arose from work on models where any phase transition is associated with the change from a disordered state to an ordered state in which the particles prefer to occupy one sublattice which is completely filled at close-packing. In such models it is a reasonable requirement that to approximate(in a semi-infinite system) a transition associated with the appearance of this type of long-range order, the boundary conditions must be compatible with a complete filling of the appropriate sublattice at close-packing.The question is how to interpret this requirement and establish which boundary conditions are suitable for the SQ12 model where we do not have a unique close-packed configuration; to resolve this we must first define the type of ordering that can exist in the model.

Bellemans and Nigam[25] have suggested that we divide the lattice into "A" and "B" sublattices, each sublattice of an $M \times N$ lattice consisting of $N/2$ horizontal lines of M sites, an "A" line lying between two "B" lines and vice versa. At close-packing, one or other of these sublattices is preferentially occupied in spite of the ability of whole rows and columns of particles to slide freely with respect to each other. A tendency towards this type of order occurs with M even or odd and with both periodic and free boundaries, the close-packed configuration(s) of the $M \times \infty$ lattices in each case being available on the close-packed $\infty \times \infty$ lattices. We thus do not have a priori grounds for rejecting any particular choice of boundary conditions.

We used MNEIGM to study periodic lattices of even width, M, up to 18 sites for $0.96 \leq u \leq 1.0$. As usual, we computed $d\rho/d\mu$ and $d^2\rho/d\mu^2$ by numerical differentiation; for a sample of values of M, the plot of $d^2\rho/d\mu^2$ is shown in fig. 4.3.1. The graph is identical to that obtained by Ree and Chesnut[24] (who studied the same lattices); indeed our estimates of $u_1(M)$, $u_2(M)$, $\rho_1(M)$, and $\rho_2(M)$ differ from theirs by at most ± 2 in the fifth significant figure.

Lattices of odd and even width, M, up to 14 sites but with free boundaries have also been studied. The variation of $d^2\rho/d\mu^2$ with u for $0.962 \leq u \leq 1.0$ is shown in fig. 4.3.2 for a few values of M.

This model is very different from those studied so far and consequently the methods we have been using to locate a possible phase transition are of little relevance. The results for $M \times \infty$ lattices leave little room for doubt that there is no first-order EPT in the SQ12 model, a conclusion supported by the limited information available from series expansions[25]. Rather, the problem of interest is to determine whether there is any transition at all in the infinite system. It is tempting to extrapolate from the results for periodic lattices of even width and conclude (with Ree and Chesnut[24]) that there is a third-order EPT around u=0.995. The behaviour of the even-free* lattices suggests a transition, still around u=0.995, but of a different nature — either a third-order EPT with totally different values for the discontinuity in $d^2\rho/d\mu^2$, or a negative infinity in $d^2\rho/d\mu^2$. On the other hand, by looking only at the odd-free lattices we should conclude that there is no phase transition in this range of u.

There are two plausible explanations of the above results for $M \times \infty$ lattices:

(1) There is a phase transition around u=0.995. The values of M studied in the even-periodic and ~~odd~~ even-free cases are too small for us to resolve the nature of the transition, although we can confidently exclude a first-order EPT or a λ-transition. The odd-free lattices are misleading just as the odd-periodic lattices are misleading in the SQ1 model — because they distort the close-packing properties of the system. For the SQ12 model, approximately half of the close-packed configurations available on an even-periodic lattice are excluded on the odd-free lattice.

(2) The SQ12 model has no phase transition. The form of the $d^2\rho/d\mu^2$ plot for the even-periodic and even-free lattices is related to the residual entropy at close packing in such $M \times \infty$ lattices.

* i.e lattices of even width with free boundaries.

We do not believe that it is possible by any numerical manipulation of our results to distinguish between these possibilities. Nor will further useful information be obtained by considering a few larger values of M for either free or periodic boundary conditions. To convincingly determine whether or not there is a transition we should use series expansions to supplement the information obtained by the matrix method; hopefully we could glean sufficient information from the series expansions to distinguish between the two (well defined) alternatives left open by the matrix method. However, the difficulties associated with the high-activity expansion have already been mentioned; we may work on them in the future, but for the present have made no improvement on the two significant terms of Bellemans and Nigam.

Nevertheless, there is an intuitive argument which, without proposing a phase transition, explains the form of the results for semi-infinite lattices with the three types of boundary conditions (even-periodic, even-free, and odd-free). Before proceeding with it, we re-emphasise that we have no rigorous conclusion for the SQ12 model — we are aware that in lattice statistics plausible arguments have, in the past, frequently proved misleading*; the reader is asked to keep this in mind when considering the argument.

In appendix I we prove that if $P_{EP}(M)$, $P_{EF}(M)$, and $P_{OF}(M)$ denote the grand canonical pressure of the $M \times \infty$ lattices with respectively even-periodic, even-free, and odd-free boundaries, then

$$P_{EP}(M) \underset{z\to\infty}{\sim} (2M)^{-1}\log 2 + \tfrac{1}{4}\log z + O(z^{-1}) \tag{4.3.4}$$

$$P_{EF}(M) \underset{z\to\infty}{\sim} (2M)^{-1}\log(M/2+1) + \tfrac{1}{4}\log z + O(z^{-1}) \tag{4.3.5}$$

$$P_{OF}(M) \underset{z\to\infty}{\sim} \frac{M+1}{4M}\log z + O(z^{-1}) \tag{4.3.6}$$

We then define $T_{EP}(M) \equiv P_{EP}(M) - P_{EP}(\infty)$, and similarly $T_{EF}(M)$ and $T_{OF}(M)$**. It is immediate that when $z=\infty$

$$T_{EP}(M) = (2M)^{-1}\log 2 \tag{4.3.7}$$

$$T_{EF}(M) = (2M)^{-1}\log(M/2+1) \tag{4.3.8}$$

$$T_{OF}(M) = 0 \tag{4.3.9}$$

We also know that when $z=0$, $T_{EP}(M) = T_{EF}(M) = T_{OF}(M) = 0$.

* e.g. for this very model, Hoover, Alder, and Ree[49] published an argument for the wrong high-activity series.

**Except that $-T_{OF}(M) = \frac{M}{M+1} P_{OF}(\infty) - P_{OF}(M)$

We consider first the even-periodic case. We note that

$$T_{EP}(\mu) = \lim_{N\to\infty} (MN)^{-1}\log\left\{\sum_{i=1}^{d(N)}\left(\frac{\lambda_i(N)}{\lambda_1(N)}\right)^{N}\right\} \qquad (4.3.10)$$

We know that $d(N)\sim a^N$ where $a = \frac{1}{2}(1+\sqrt{5}) = 1.618$ and thus $T_{EP}(M)\leq M^{-1}\log a = 0.481/M$. At close-packing, $T_{EP}(M) = 0.346/M$. We now display (fig. 4.3.3) two possible forms of $T_{EP}(M)$ and the corresponding plots of the first three derivatives of this quantity with respect to μ. We can rule out the possibility that T_{EP} is of the form marked (2) since then for $\mu \gtrsim \mu_1$ we should have $\rho(M) \lesssim \rho(\infty)$, i.e. we should observe the intersection property noted for previous models. For the even-free case, $\rho(M)$ is in fact a monotonic decreasing function of M for $M \leq 18$ and $0.96 \leq u \leq 0.9999$. From the proposed variation of T_{EP} with μ we can understand qualitatively fig. 4.3.1 — going from left to right we should have successively ranges where $d^2\rho/d\mu^2$ decreases, increases, and finally decreases with M. Thus we see that the form of fig. 4.3.1, which <u>could</u> signal the growth of a true third-order EPT around u=0.995, could also arise purely as a consequence of the necessity for $T_{EP}(M)$ to be a sigmoid function of μ for values of μ greater than about 3.0.

The argument is essentially the same for the even-free case where at $z=\infty$, $T_{EF}(M) = (2M)^{-1}\log(M/2 + 1)$. In this case we are not yet (i.e. by M=14) able to observe the intermediate range of of u where $d^2\rho/d\mu^2$ increases with M, but it is possible that the crowding of the curves around u=0.987 signals the appearance of this stage at M=16 or M=18. It might be valuable to consider the case M=16 for a few values of u near this point.

For the odd-free case we expect the sigmoid form to be absent since $T_{OF}(M) = 0$ at $z=\infty$. We should anticipate that there will be no irregularities in the behaviour of $d^2\rho/d\mu^2$ for the $M\times\infty$ lattices and furthermore that the plot of this function for the $M\times\infty$ lattice should resemble that of the $\infty\times\infty$ lattice. The former point is evident from fig. 4.3.2: we can provide some (admittedly meagre) evidence for the latter point by using the high-activity series of Bellemans and Nigam[25]

$$\rho = \tfrac{1}{4} - \tfrac{1}{8}z^{-\frac{1}{2}} - \tfrac{1}{4}z^{-1} + O(z^{-\frac{3}{2}}) \qquad (4.3.11)$$

from which

$$d^2\rho/d\mu^2 = -\tfrac{1}{32}z^{-\frac{1}{2}} - \tfrac{1}{4}z^{-1} + O(z^{-\frac{3}{2}}) \qquad (4.3.12)$$

We have plotted this approximation to $d^2\rho/d\mu^2$ on fig. 4.3.2 for four values of u, assuming the error to be of order of magnitude $2z^{-\frac{3}{2}}$. The results are consistent with our assertion that the odd-free lattices are similar in properties to the $\infty\times\infty$ lattice.

We are aware of the inadequacy of the above analysis, and hope to improve on it after some further work on the model. However, we feel that it provides some clarification of our assertion that the phase transition proposed by previous workers for this model could be an artifact of the matrix method, though we are of course still a long way from demonstrating that there is no phase transition present. Yet perhaps the most interesting aspect of the analysis is that we have been led back to the original theme of the thesis, namely the relation between the residual entropy at close-packing in such models as the SQ12 lattice gas, and the occurrence of EPTs. We have seen that the existence of this residual entropy is, for the even-periodic lattice, related to the absence of an intersection property in the density; the sigmoid form of the plot of $T_{EP}(M)$ against μ can only occur when the residual entropy per lattice site of an $M\times\infty$ lattice is non-vanishing, and this sigmoid form is necessary for there to be no intersection point (i.e. a point where $\rho(M,u) = \rho(M+2,u)$ with $0<u<1$). Furthermore, we can conjecture that the existence of such an intersection point for $M\times\infty$ lattices is a necessary condition for a first-order EPT and probably for a λ-transition. We believe that an argument could be developed along these lines which could rigorously exclude first-order EPTs and λ-transitions from a class of hard-core lattice gases with non-unique close-packed configurations.

To sum up this rather long section, we have neither proved nor disproved the existence of the third-order EPT proposed by Ree and Chesnut[24] for the SQ12 model. We have invented an argument which, without assuming any phase transition, explains the plot of $d^2\rho/d\mu^2$ against u for different types of boundary condition. The key to the argument is the effect of the residual entropy per lattice site which persists at close-packing in certain $M\times\infty$ lattices; a byproduct is a little insight on why such models with no unique close-packed configuration do not exhibit a first-order EPT.

4.4 Concluding Remarks.

We are now in a position to reflect on the two aims behind the work reported in this thesis.

We started with the idea of Orban and Bellemans relating the occurrence of a first-order EPT in a two-dimensional lattice gas with extended hard core, to the existence of a unique close-packed configuration in the model. We now know from the SQ124 model that (even when the hard core extends beyond nearest neighbour sites) the existence of a unique close-packed configuration is not a sufficient condition for a first-order EPT. With the benefit of our results for the other hard-core lattice gases we can now reconsider the relationship between behaviour at close-packing and the nature of the phase transition. Thanks to our work on the SQ12 model we now realise the following result to be obvious:

Theorem T1. For any two-dimensional hard-core lattice gas, the vanishing of the entropy per lattice site at close-packing is a sufficient condition for there to be an intersection property in the density of $M\times\infty$ even-periodic lattices.

We believe, but have not proved, the following result:

Conjecture C1. For any two-dimensional lattice gas, the existence of an intersection property in the density is a necessary condition for a first-order EPT or a λ-transition.

T1 and C1 alone do not relate behaviour at close-packing to the nature of the phase transition. We know that the converse of C1 is not true (consider a lattice gas with an attractive potential at a temperature immediately above its critical point) and are led to consider whether the converse of T1 may be true. Truth of this converse of T1 and of C1 would imply:

Conjecture C2. For any two-dimensional hard-core lattice gas, the vanishing of the entropy per lattice site is a neccessary condition for a first-order EPT or a λ-transition.

It would be rash to venture an opinion on the validity of C2 as we only have results for one relevant model (SQ12), and it is possible that the SQ1234 or SQ12345 models might provide counterexamples. To examine the

intersection properties and to evaluate the entropy at close-packing for these two models would be perfectly feasible; this would provide a good test of C2 as these two models seem[28] to differ in properties from each other and from the SQ12 model.

The other aim in the present work was to re-examine some of the hard-core lattice gases studied by other workers, in particular such models as TR12 and SQ123 for which there were reports of first-order EPTs. The main problem has already been emphasised in section 2.7 — we need a better method of deducing the nature of the transition from results for $M \times \infty$ lattices. An appealing result which would help substantially would be the following:

Conjecture C3. If, for a two-dimensional lattice gas, $d\rho/d\mu$ has a maximum at $u = u_0(M)$, and if $u_t = \lim_{M\to\infty} u_0(M)$,

(1) There is a λ-transition at u_t if $(d\rho/d\mu)_{max} \underset{(M\to\infty)}{\sim} A \log M$

(2) There is a first-order EPT at u_t if $(d\rho/d\mu)_{max} \underset{(M\to\infty)}{\sim} A.M^{\alpha} \quad (\alpha > 0)$.

A proof of C3 will be difficult to find, yet we believe that this result, or one of comparable power, is essential before we can use the matrix method to unambiguously identify first-order EPTs. The alternative is to look for our key under a different lamp post.

APPENDIX I: Close-Packed Configurations of the SQ12 Model.

(1) Even-Periodic Lattices.

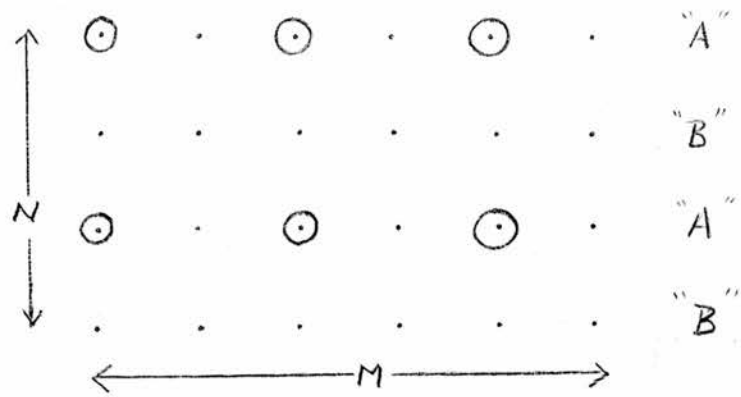

We start with the configuration shown above which contributes $z_A^{MN/4}$ to the grand partition function (GPF). (Note that we are using z_A, z_B as aids to enumerating the configurations although at close-packing both are infinite.)

Each horizontal line can be rotated by one site independently of any other and thus the total contribution to the GPF is $2^{N/2} z_A^{MN/4}$.
We could similarly have started with all the particles on the "B" sublattice with a similar contribution to the GPF of $2^{N/2} z_B^{MN/4}$.
Starting with the original configuration we choose one of the M/2 occupied columns and rotate it by one site. This gives a contribution to the GPF of $C_1^{M/2} z_B^{N/2} (z_A^{N/2})^{M/2-1}$.
We can do this with 1,2,3,.... (M/2 - 1) columns and get new configurations. This gives a total contribution to the GPF of $\sum_{J=1}^{M/2-1} C_J^{M/2} (z_B^{N/2})^J (z_A^{N/2})^{M/2-J}$

$$= (z_A^{N/2} + z_B^{N/2}) - z_A^{MN/4} - z_B^{MN/4}$$

Another contribution identical to the above is obtained by starting with the original contribution and rotating it horizontally by one site before starting to rotate columns.

Summing these contributions, we find that the GPF, $\underline{\underline{W}}(M,N,z_A,z_B)$ is given by

$$\underline{\underline{W}}(M,N,z_A,z_B) = (2^{N/2}-2)\, z_A^{MN/4} + (2^{N/2}-2)\, z_B^{MN/4} + 2(z_A^{N/2} + z_B^{N/2})^{M/2}$$

As a check we set $z_A = z_B = 1$ to get $\underline{\underline{W}}(M,N,1,1) = 2(2^{M/2} + 2^{N/2} - 2)$ a result identical to that of Bellemans and Nigam[25].

Letting $N \to \infty$, and setting $z_A = z_B$, it follows that the grand canonical pressure $P(M,\infty,z_A,z_B)$ is given by

$$P(M,\infty,z_A,z_B) = (2M)^{-1}\log 2 + \tfrac{1}{4}\log z \qquad \text{(setting } z_A = z_B = z\text{)}$$

(2) Even-free lattices

The derivation is almost identical to that for even-periodic case. The result is

$$P(M,\infty,z,z) = (2M)^{-1}\log (M/2 + 1) + \tfrac{1}{4}\log z$$

(3) Odd-free lattices

Here, there is only one permissible configuration on the single horizontal ring of M sites. If we assume the boundary conditions in the N direction to be periodic, the GPF is given by

$$\underline{\underline{H}}(M,N,z_A,z_B) = (z_A^{M/2} + z_B^{M/2})^{N\left(\frac{M+1}{2}\right)}$$

and hence

$$P(M,\infty,z,z) = \frac{M+1}{4M}\log z$$

APPENDIX II: Eigenvalues and Eigenvectors of Large Matrices.

A few years ago, Nesbet[50] introduced an algorithm for the determination of eigenvalues and eigenvectors of large symmetric matrices. The algorithm has recently been modified by Shavitt[51] for efficient application to sparse symmetric matrices and extended by Bender and Shavitt[37] to cover extremal eigenvalues of nonsymmetric matrices. A well-known property of the Rayleigh quotient[32] is exploited, namely that if we have estimates $\underset{\sim}{b}$ and $\underset{\sim}{c}$ for corresponding left and right eigenvectors of a normal[32] matrix A, and if the errors in $\underset{\sim}{b}$ and $\underset{\sim}{c}$ are of (absolute) order ε, then the generalised Rayleigh quotient $E \equiv (\underset{\sim}{b}^T A \underset{\sim}{c})/(\underset{\sim}{b}^T \underset{\sim}{c})$ gives an estimate of the corresponding eigenvalue, accurate to order ε^2. When the matrix is non-normal Wilkinson[32] has shown that E may still provide a good estimate of the eigenvalue; the error in this case is of order $\varepsilon^2/(\underset{\sim}{b}^T \underset{\sim}{c})$ and in practice one is unlikely to be concerned with cases where $(\underset{\sim}{b}^T \underset{\sim}{c})$ is small since the eigenvalue problem is not then a priori well-posed.[52] In the most general version of the algorithm [37] we start with trial vectors $\underset{\sim}{b}$ and $\underset{\sim}{c}$ and compute E as an estimate of the eigenvalue, the next trial values of $\underset{\sim}{b}$ and $\underset{\sim}{c}$ being generated by applying one step of the simple Gauss-Seidel[53] iterative process to the matrix A-EI (where I is the unit matrix). It is at this point that the convergence can be improved. Knowing that in the solution of linear equations the extrapolated Gauss-Seidel (or successive over-relaxation (SOR)) method can frequently be made to converge faster than the basic Gauss-Seidel scheme, we found it natural to investigate the effect of replacing the single Gauss-Seidel iteration in Nesbet's algorithm by an SOR iteration. In this appendix we show how this modification may very simply be incorporated in the iterative scheme given by Bender and Shavitt[37] and we discuss the results of applying the modified algorithm to the matrices of the SQ124 model.

The SOR Method.

Both Gauss-Seidel and SOR are members of the same class of iterative methods for the solution of sets of linear equations. To solve the set of equations $A\underset{\sim}{x} = \underset{\sim}{b}$ we split the matrix A into the form A = M-N and then iterate as follows:

$$\underset{\sim}{x}_0 \text{ arbitrary,}$$

$$M\underset{\sim}{x}_{m+1} = N\underset{\sim}{x}_m + \underset{\sim}{b}, \qquad m=1,2,3,\ldots\ldots \tag{A2.1}$$

In practice the splitting of A is chosen to make the solution of (A2.1) simple or even trivial (though it should be emphasised that there are restrictions on the choice of splitting if the iterative scheme is to converge — see Varga[53] for details). The Gauss-Seidel method is defined by the splitting

$$M = D-E$$
$$N = F \qquad (A2.2)$$

where D is diagonal and E,F are respectively strictly lower and upper triangular matrices. However this particular splitting is just one member of the one-parameter family of splittings defined by

$$M = \omega^{-1}(D-\omega E)$$
$$N = \omega^{-1}(\omega F+(1-\omega)D) \qquad (A2.3)$$

SOR is the iterative scheme defined by the splitting (A2.3) and it can be shown that SOR <u>may</u> converge when $0<\omega<2$. If $\omega=1$ we retrieve the basic Gauss-Seidel scheme, but it is frequently found that with the choice of an alternative value of ω (usually between 1 and 2) we achieve faster convergence to the solution of a set of linear equations.

<u>Modification of the Algorithm</u>.

The most general current version of the algorithm was given by Bender and Shavitt[37] and we now show how their scheme may be modified to incorporate SOR in the solution of the eigenvalue problem

$$A\underset{\sim}{c} = E\underset{\sim}{c}$$
$$\underset{\sim}{b}A = E\underset{\sim}{b} \qquad (A2.4)$$

Given estimates $\underset{\sim}{b}$ and $\underset{\sim}{c}$ for the left and right eigenvectors we guess initially that the eigenvalue is

$$E = N/D = (\underset{\sim}{b}^{T}A\underset{\sim}{c})/(\underset{\sim}{b}^{T}\underset{\sim}{c}) \qquad (A2.5)$$

Bender and Shavitt modify $\underset{\sim}{b},\underset{\sim}{c}$, and E thus:

$$\sigma_\mu = \sum_{\lambda=1}^{n} A_{\mu\lambda} c_\lambda - Ec_\mu \qquad (A2.6)$$
$$\sigma'_\mu = \sum_{\lambda=1}^{n} b_\lambda A_{\lambda\mu} - Eb_\mu \qquad (A2.7)$$
$$\Delta c_\mu = \sigma_\mu /(E - A_{\mu\mu}) \qquad (A2.8)$$
$$\Delta b_\mu = \sigma'_\mu /(E - A_{\mu\mu}) \qquad (A2.9)$$
$$\Delta D = (\Delta b_\mu)c_\mu + (\Delta c_\mu)b_\mu + (\Delta b_\mu)(\Delta c_\mu) \qquad (A2.10)$$
$$\Delta E = \Delta b_\mu \sigma_\mu /(D+\Delta D) = \Delta c_\mu \sigma'_\mu /(D+\Delta D) \qquad (A2.11)$$

Equations (A2.8) and (A2.9) are the results of a single Gauss-Seidel iteration on the equations (A2.4). Equation (A2.10) is obvious. Equation (A2.11) may be verified by evaluating the Rayleigh quotient

$$E + \Delta E = ((\underset{\sim}{b}+\Delta\underset{\sim}{b})^{T} A(\underset{\sim}{c}+\Delta\underset{\sim}{c}))/((\underset{\sim}{b}+\Delta\underset{\sim}{b})^{T}(\underset{\sim}{c}+\Delta\underset{\sim}{c})).$$

To incorporate SOR into the algorithm we have only to replace the equations (A2.8), (A2.9), and (A2.11) by:

$$\Delta c_{\mu} = \omega \sigma_{\mu} / (E - A_{\mu\mu}) \qquad (A2.8')$$

$$\Delta b_{\mu} = \omega \sigma'_{\mu} / (E - A_{\mu\mu}) \qquad (A2.9')$$

$$\Delta E = (\Delta b_{\mu}) \sigma_{\mu} (2-\omega)/(D + \Delta D) \qquad (A2.11')$$

These equations are obtained in a similar manner to (A2.8), (A2.9), and (A2.11).

Use of the Modified Algorithm.

The algorithm, modified to incorporate SOR, was tested by the author on one of the sequences of matrices which arose in the study of the SQ124 model. In this appendix we use the shorthand P_m for the reduced transfer matrix P of a periodic lattice of width M sites. For the tests we set the activity, z, arbitrarily to unity. The matrices are irreducible and the matrix elements are all non-negative. The thermodynamic properties derive from the eigenvalue of maximum modulus (necessarily real and positive) and its derivatives with respect to z. Denoting by E, $\underset{\sim}{b}$, and $\underset{\sim}{c}$, respectively, the maximum eigenvalue and the corresponding left and right eigenvectors of P_m, we know that

$$\frac{dE}{dz} = \frac{(\underset{\sim}{b}^{T} P'_{m} \underset{\sim}{c})}{(\underset{\sim}{b}^{T}\underset{\sim}{c})} \qquad (A2.13)$$

Thus to compute dE/dz we require (to high accuracy) a knowledge of $\underset{\sim}{b}$ and $\underset{\sim}{c}$ as well as of E.

We studied the matrices P_4 (of dimension 5) to P_{10} (of dimension 41). Using for $\underset{\sim}{b}$ and $\underset{\sim}{c}$ the deliberately poorly chosen starting vectors (1,1,.....1) and its transpose, we noted, for a number of values of ω, the number of iterations $n(\omega)$ required before Δb_{μ} and Δc_{μ} were less than a given tolerance (10^{-6}) for all μ. To eliminate spurious effects due to the very inaccurate starting vectors, ten iterations with

ω =1 were executed before setting ω to any other value. The variation of $n(\omega)$ with ω is shown in fig. A2.1 and it is clear that there is an optimum value of ω around ω=1.4 for which substantial acceleration of convergence is achieved. The work was repeated for a few different values of z with the same results. Similar tests have been carried out on the matrices from a number of different models and have yielded the same qualitative conclusion, i.e. there is an optimum value of ω for which the convergence is substantially faster than with ω=1.

The obvious disadvantage of the modified algorithm is the lack of a simple method of obtaining the optimum value of ω. However, this can be overcome in two situations:

(i) If we have a family of matrices of increasing dimension (as in the present work) a few test calculations on the smaller matrices may indicate a suitable value of ω. (e.g. ω=1.4 proved satisfactory for the SQ124 matrices P_{12} (dimension 97) and P_{14} (dimension 241) over a wide range of values of z).

(ii) We are likely to be using the algorithm mainly on matrices which are too large to store in the core of the computer as an ordinary two-dimensional array (since otherwise methods based on similarity transformations are superior[32]), in which case each such iteration may require a few seconds of computer time. In circumstances where the user may intervene during execution of the program, the value of ω may be changed if the original choice proves unsatisfactory. We have a subroutine MNTYPE, written by Dr. R. Erskine, which enables the user of the St. Andrews University computer to change the value of ω by an entry on the Console Typewriter. The author has found this "experimental" approach successful in dealing with a number of matrices of dimension greater than 250.

APPENDIX III: DERIVATION OF d(M) AND σ(M), THE DIMENSIONS OF THE TRANSFER MATRIX BEFORE AND AFTER SYMMETRY REDUCTION.

(i) Recurrence Relation for d(M).

The problem is to find d(M), the dimension of the unreduced transfer matrix, for a periodic lattice of width M. If the hard-core interaction extends over q consecutive rings of lattice sites we consider the transfer matrix, B_1, for a lattice of width (q-1) sites and with free boundary conditions. Thus if $\{\lambda_i : i=1,2,\ldots,d(q-1)\}$ are the eigenvalues of this matrix evaluated at z=1, then

$$d(M) = \sum_{i=1}^{d(q-1)} \lambda_i^M \qquad (A3.1)$$

If the coefficients of the characteristic equation of B_1 can be calculated, Newton's formulae[47] may be used to construct a recurrence relation for d(M). This is now illustrated with an example, the unoriented SQ1 model for which

$$B_1 = \begin{bmatrix} 1 & z \\ 1 & 0 \end{bmatrix} \qquad (A3.2)$$

The characteristic equation of B_1 is

$$\lambda^2 - \lambda - z = 0. \qquad (A3.3)$$

Setting z=1 and applying Newton's formulae we get the recurrence relation

$$\underline{d(M+2) = d(M+1) + d(M)} \qquad M \geq 1 \qquad (A3.4)$$

Since d(1)=1, d(2)=3, equation (A3.4) determines d(M) for all $M \geq 3$.

The SQ124 model provides a less trivial example. In this case B_1 is of dimension 5 and has a characteristic equation

$$(\lambda^2 - z)(-\lambda^3 + \lambda^2 + \lambda z + z) = 0. \qquad (A3.5)$$

Newton's formulae give for s_M, the sum of the M'th powers of the roots of the right-hand factor:

$$s_1 = 1 \qquad (A3.6)$$

$$s_2 = 1+2 = 3 \qquad (A3.7)$$

$$s_3 = 3+3+1 = 7 \qquad (A3.8)$$

$$\underline{s_{m+3} = s_{m+2} + s_{m+1} + s_m} \qquad M \geq 1,\ z=1. \qquad (A3.9)$$

We can calculate d(M) from this recurrence relation as $d(M) = s_M + (1+(-1)^M)$.

(ii) Use of the Polya theorem to calculate $\sigma(M)$.*

The procedure just outlined for computing d(M) is tractable for all the models considered. The determination of $\sigma(M)$ is much more difficult; in principle the Polya theorem provides a recipe but in practice the procedure is too complex for all but the simplest models. Ree and Chesnut[23] have outlined the method for the unoriented SQ1 model; we shall illustrate it on an even simpler example, the oriented SQ1 model.

The symmetry group is D_M, the dihedral group of order M, and the figure counting series is 1+x. Thus the counting series for inequivalent configurations is $Z(D_M, 1+x)$ where Z denotes the cycle index. Now

$$Z(D_M) = (2M)^{-1} \sum_{M/k} \phi(k)\, y_k^{M/k} + \begin{cases} \frac{1}{2} y_1 y_2^{\frac{M-1}{2}} & M \text{ odd} \\ \frac{1}{4}\left(y_2^{M/2} + y_1^2 y_2^{\frac{M-2}{2}}\right) & M \text{ even} \end{cases} \qquad (A3.10)$$

where the summation is over all divisors of M between 1 and M, and $\phi(k)$ denotes the number of relative primes to k which are less than k. To evaluate $Z(D_M, 1+x)$ we substitute $(1+x^K)$ for y_k in (A3.10) and by putting x=1 in the result obtain $\sigma(M)$, the dimension of the matrix after symmetry reduction.

*The mathematics used in this section is taken from Harary[48] to which the reader is referred for details.

REFERENCES

1. D.S. Gaunt and M.E. Fisher, J. Chem. Phys. 43,2840 (1965)
2. D.S. Gaunt, J. Chem. Phys. 46,3237 (1967)
3. F. Calogero, J. Math. Phys. 12,419 (1971)
4. D. Ruelle, "Statistical Mechanics: Rigorous Results" (Benjamin 1969)
5. A.B. Pippard, "The Elements of Classical Thermodynamics" (C.U.P. 1966)
6. R.B. Griffiths, Phys. Rev. 136A,437 (1964)
7. R.L. Dobrušin, Funkcional Anal. i Priložen 2, 31 and 44 (1968); translated in Funct. Anal. Appl. 2,292 and 302 (1968)
8. H.J. Brascamp, Commun. Math. Phys. 18,82 (1970)
9. J.E. Mayer, J. Chem. Phys. 16,665 (1948)
10. M.E. Fisher, J. Math. Phys. 4, 278 (1963)
11. R.J. Baxter, J. Math. Phys. 11, 3116 (1970)
12. Chapter I of J. Zinn-Justin, Physics Reports 1,55 (1971) summarises the elementary properties of Padé Approximants; ref. 13 (below) contains an account of their use in the study of the critical region.
13. M.E. Fisher, Rep. Prog. Phys. 30,615 (1967)
14. A. Bellemans and S. Fuks, Physica 50,348 (1970)
15. C. Gruber and H. Kunz, Commun. Math. Phys. 22, 133 (1971)
16. N. Karayianis, C.A. Morrison, and D.E. Wortman, J. Math. Phys. 7,1458 (1966)
17. L.K. Runnels, Phys. Rev. Lett. 15,581 (1965)
18. L.K. Runnels and L.L. Combs, J. Chem. Phys. 45,2482 (1966)
19. L.K. Runnels, L.L. Combs, and J.P. Salvant, J. Chem. Phys. 47,4015 (1967)
20. L.K. Runnels, J. Math. Phys. 11, 842 (1970)
21. L.K. Runnels, J.P.Salvant and H.R. Streiffer, J.Chem. Phys. 52, 2352 (1970)
22. L.K. Runnels, J.R. Craig, and H.R. Streiffer, J. Chem. Phys. 54,2004 (1971)
23. F.H. Ree and D.A. Chesnut, J. Chem. Phys. 54,3983 (1966)
24. F.H. Ree and D.A. Chesnut, Phys. Rev. Lett. 18,5 (1967)
25. A. Bellemans and R.K. Nigam, J. Chem. Phys. 46, 2922 (1967)
26. J. Orban and A. Bellemans, J. Chem. Phys. 49,363 (1968)
27. A. Bellemans and J. Orban, Phys. Rev. Lett. 17,908 (1966)
28. J. Orban, Ph.D. Thesis, Université Libre de Bruxelles (1969)
29. D.A. Chesnut, J. Comput. Phys. 7,409 (1971)
30. G. Marsaglia, Proc. Nat. Acad. Sci. 61, 25 (1968)
31. R.M. Nisbet. and I.E. Farquhar, J. Chem. Phys. 52,3310 (1970)
32. J.H. Wilkinson, "The Algebraic Eigenvalue Problem" (Clarendon, Oxford 1965)

33. E.M. Patterson and D.E. Rutherford, "Elementary Abstract Algebra" (Oliver and Boyd 1965)
34. A.L. Dulmage and N.S. Mendelsohn, "Graphs and Matrices" in "Graph Theory and Theoretical Physics" Ed. Harary (Academic Press 1967)
35. J. Ashkin and W.E. Lamb, Jr., Phys. Rev. 64,159 (1943)
36. J. Grad and M.A. Brebner, Commun. ACM, 11,820 (1968) and references therein.
37. C.F. Bender and I. Shavitt, J. Comput. Phys. 6,146 (1970)
38. G.Forsythe, L.Straus, J. Math.and Phys. 34,153(1955)
39. See e.g. W.E. Grove, "Brief Numerical Methods" (Prentice-Hall 1966) p. 66
40. D. Shanks, J. Math. and Phys. 34,1 (1955)
41. D.S. Gaunt, Phys. Rev. 179,174 (1969)
42. J. Van Craen, Physica 49, 558 (1970)
43. A. Bellemans and J. Van Craen, Paper submitted to the I.U.P.A.P. Conference on Statistical Mechanics, Chicago 1971.
44. L. Onsager, Phys. Rev. 65,117 (1944)
45. T.D. Lee and C.N. Yang, Phys. Rev. 87,410 (1952)
46. C.N. Yang, Phys. Rev. 85, 808 (1952)
47. W.L. Ferrar, "Higher Algebra" (Clarendon, Oxford 1943)p.175
48. F. Harary, "Graphical Enumeration Problems" in "Graph Theory and Theoretical Physics" Ed. Harary (Academic Press 1967)
49. W.G. Hoover, B.J. Alder, and F.H. Ree, J. Chem. Phys.41,3528(1964)
50. R.K. Nesbet, J. Chem. Phys. 43, 311 (1965)
51. I. Shavitt, J. Comput. Phys. 6, 124 (1970)
52. Chapter II of Ref. 32
53. R.S. Varga, "Matrix Iterative Analysis" (Prentice-Hall 1962)

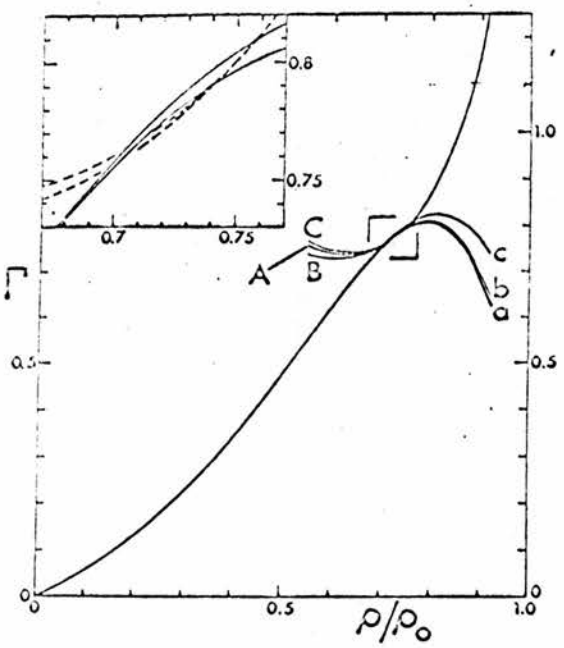

FIG. 7. Plot of the reduced pressure, $\Gamma = pa^2/k_B T$ vs density ρ. Curves a, b, c are the [6, 7], [7, 6], and [6, 6] Padé approximants to the low-density $\Gamma(\rho)$ series. The high-density curves A, B, C are derived from the [4, 4], [3, 4], and [3, 3] approximants to the $\Gamma^*(\rho')$ series. Further details of the curves a and c (solid lines) and the curves B and C (broken lines) in the transition region are given in the inset which covers the region indicated on the main plot.

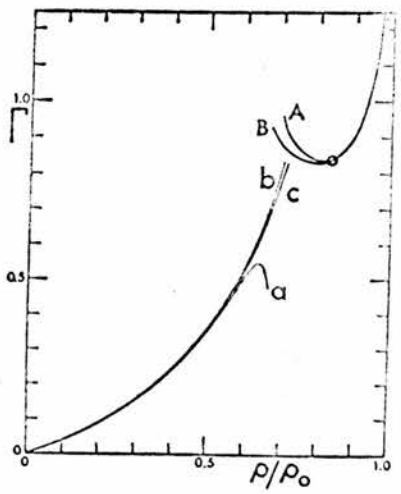

FIG. 2. Triangular lattice gas. Plot of the reduced pressure $\Gamma \equiv pr_0/k_B T$ versus reduced density ρ/ρ_0. Curves a, b, and c are the [4,4], [3,4], and [3,3] Padé approximants to the low-density $\Gamma(\rho)$ series. The high-density curves A and B are derived from the [2,2] and [1,2] approximants to the $\Gamma^*(\rho')$ series. The point (Γ_2, ρ_2) at which the high-density series are singular is indicated by a circle.

Figs. 1.2.1 and 1.2.2: Isotherms for the SQ1 (left) and TR1 models obtained by constructing Pade Approximants to the various series expansions (xeroxed from refs. 1 and 2).

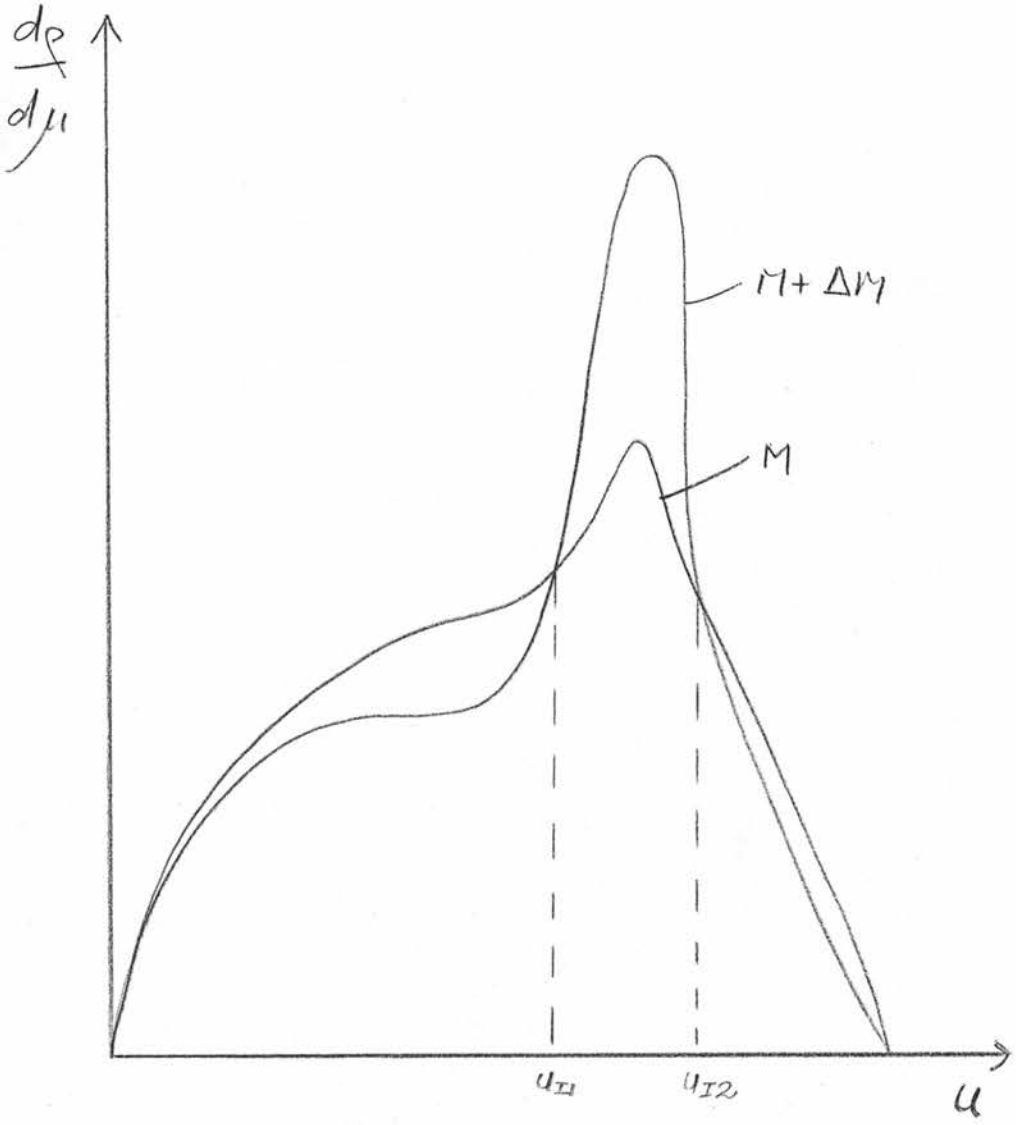

Fig. 2.5.1: Postulated variation of $\frac{d\rho}{d\mu}$ with u for lattices of width M and M + ΔM.

fig. 2.6.1: Superexchange Model. The solid lines define the underlying lattice. In addition to the nearest-neighbour exclusion there is an attractive potential across alternate sets of second-neighbours.

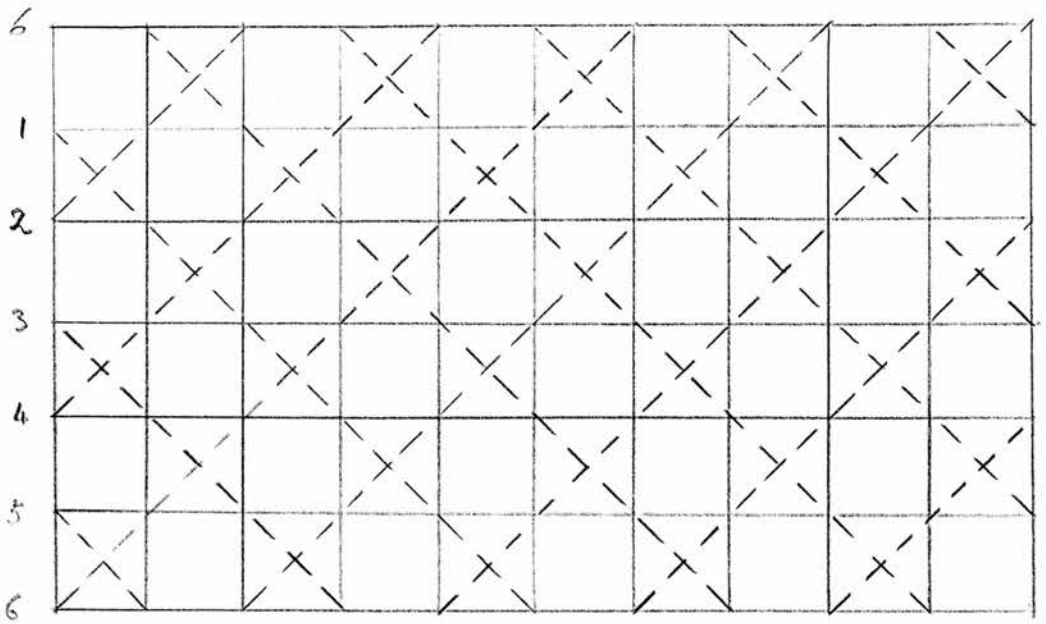

fig. 2.6.2: Superexchange Model. The lattice takes this form after the "twisting" described in section 2.6.

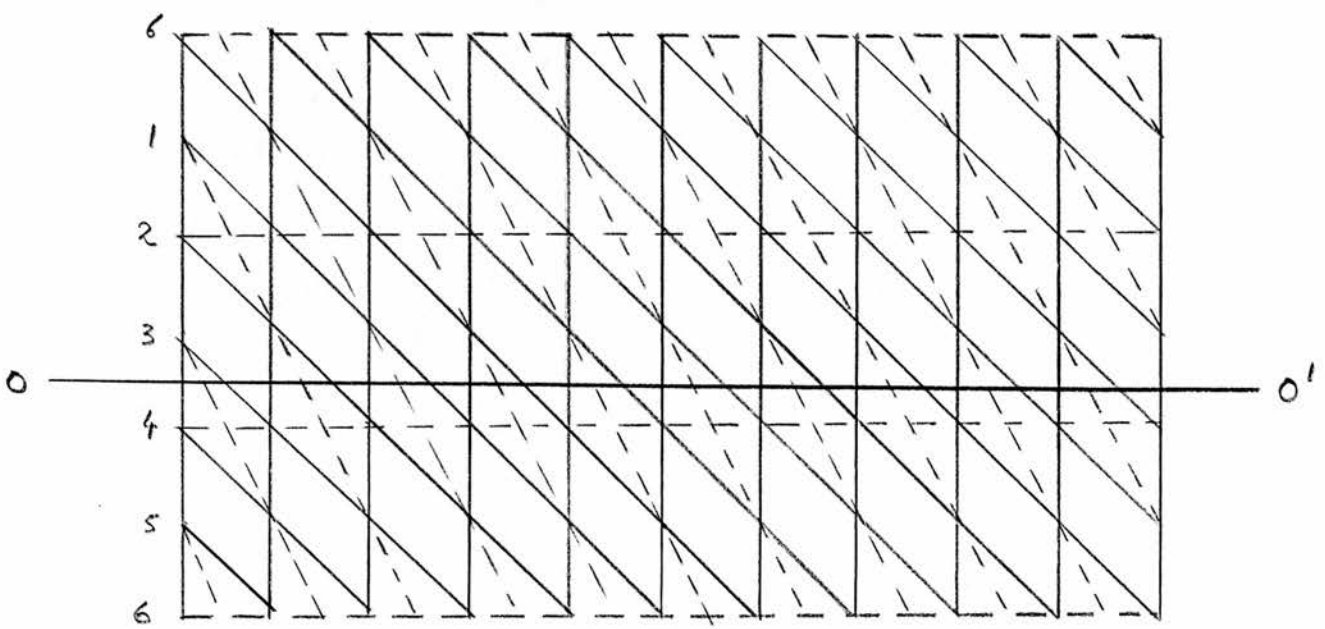

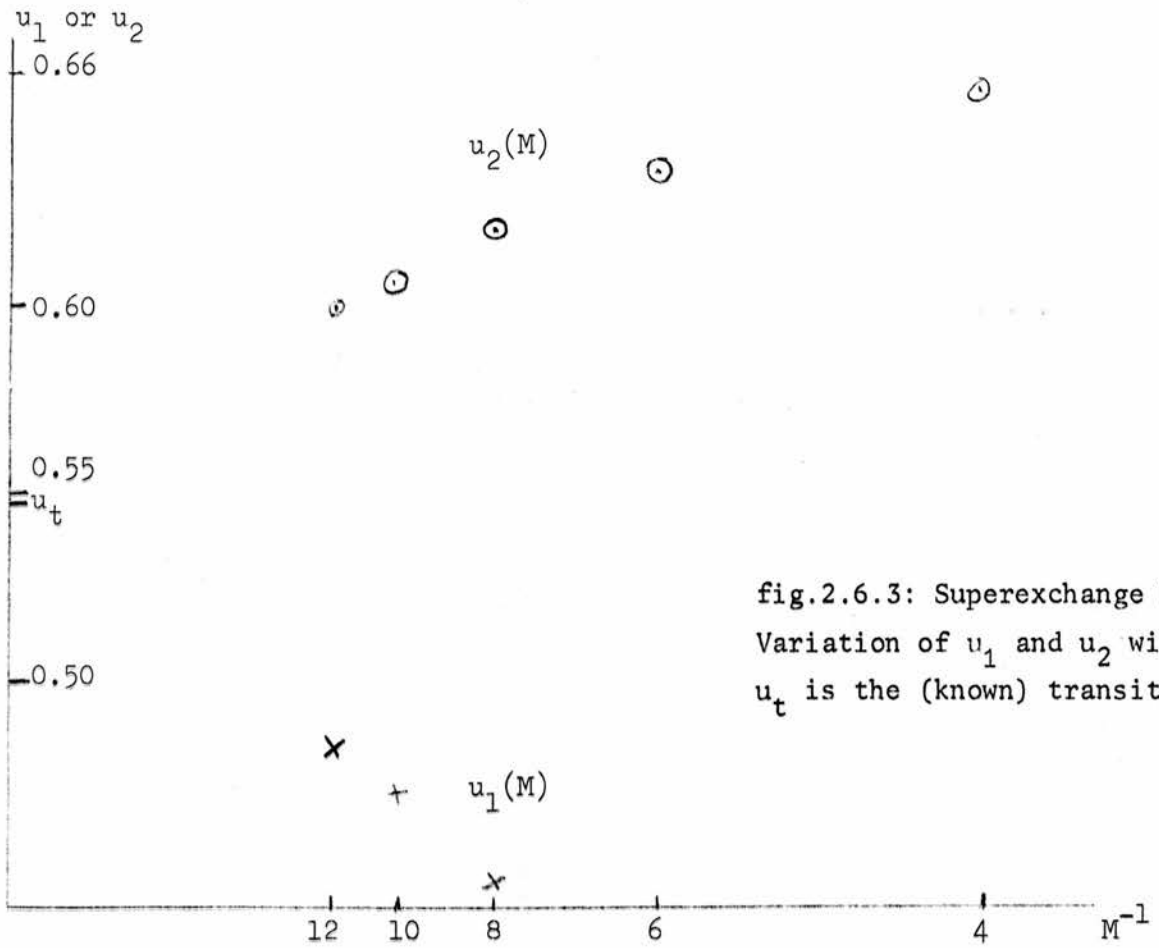

fig.2.6.3: Superexchange Model - Variation of u_1 and u_2 with M^{-1}. u_t is the (known) transition point.

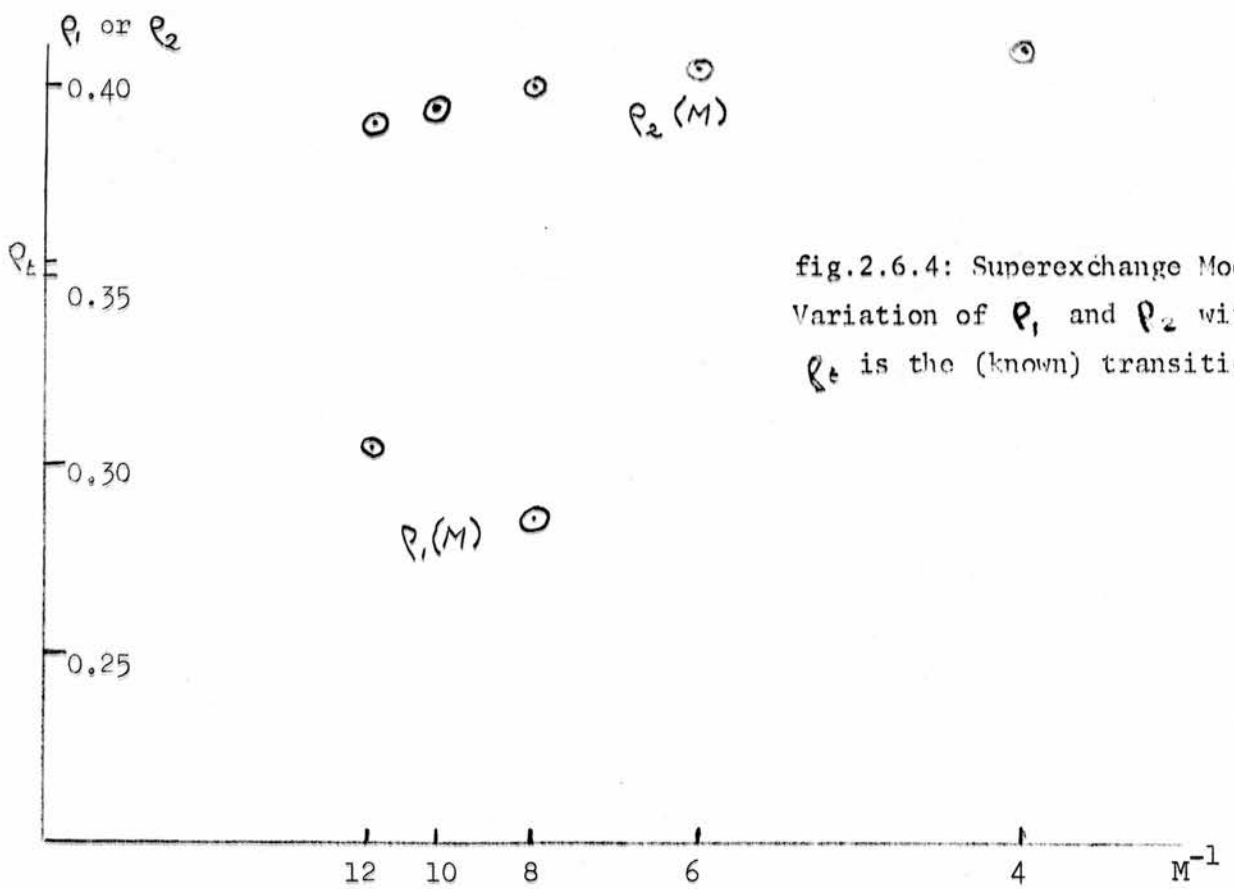

fig.2.6.4: Superexchange Model - Variation of ρ_1 and ρ_2 with M^{-1}. ρ_t is the (known) transition point.

fig. 2.6.5: Superexchange Model — Variation of $(d\rho/d\mu)_{max}$ with log M

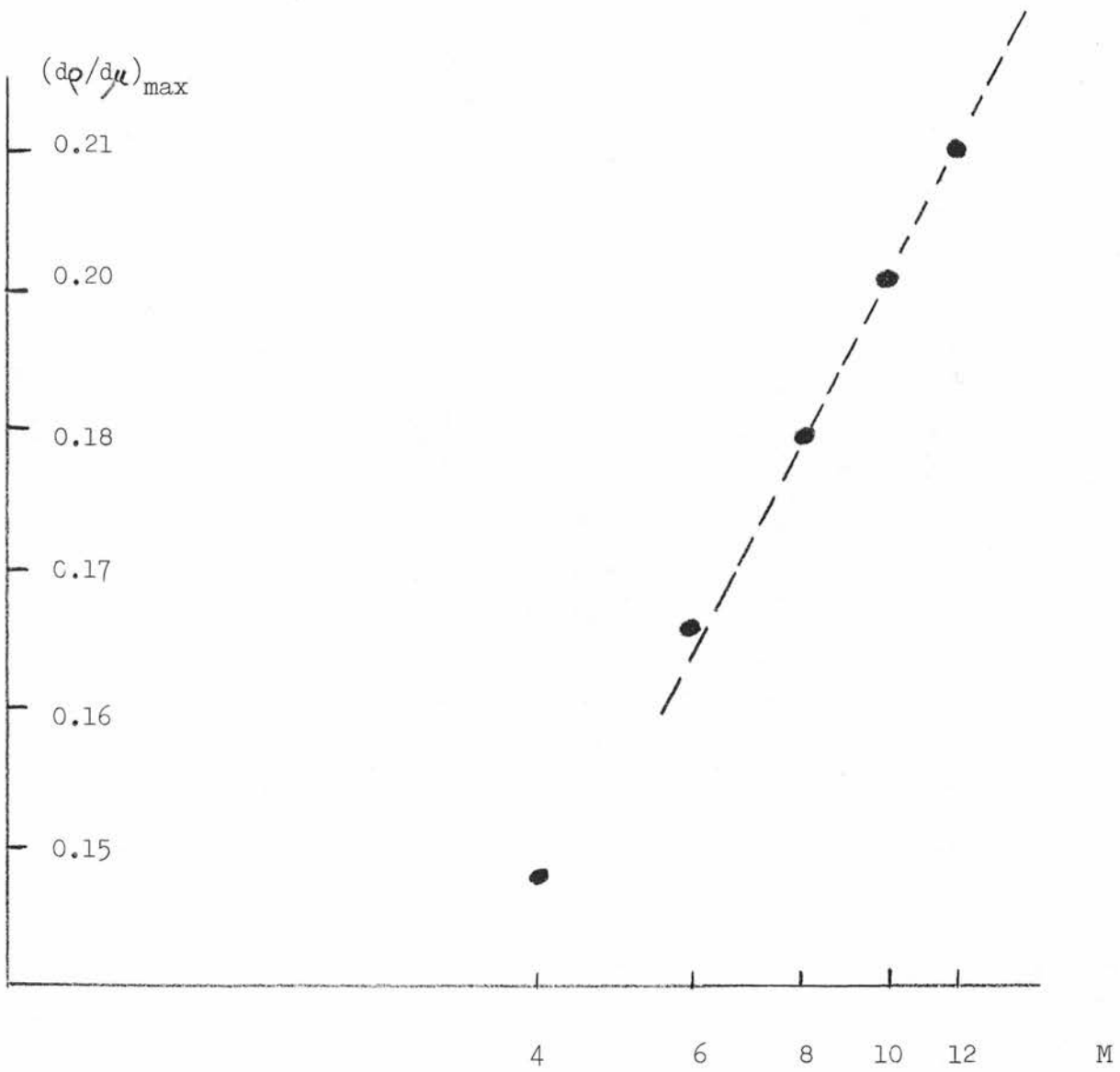

FIG 266: LATTICE GAS WITH ATTRACTION — PLOT OF $\left(\frac{dp}{d\mu}\right)_{max}$ AGAINST LOG M.

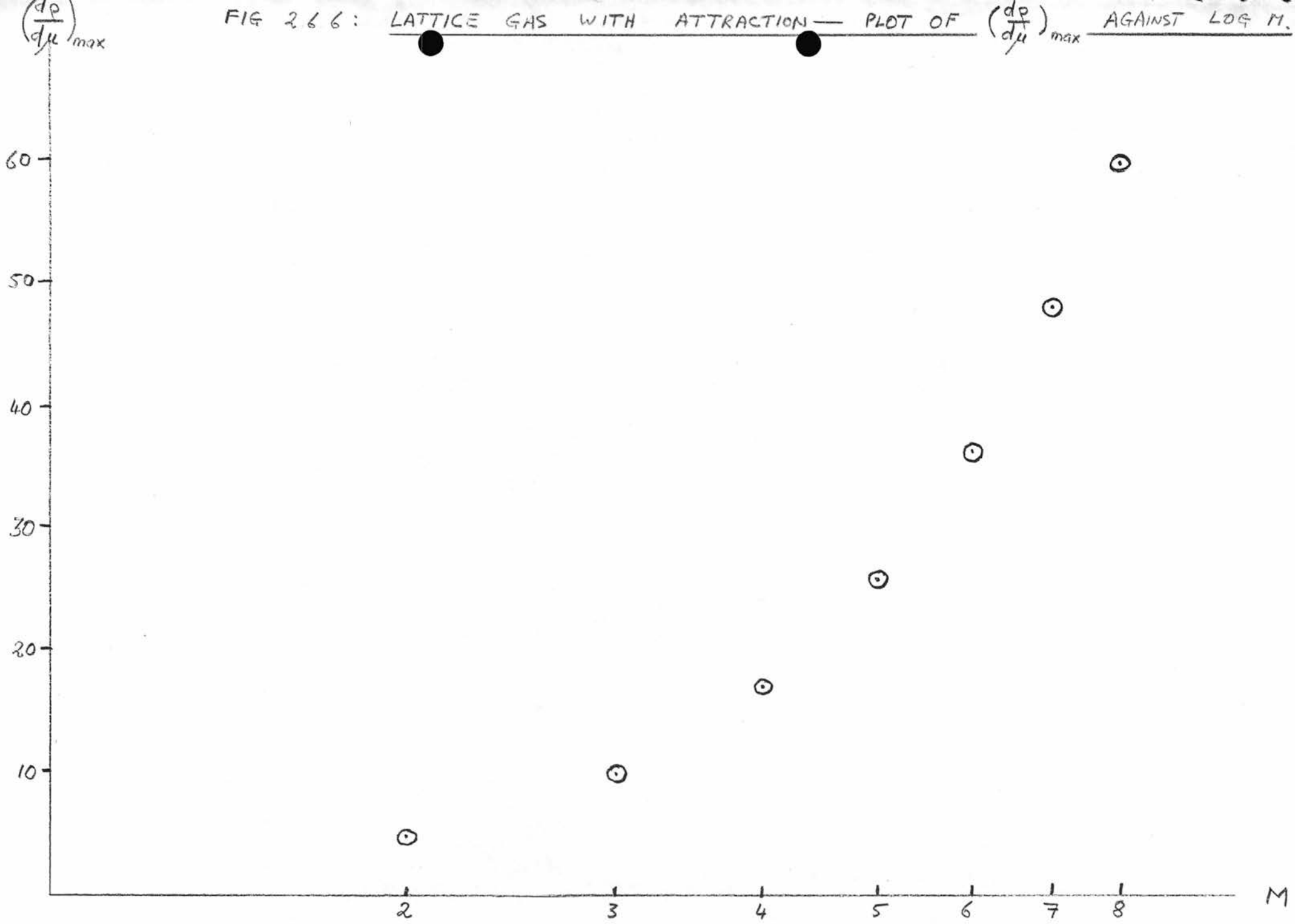

fig. 2.6.7: Lattice Gas with Attraction, $\xi = 6$ — plot of log $(d\rho/d\mu)_{max}$ against log M.

(consistent with $(d\rho/d\mu)_{max} \sim M^{\alpha}$ with $1.8 < \alpha < 1.9$)

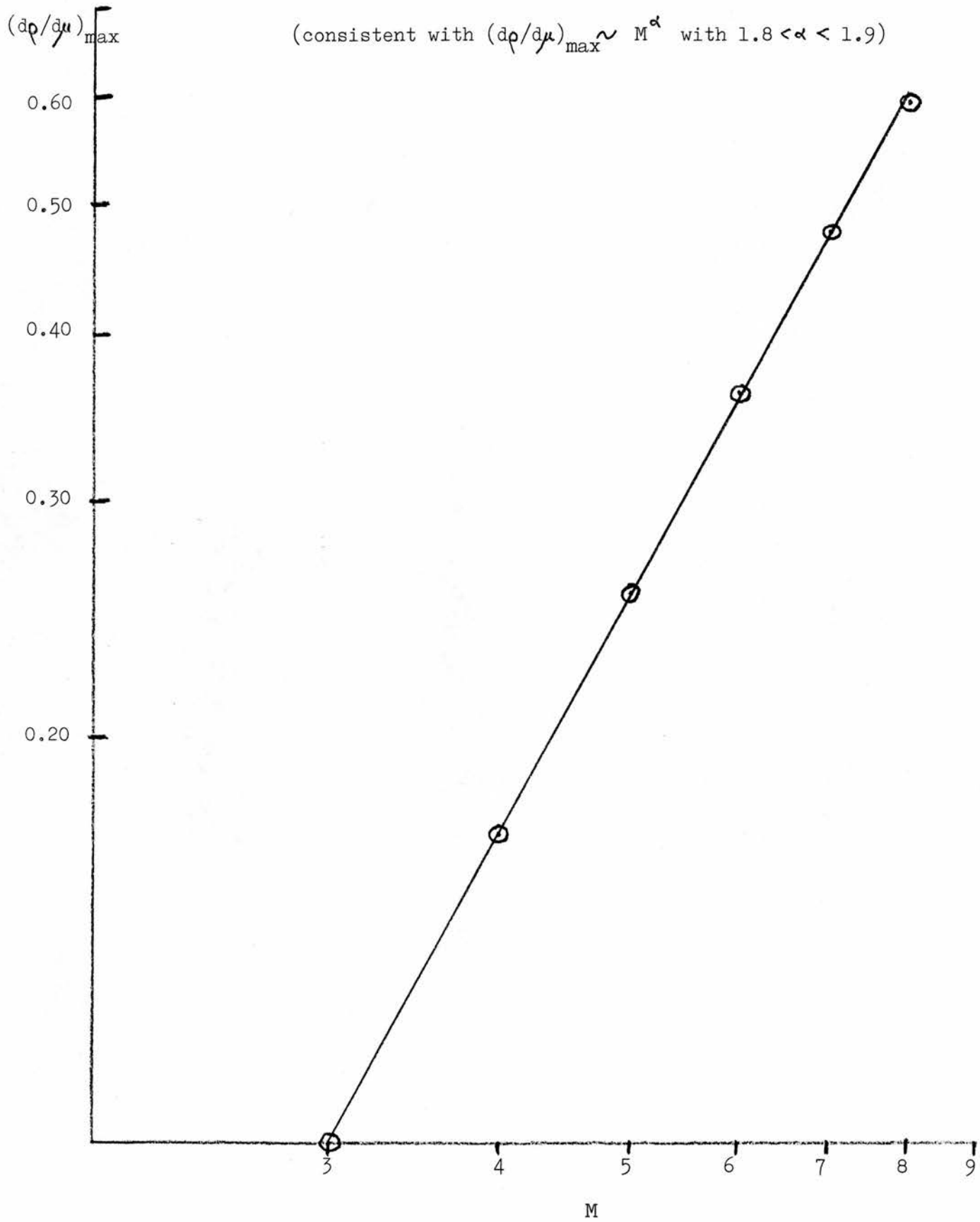

FIG. 2 6 8 : LATTICE GAS WITH ATTRACTION — PLOT OF $P_1(M)$ AND $P_2(M)$ AGAINST M^{-1}.

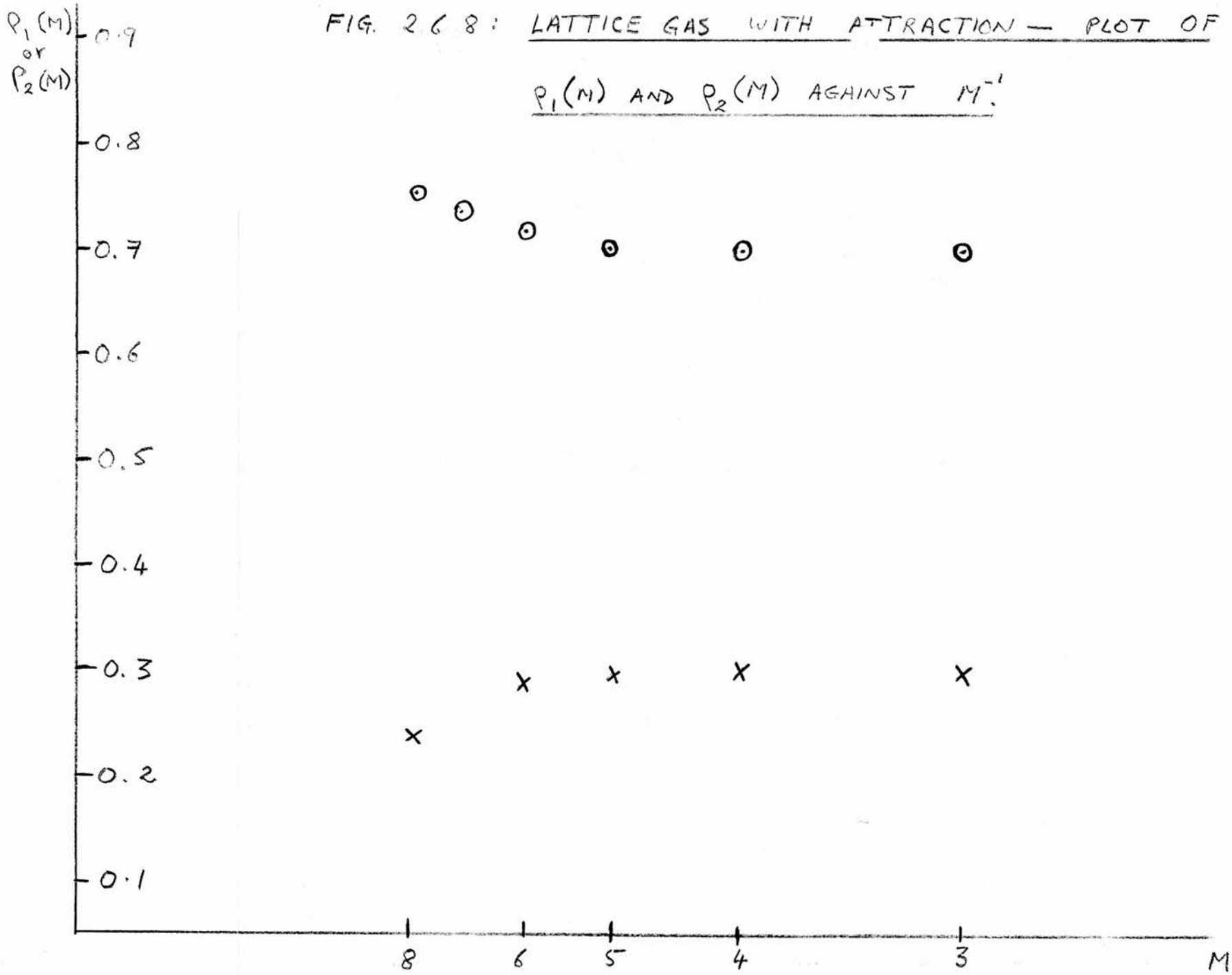

FIG 2.6.9: LATTICE GAS WITH ATTRACTION — $\zeta = 6$

PLOT OF $u_1(M)$ AND $u_2(M)$ AGAINST M^{-1}

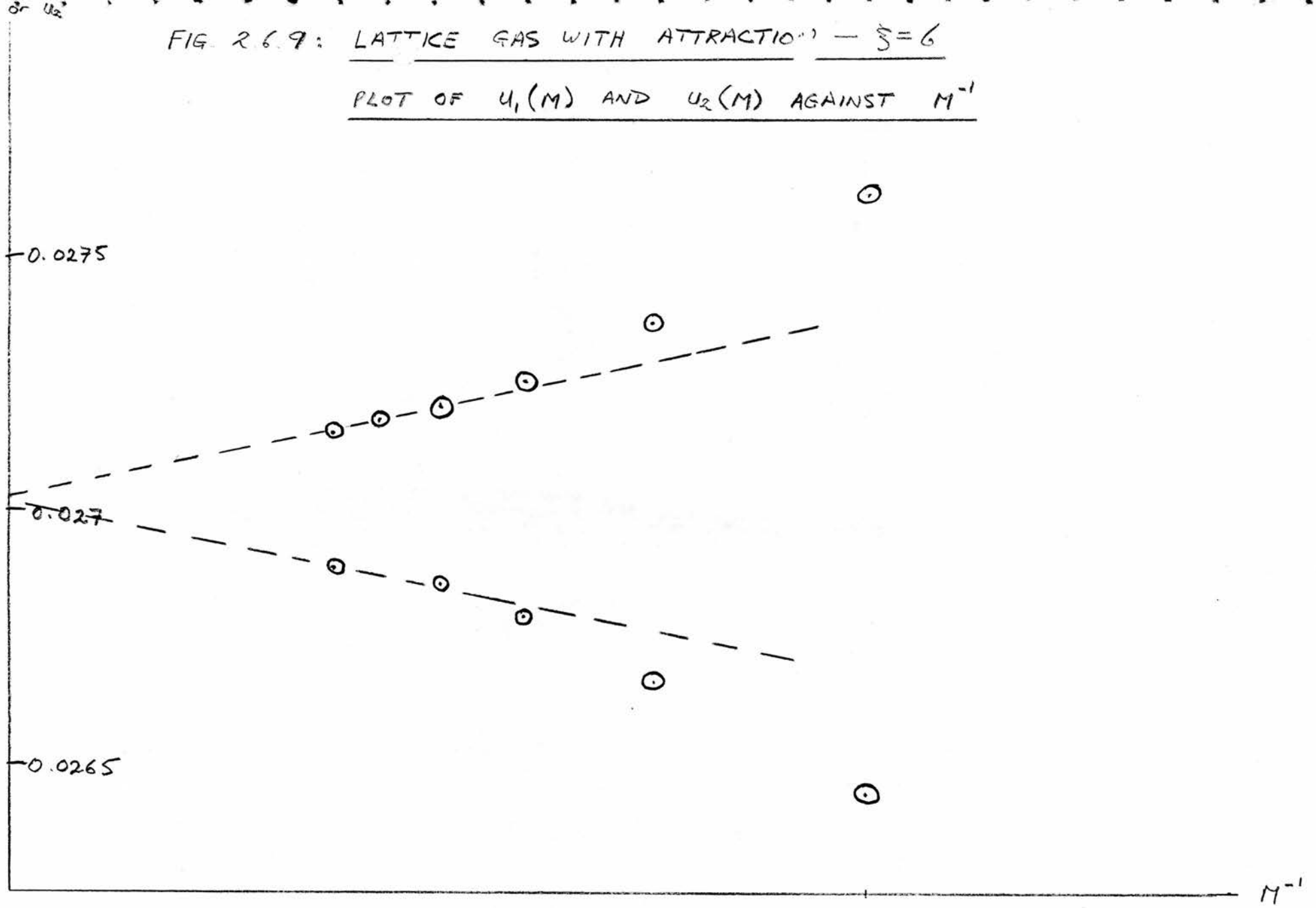

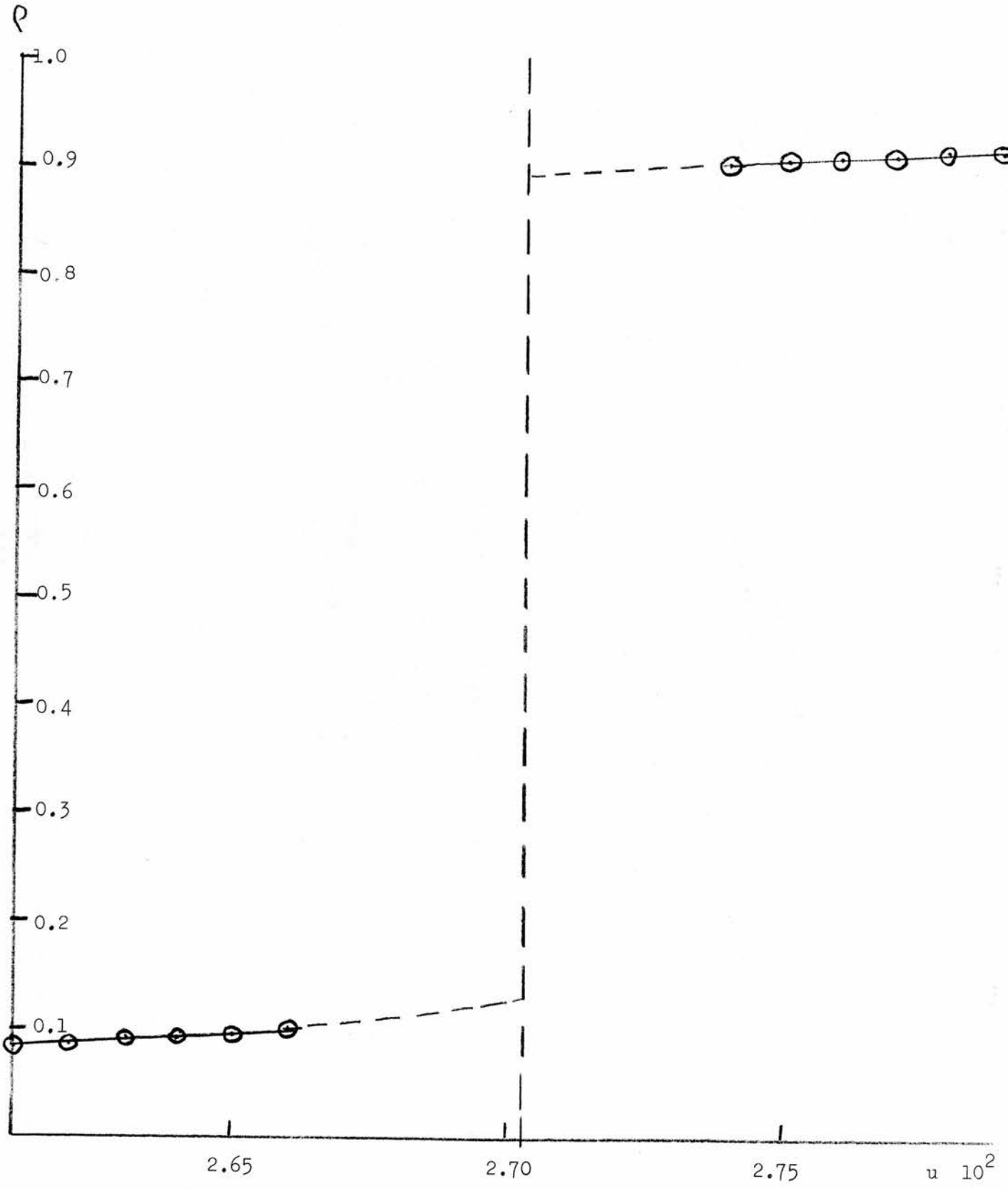

fig. 2.6.10: Lattice Gas with Attraction — Plot of ρ (obtained by e_1 transforming the results from lattices of width M=2,3,....8) against $\bar{u}$.

FIG. 2.6.11 : SQI MODEL — PLOT OF $\left(\frac{d\rho}{d\mu}\right)_{max}$ AGAINST LOG M

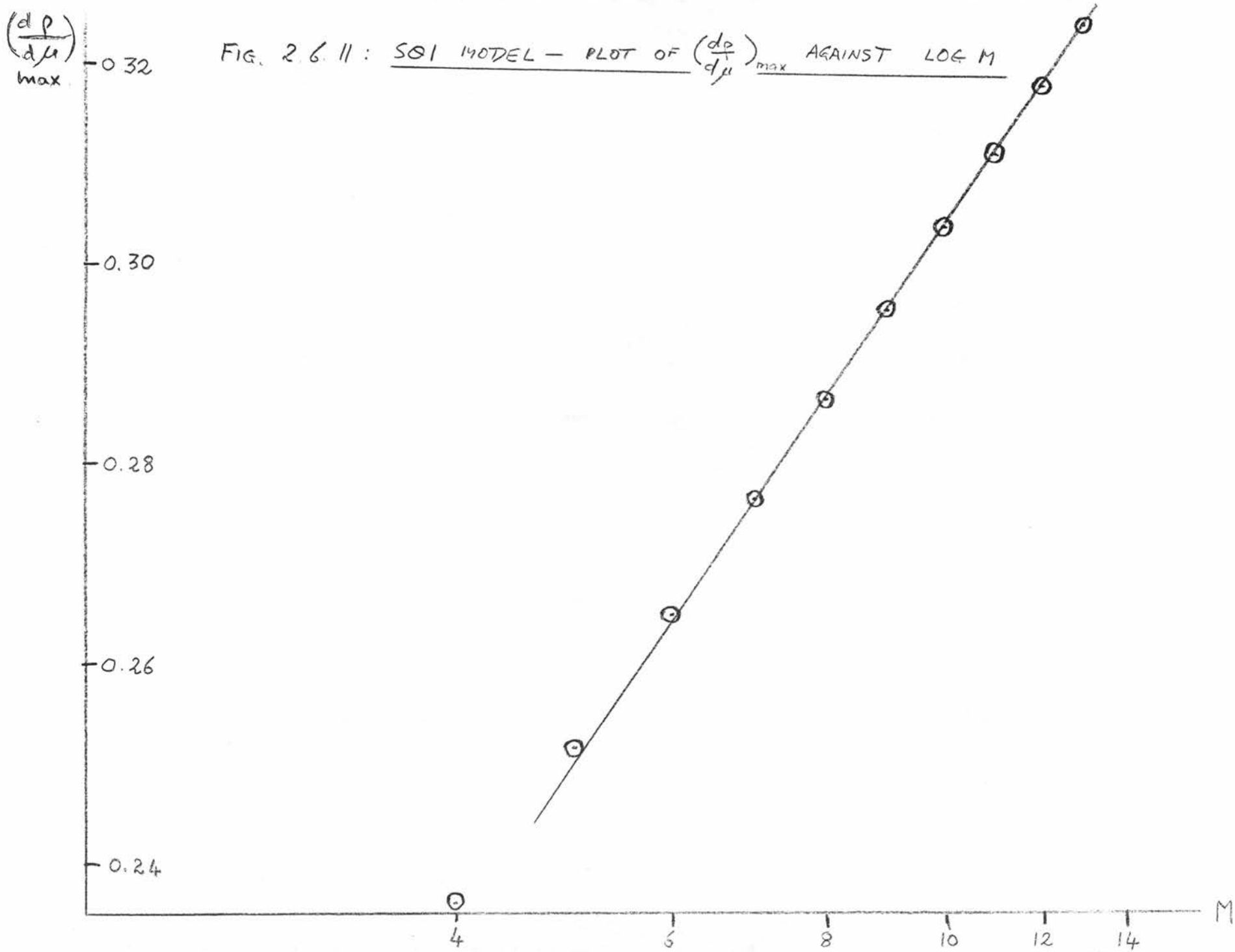

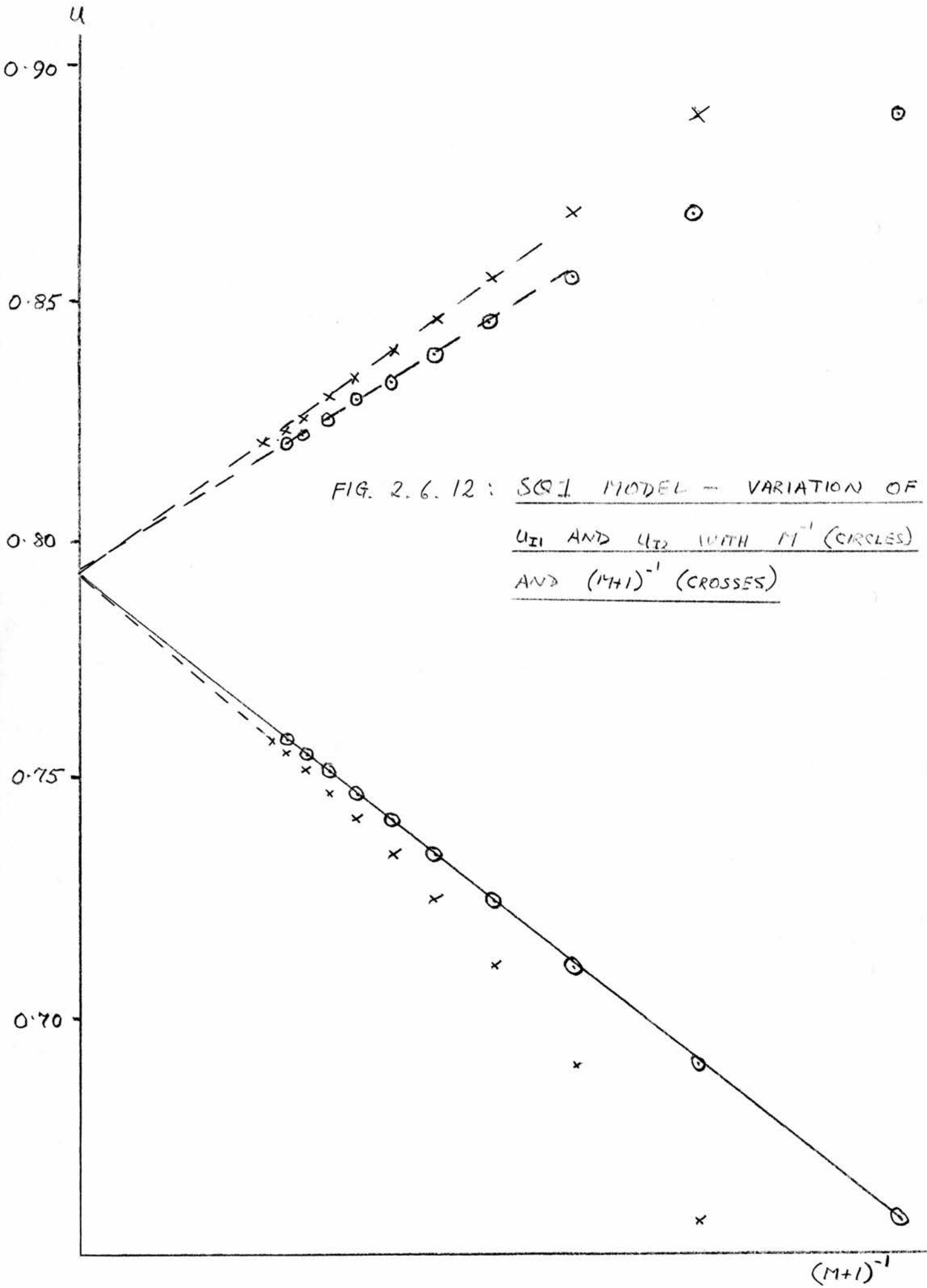

FIG. 2.6.12 : SQI MODEL – VARIATION OF u_{I1} AND u_{I2} WITH M^{-1} (CIRCLES) AND $(M+1)^{-1}$ (CROSSES)

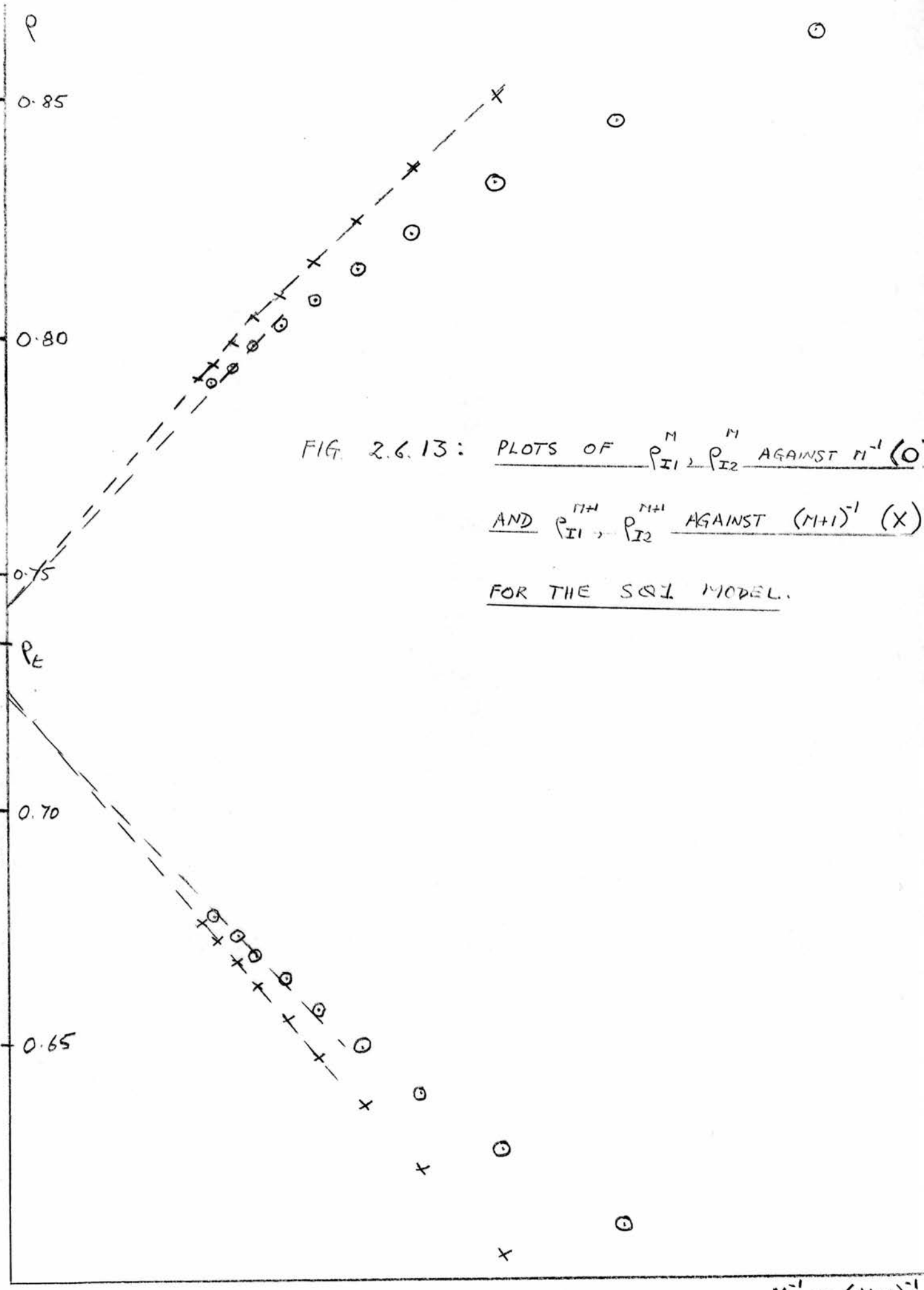

FIG. 2.6.13: PLOTS OF ρ_{I1}^{M}, ρ_{I2}^{M} AGAINST M^{-1} (O) AND ρ_{I1}^{M+1}, ρ_{I2}^{M+1} AGAINST $(M+1)^{-1}$ (X) FOR THE SOI MODEL.

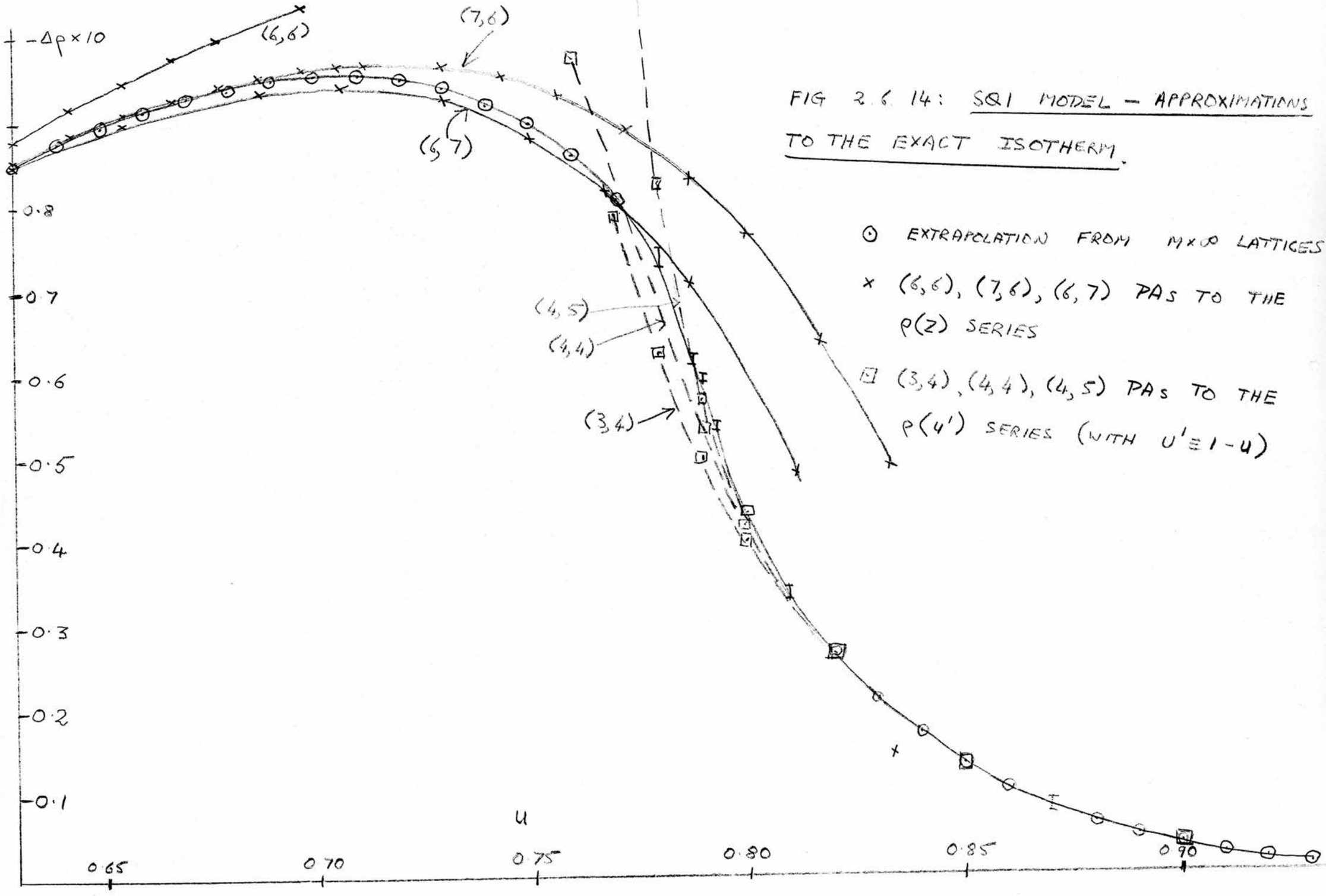

FIG 2.6.14: SQ1 MODEL — APPROXIMATIONS TO THE EXACT ISOTHERM.

⊙ EXTRAPOLATION FROM M×∞ LATTICES

× (6,6), (7,6), (6,7) PAs TO THE P(Z) SERIES

⊡ (3,4), (4,4), (4,5) PAs TO THE P(4') SERIES (WITH $u' \equiv 1-u$)

FIG. 2.6.15: VARIATION OF $\Delta\rho$ ($\equiv \rho - u$) WITH $u \in (0.75, 0.83)$ FOR THE SQI MODEL.

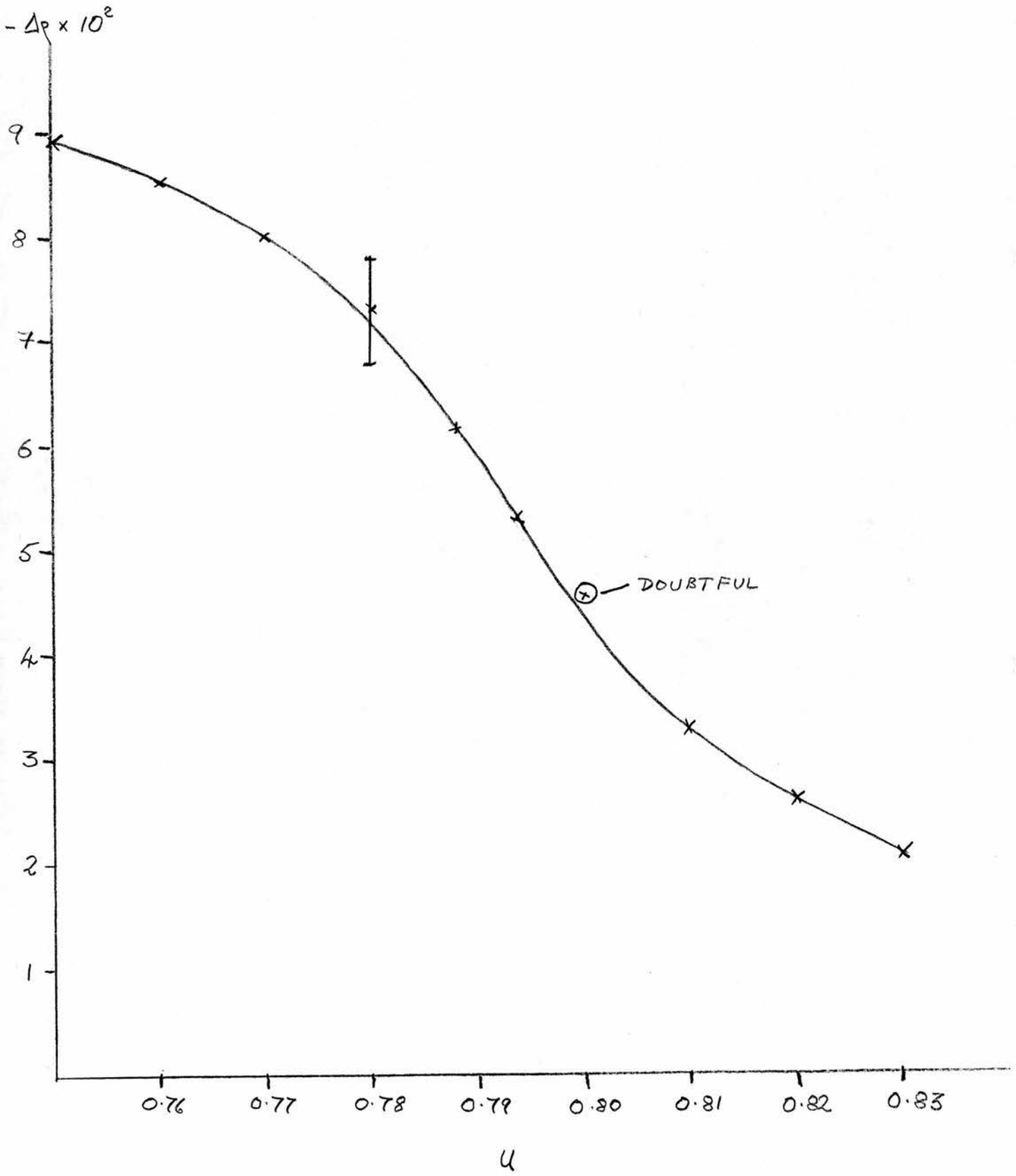

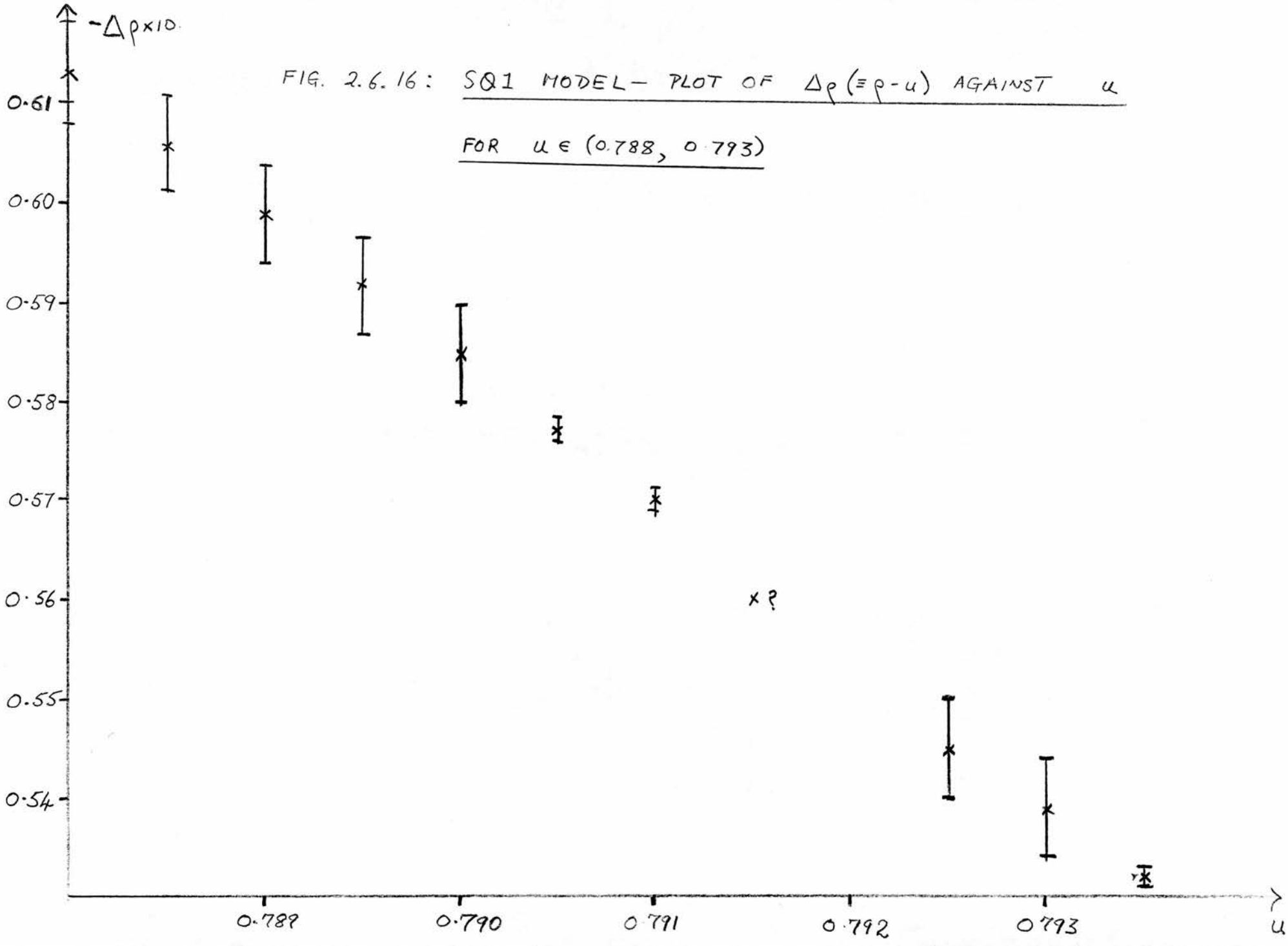

FIG. 2.6.16: SQ1 MODEL — PLOT OF $\Delta\rho$ ($\equiv \rho - u$) AGAINST u FOR $u \in (0.788, 0.793)$

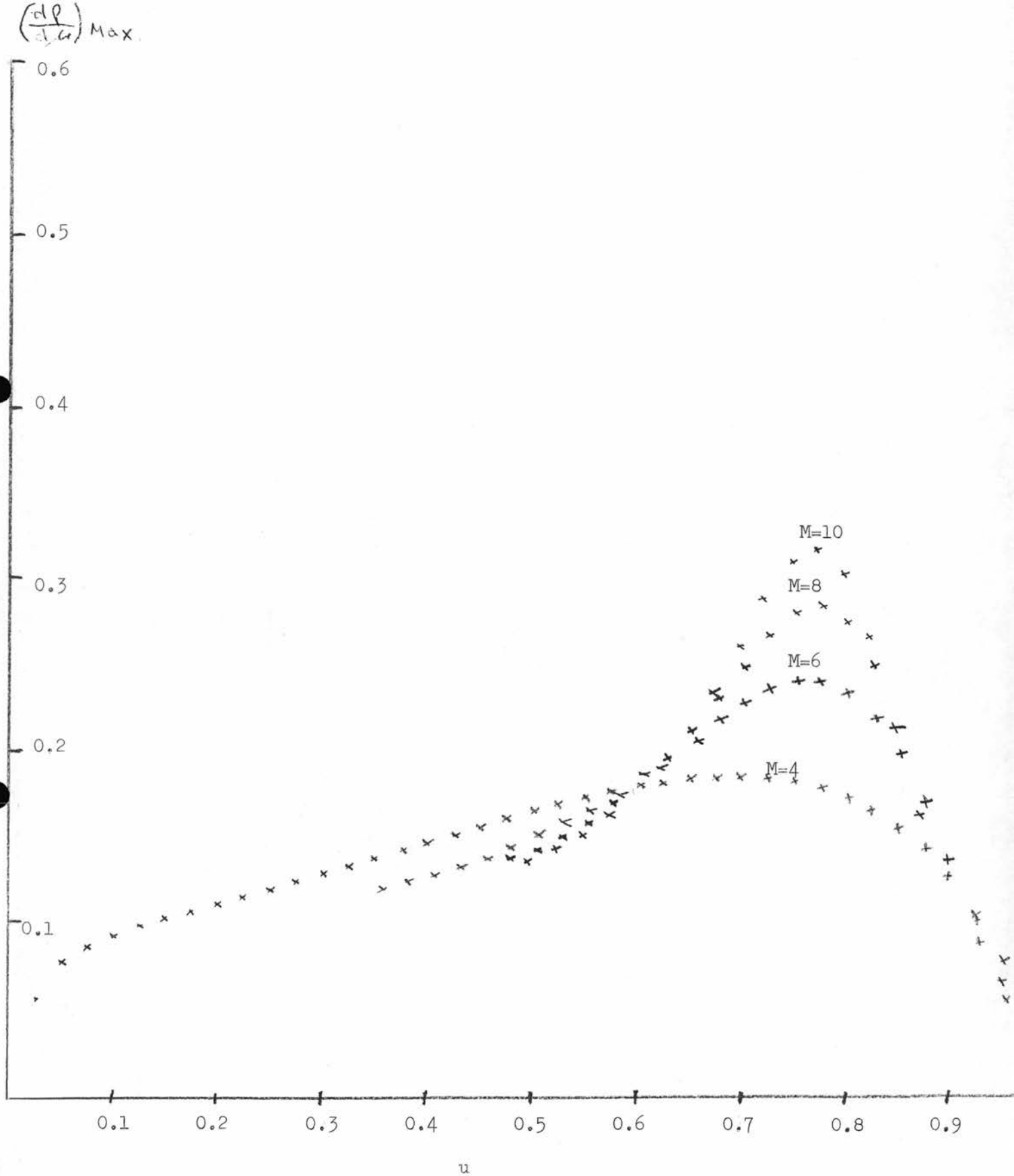

Fig. 3.1.1: SQ124 Model — variation of $\left(\frac{dp}{du}\right)_{max}$ with u for even-periodic lattices.

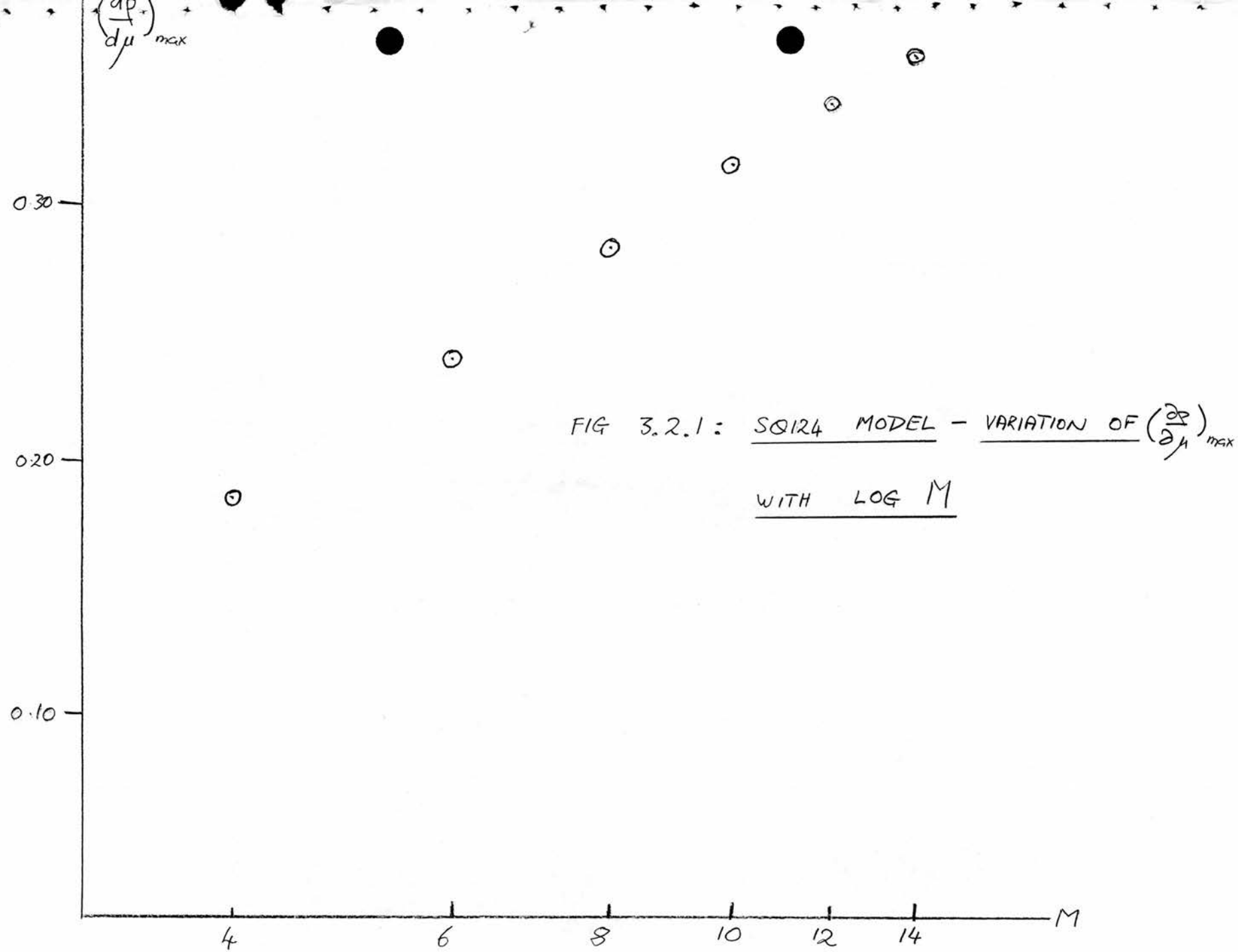

FIG 3.2.1 : SQ124 MODEL – VARIATION OF $\left(\frac{\partial p}{\partial \mu}\right)_{max}$ WITH LOG M

FIG. 3.3.1: PLOT OF ΔP ($\equiv P/kT - \frac{1}{4}\log Z$) AGAINST u FOR THE SQ124 MODEL.

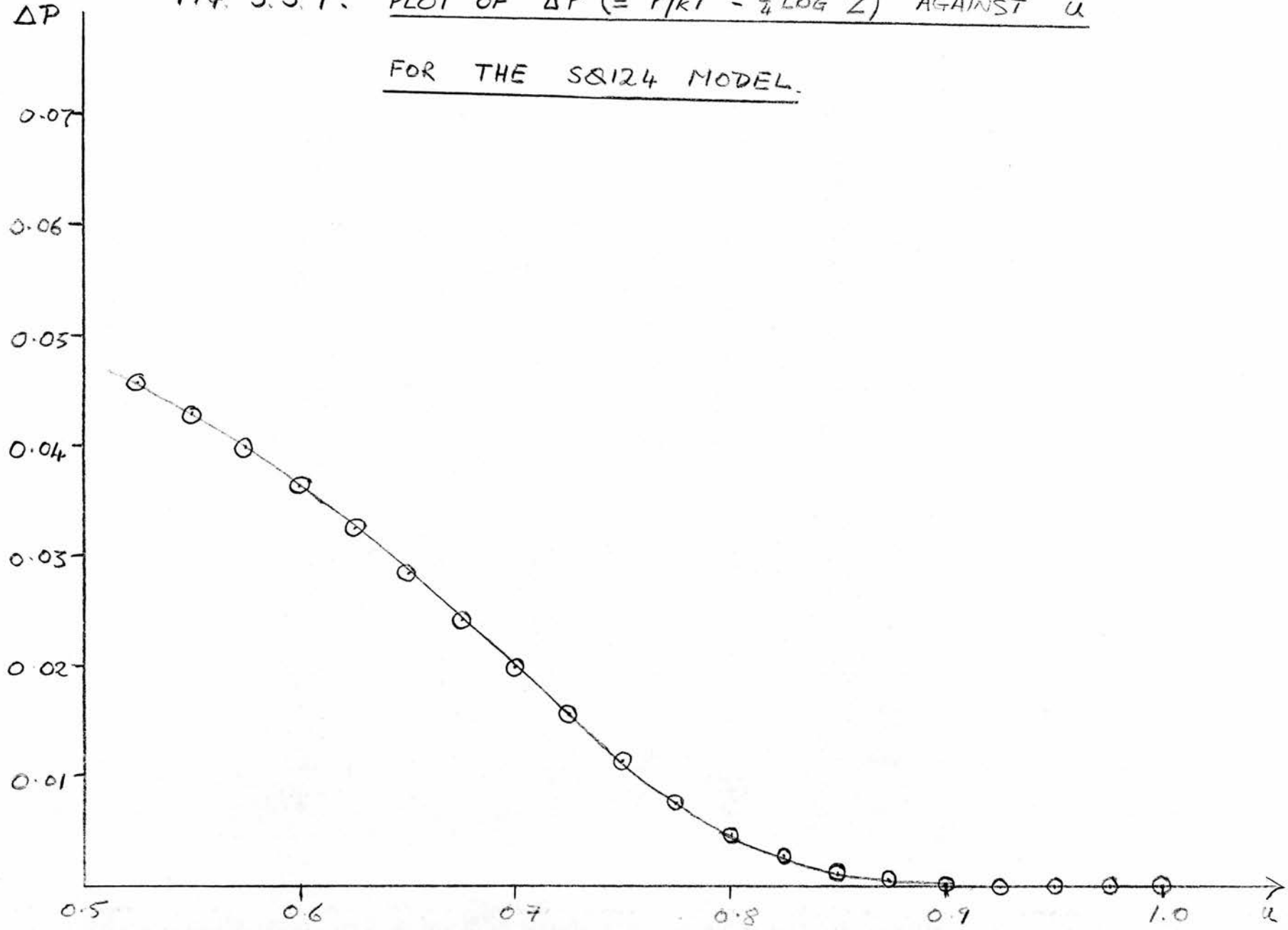

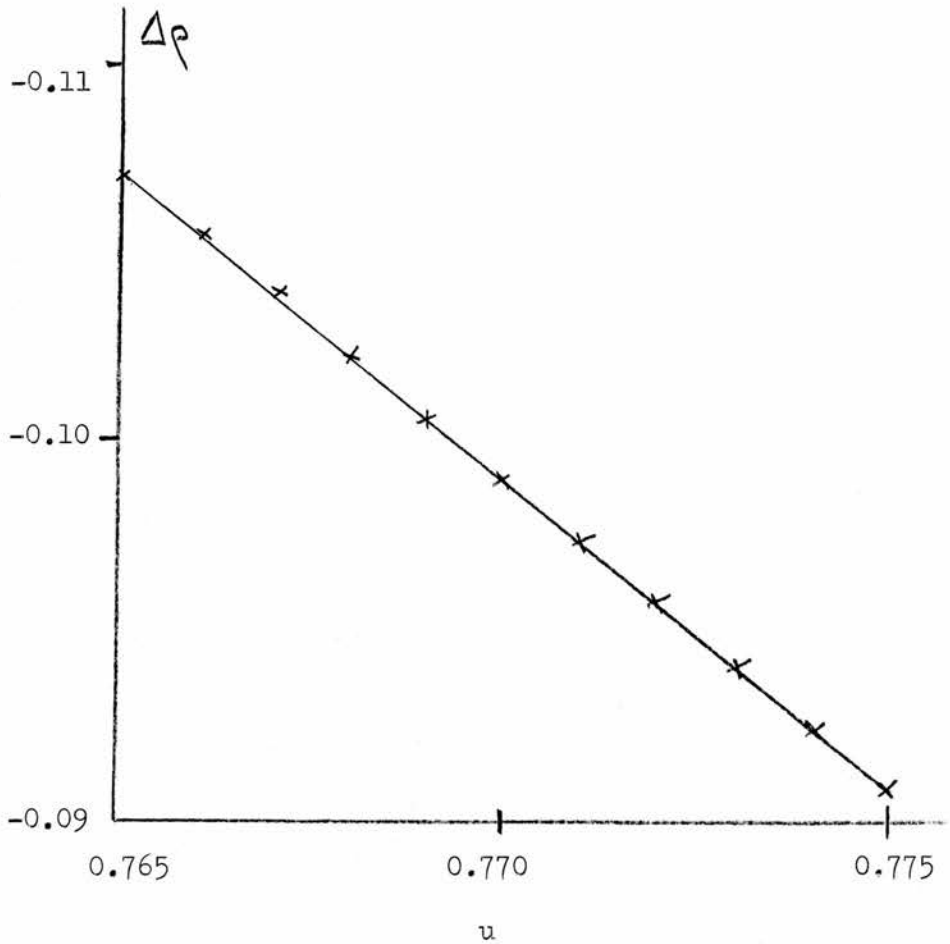

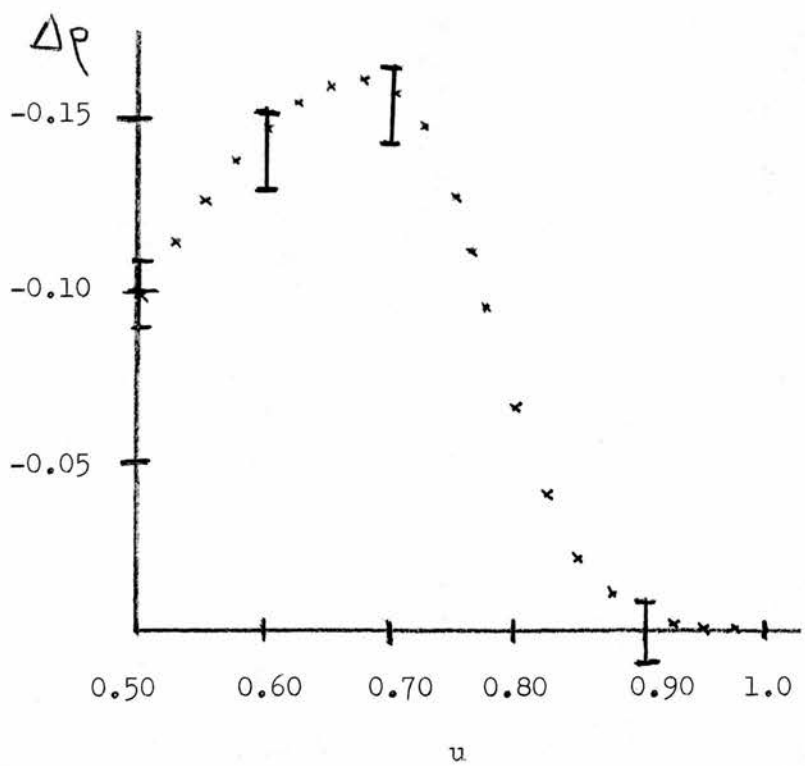

Fig. 3.3.2 (below) and fig. 3.3.3 (above): SQ124 model — exact isotherm of the infinite lattice. The results are from extrapolation of densities of periodic lattices. The points marked I are from lattices with free boundaries. The accuracy of the points in fig. 3.3.3 is uncertain.

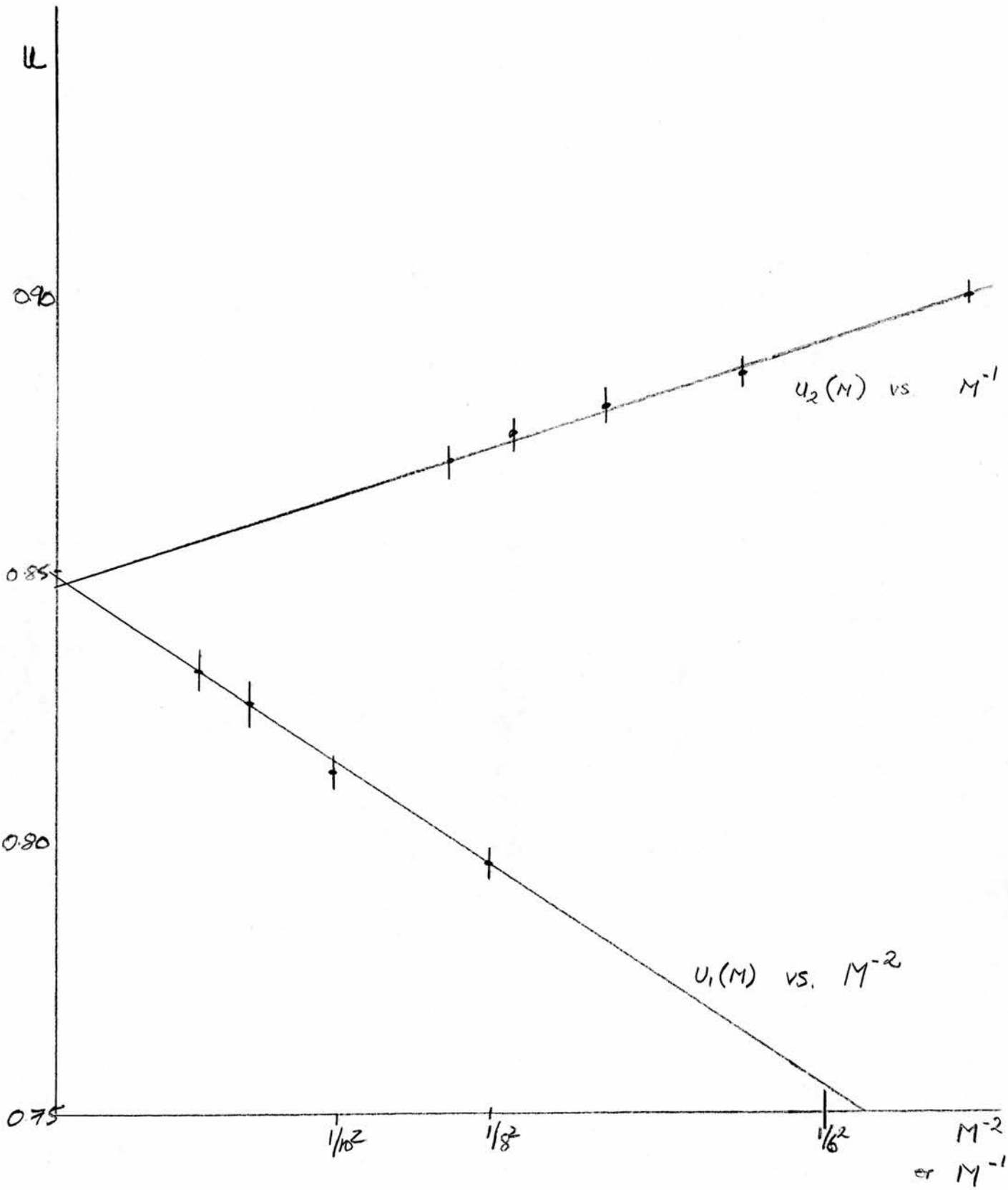

Fig. 4.1.1: TR12 Model — variation of u (M) and u (M) with M. (A tracing of a graph kindly communicated to the author by Dr. J Orban)

Fig. 4.2.1: SQ123 Model -- Close-packed Configurations.

(1) Infinite Lattice.

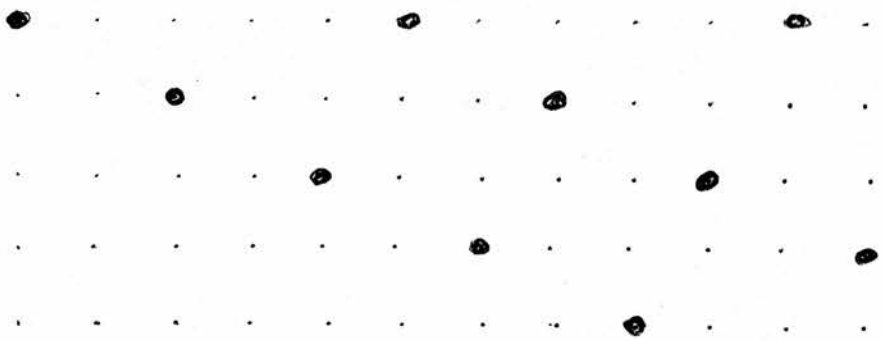

$\rho_{max} = \frac{1}{5}$

(2) Free Boundary Conditions, M=4.

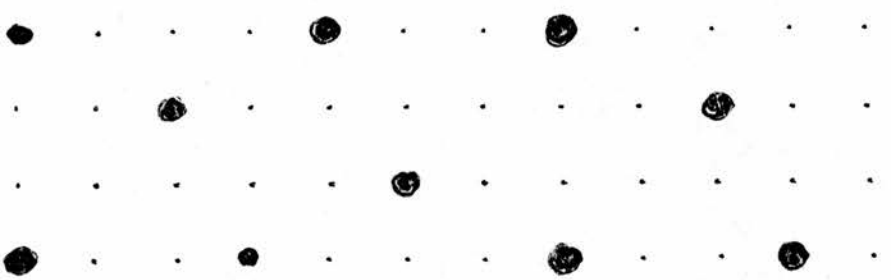

$\rho_{max} = \frac{3}{14}$

$\therefore = 0.214$

(3) Almost-Periodic Boundary Conditions, M=4.

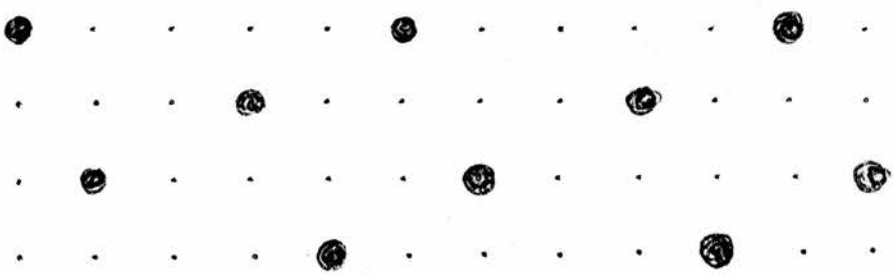

$\rho_{max} = \frac{1}{5}$

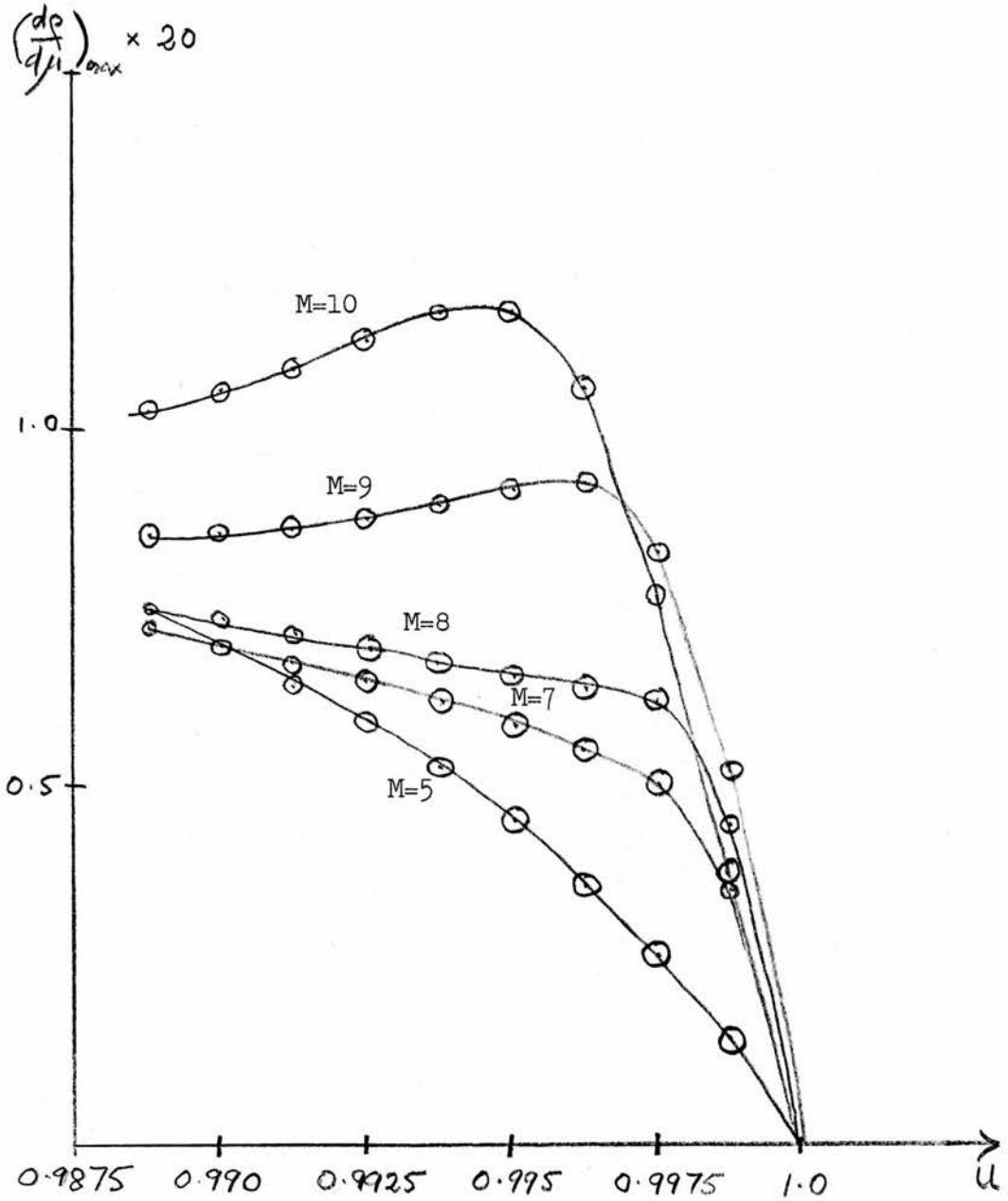

Fig. 4.2.2: SQ123 Model with almost-periodic boundary conditions — Variation of $(dp/du)_{max}$ with u.

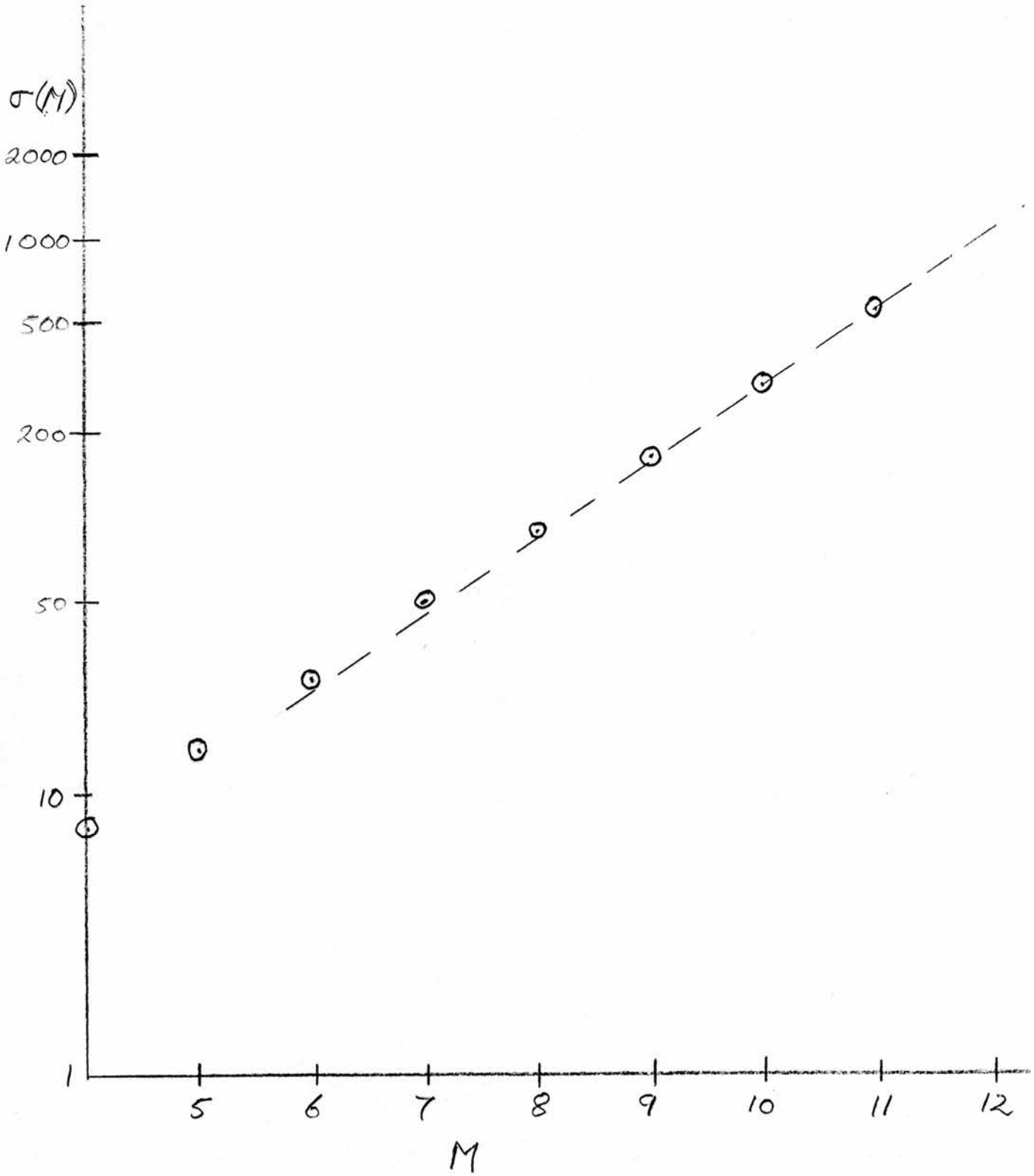

Fig. 4.2.3: Dimension of the transfer matrix for the SQ123 model with "almost-periodic boundary conditions".

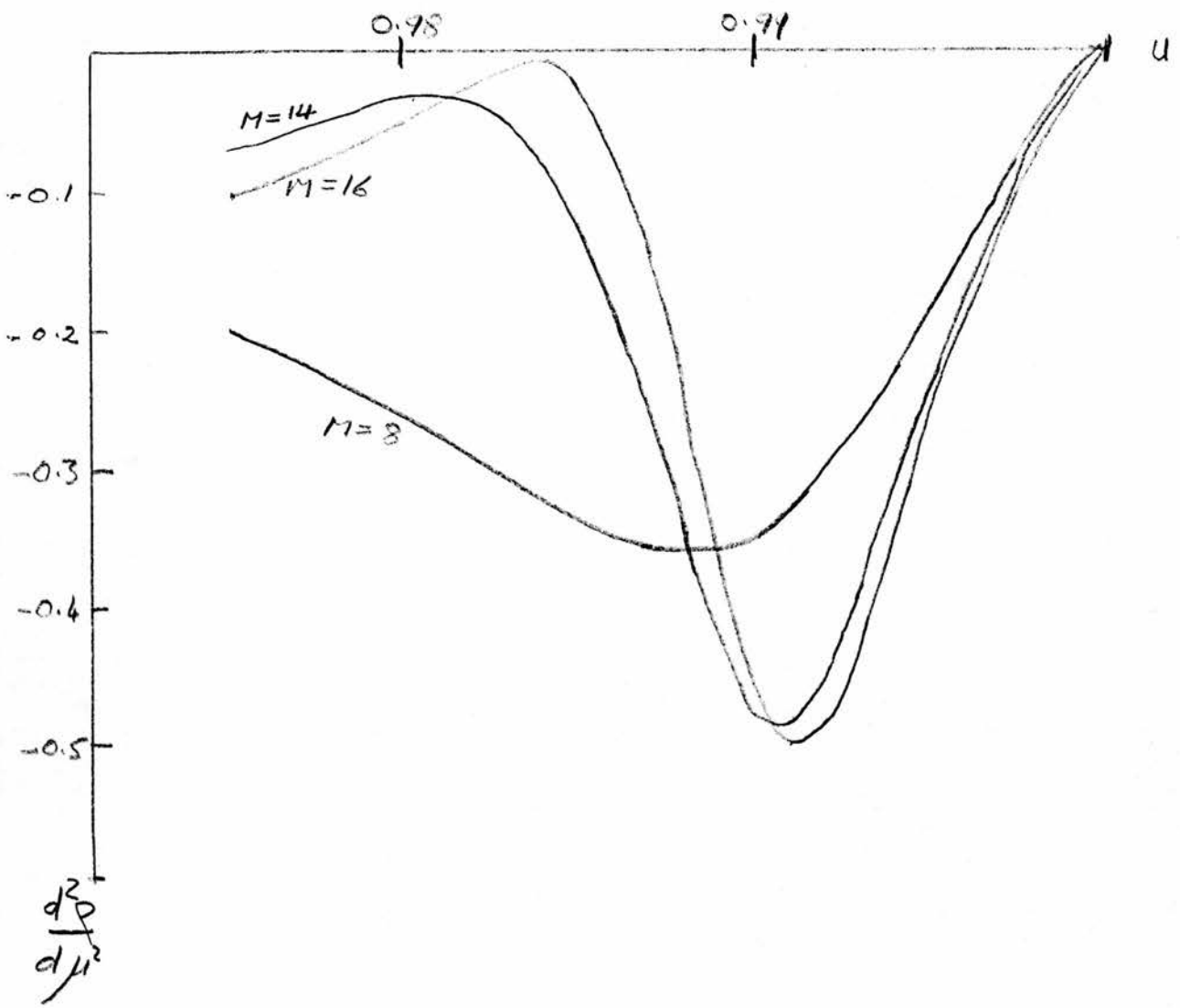

FIG 4.3.1 : SQ12 MODEL : VARIATION OF $\frac{d^2\rho}{d\mu^2}$ WITH u FOR EVEN-PERIODIC LATTICES

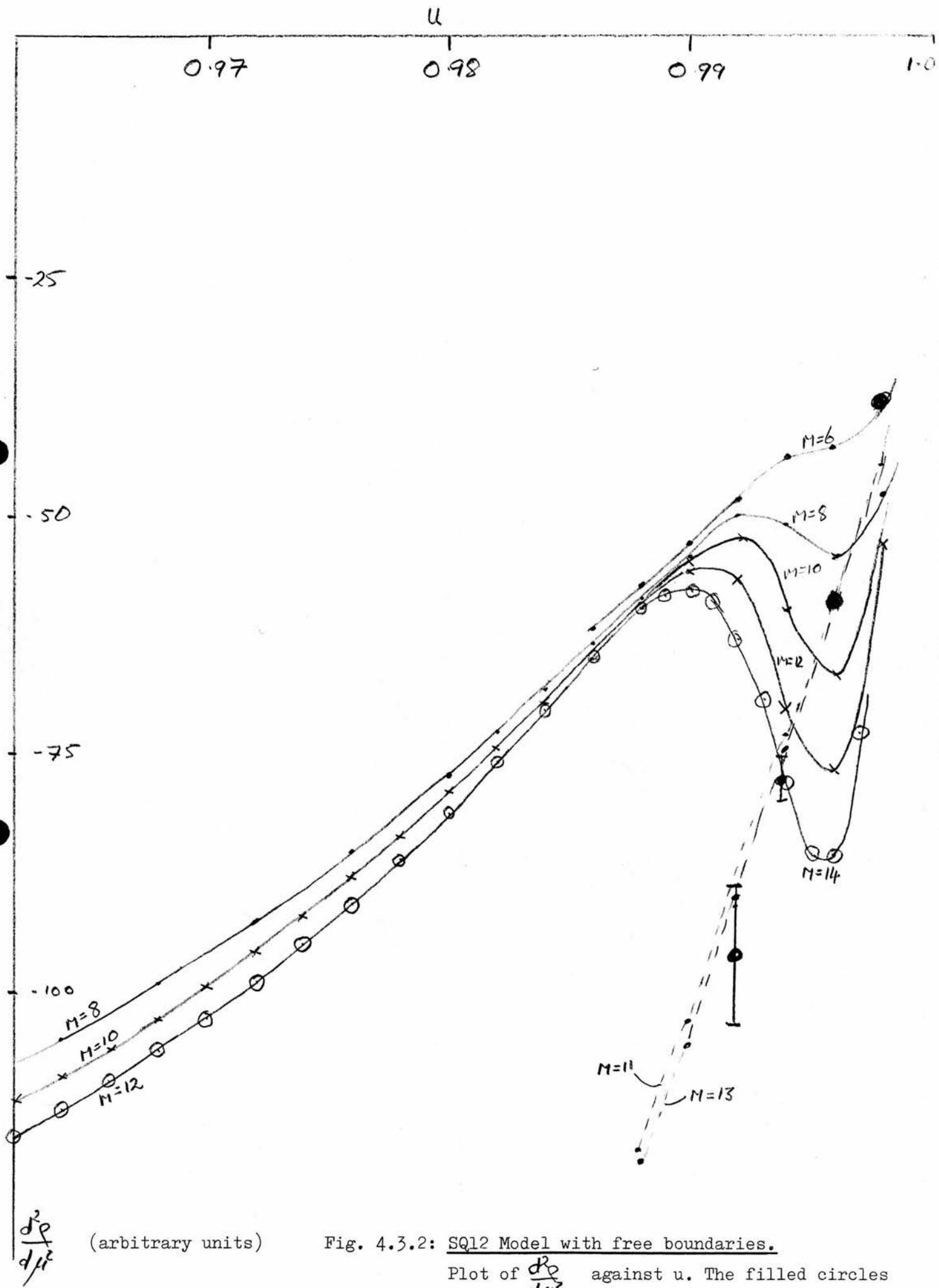

Fig. 4.3.2: SQ12 Model with free boundaries.
Plot of $\frac{d^2\rho}{d\mu^2}$ against u. The filled circles are the values obtained from the series of ref.25

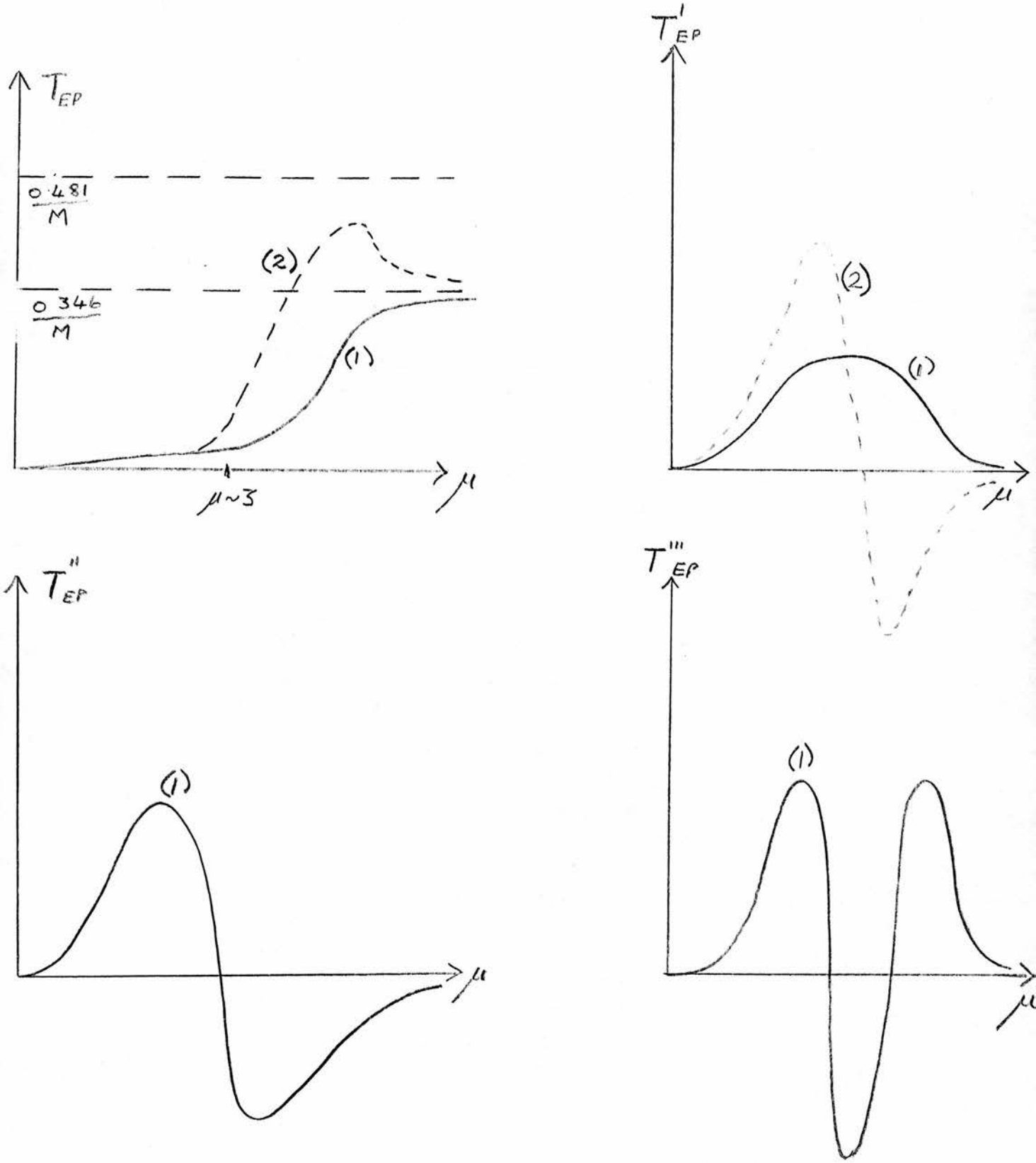

Fig. 4.3.3: Possible behaviour of T_{EP} and its derivatives in the SQ12 model.

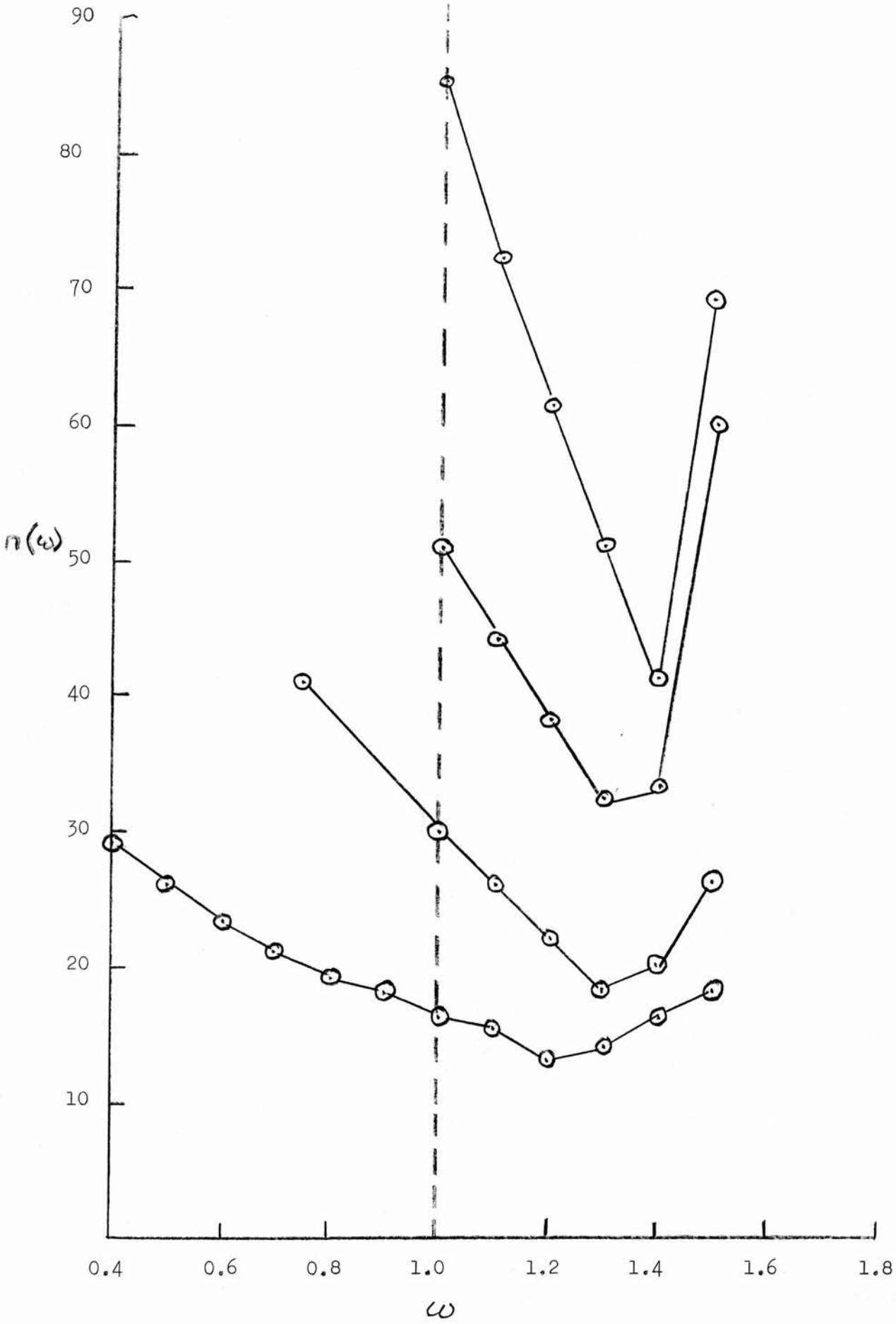

Fig. A2.1: Variation of $n(\omega)$, the number of iterations required for convergence, with ω, the SOR acceleration parameter, for the SQ124 matrices.